

Generation and Maintenance of T Follicular Helper Cells

Dissertation

Zur Erlangung des Doktorgrades

der Mathematisch-Naturwissenschaftlichen Fakultät

der Christian-Albrechts-Universität zu Kiel

vorgelegt von

**Julia Ritzau-Jost
geb. Kuhrau**

Kiel, 12.07.2021

President of the Christian-Albrechts-Universität zu Kiel:

Prof. Dr. Simone Fulda

Dean of the Faculty of Mathematics and Natural Sciences of the Christian-Albrechts
Universität zu Kiel:

Prof. Dr. Frank Kempken

1st Reviewer: Prof. Dr. Thomas Bosch

2nd Reviewer: Prof. Dr. Andreas Hutloff

Day of defense: 12.05.2022

This thesis was carried out from November 2016 to July 2021 under the supervision of Prof. Dr. Hutloff in the research group 'Chronic Immune Reactions' at the German Rheumatism Research Center, Berlin, and the department 'Molecular Immune Regulation' at the Institute of Immunology, Christian-Albrechts-Universität zu Kiel, and in cooperation with the department 'Molecular Immunology' at the Robert Koch Institute, Berlin.

Table of Contents

I Abbreviations	V
II List of Figures	VIII
III List of Tables	IX
IV Abstract	X
V Zusammenfassung	XI
1 Introduction	1
1.1 T_{fh} cell-dependent GC reactions and the humoral immune response	1
1.2 T_{fh} cell generation and maintenance	5
1.3 Clinical relevance of T_{fh} cells	9
1.4 Identification of T_{fh} cell signature genes by genetic modification of antigen-specific T cells	10
1.4.1 The adoptive transfer of genetically modified transgenic T cells.....	10
1.4.2 Principle of the CRISPR Cas9 system	11
1.5 Objectives	13
2 Methods	14
2.1 Mice	14
2.2 Cloning of plasmids for genetic manipulation of T cells	15
2.2.1 Cloning of overexpression plasmids.....	15
2.2.2 Cloning of sgRNAs for knock out of genes.....	16
2.2.3 Generation of plasmids for genetic manipulation of target cells.....	18
2.3 Retroviral infection	19
2.3.1 HEK cell cultures and transfection by calcium phosphate precipitation	19
2.3.2 Retroviral transduction of transgenic T cells	19
2.3.2.1 <i>In vitro</i> polarization of Th ₂ subsets	20
2.4 Mouse models	20
2.4.1 Adoptive transfer	20
2.4.2 Immunization methods	21
2.4.2.1 Subcutaneous immunization.....	21
2.4.2.2 Intranasal immunization	21
2.4.3 Tamoxifen administration	21
2.4.4 Lymphocyte isolation out of tissue	22
2.4.4.1 Lymphocyte isolation of draining lymph nodes	22
2.4.4.2 Lymphocyte isolation of lung tissue	22
2.5 Fluorescence-activated cell sorting	22
2.5.1 Sort of T _{fh} and non-T _{fh} cells for transcriptome analysis	23
2.5.2 Sort of fluorescence ⁺ cells.....	23
2.5.3 Cell staining of surface molecules and intracellular staining	23
2.5.3.1 Restimulation of isolated cells.....	24
2.6 Next generation sequencing	26
2.7 Proof of Cas9 knock out efficiency	26
2.7.1 T7 Endonuclease Assay.....	27
2.7.2 Sanger sequencing	27
2.8 Statistics	27
3 Results	28

3.1 Screening for new T_{fh} signature target genes	28
3.2 The T_{fh} signature gene <i>Tnfrsf11</i> is highly upregulated on T_{fh} cells but not involved in T_{fh} cell generation and maintenance	30
3.2.1 Early <i>Tnfrsf11</i> -depletion does not alter T _{fh} cell and B _{GC} cell generation.....	30
3.2.2 <i>Tnfrsf11</i> -depletion in primed T cells affects memory T _{fh} cell maintenance in draining lymph nodes.....	33
3.2.3 T cell-specific <i>Tnfrsf11</i> -depletion does not affect transgenic T and B cell migration behavior in inflamed lung tissue.....	36
3.2.4 Transcriptome analysis of <i>Tnfrsf11</i> -depleted T _{fh} and non-T _{fh} cells reveals differentially regulated genes.....	39
3.3 Screening for T_{fh} signature gene function by overexpression and CRISPR Cas9-mediated knock out in transgenic T cells	41
3.3.1 Overexpression of seven negatively regulated T _{fh} cell signature genes reveal a unique function of RAR α in T _{fh} cell generation.....	41
3.3.1.1 Nuclear retinoic acid receptor α promotes germinal center responses.....	45
3.3.2 CRISPR Cas9-mediated knock out of eleven positively regulated T _{fh} cell signature genes in antigen-specific T cells.....	48
3.3.2.1 Establishment of an <i>in vivo</i> CRISPR Cas9-mediated knock out system.....	48
3.3.2.2 Verification of knock out efficiency of genes of interest.....	49
3.3.2.3 Proof of principle of successful knock out and functional effects on T _{fh} cell numbers <i>in vitro</i> and <i>in vivo</i>	51
3.3.2.3.1 Successful <i>in vitro</i> knock out of <i>Cd44</i> and <i>Tigit</i>	51
3.3.2.3.2 Constitutive <i>in vivo</i> knock out of <i>Cd40lg</i> and <i>Il21</i> diminishes T _{fh} cell help.....	53
3.3.2.3.3 Verification of an inducible <i>in vivo</i> Cas9-mediated <i>Cd40lg</i> knock out.....	55
3.3.2.3.4 Fluorophore-dependent long-term stability of retrovirally infected cells.....	56
3.3.3 Functional screening of eleven T _{fh} signature genes by CRISPR Cas9-mediated knock out.....	60
3.3.3.1 The cell signaling regulator <i>Sostdc1</i> is highly upregulated in T _{fh} cells but not involved in T _{fh} cell generation or maintenance.....	66
4 Discussion	70
4.1 T cell specific RANKL expression does not play a major role in T_{fh} cell generation, maintenance, and tissue inflammation	72
4.2 RARα signaling has a key role in the humoral immune response	76
4.3 CRISPR Cas9-mediated knock out in transgenic T cells provides an efficient method for screening of gene function	78
4.4 Limitations of the adoptive transfer model at the example of <i>Sostdc1</i> knock out in antigen-specific T cells	80
5 Conclusion	83
6 Literature	84
7 Acknowledgements	107
8 Curriculum Vitae	109
9 List of publications	110
Declaration	111

I Abbreviations

Ascl2	achaete-scute complex homolog 2
APC	antigen-presenting cell
ATRA	<i>all-trans</i> retinoic acid
BCR	B cell receptor
Bcl-6	B cell lymphoma 6 protein
BFP	blue fluorescent protein
β-ME	beta-mercaptoethanol
BMP	bone morphogenic protein
BTLA	B- and T-lymphocyte attenuator (CD272)
Ca ²⁺	calcium
CCL	C-C-chemokine ligand
CCR	C-C-chemokine receptor
CD	cluster of differentiation
CD40L	CD40 Ligand (CD154)
CD62L	L-selectin
cDNA	complementary DNA
CFA	complete Freund's adjuvant
c-Maf	musculoaponeurotic fibrosarcoma oncogene homolog
CRISPR	clustered regularly interspaced short palindromic repeats
CTLA-4	cytotoxic-T-lymphocyte-associated protein 4 (CD152)
CXCL	C-X-C motif chemokine
CXCR	C-X-C chemokine receptor
DAPI	4',6-diamidino-2-phenylindole
DC	dendritic cell
dLN	draining lymph node
DSB	DNA double-strand break
Ebi2	Epstein-Barr virus-induced G protein coupled receptor 2
EDTA	ethylenediaminetetraacetic acid
EV	empty vector
FACS	fluorescence activated cell sorting
FC	fold change
FCS	fetal calf serum
FDC	follicular dendritic cell
FRC	fibroblastic reticular cell
GC	germinal center
GFP	green fluorescent protein
HDR	homology directed repair
HEK	human embryonic kidney
HEPES	4-(2-hydroxyethyl)-1-piperazineethanesulfonic acid
ICOS	inducible T cell costimulator
IFA	incomplete Freund's adjuvant

I Abbreviations

IFN γ	interferon gamma
Ig	immunoglobulin
IL	interleukin
IL2Ra	interleukin-2 receptor alpha (CD25)
i.p.	intraperitoneal
IRES	internal ribosome entry site
KCl	potassium chloride
KHCO ₃	potassium bicarbonate
Klf2	Kruppel-like factor 2
KO	knock out
LCMV	lymphocytic choriomeningitis virus
LEF1	lymphoid enhancer-binding factor 1
LFA-1	lymphocyte function-associated antigen 1
LN	lymph node
LTR	long terminal repeat
MACS	magnetic activated cell sorting
MFI	mean fluorescence intensity
MHC	major histocompatibility complex
MSCV	murine stem cell virus
NaCl	sodium chloride
Na ₂ HPO ₄	disodium hydrogen phosphate
NFAT	nuclear factor of activated T cells
NH ₄ Cl	ammonium chloride
NHEJ	nonhomologous end-joining
NIP	3-iodo nitrophenol
NP	nitrophenol
OE	overexpression
PAM	protospacer adjacent motif
PBS	phosphate-buffered saline
PC	plasma cell
PCR	polymerase chain reaction
PFA	paraformaldehyde
PI	propidium iodide
PMA	phorbol 12-myristate 13-acetate
pMHC	peptide-major histocompatibility complex
PD-1	programmed cell death protein 1
PSGL-1	selectin P ligand
RA	retinoic acids
RANKL	receptor activator of NF- κ B ligand
RAR	retinoic acid receptor
RAR α	retinoic acid receptor alpha
RNA	ribonucleic acid
RXR	retinoic x receptor

I Abbreviations

S1PR2	sphingosine-1-phosphate receptor 2
SAP	SLAM-associated protein
s.c.	subcutaneous
SD	standard deviation
sgRNA	single guide RNA
SHM	somatic hypermutation
shRNA	small hairpin RNA
SLAM	signaling lymphocyte activation molecule
SLO	secondary lymphoid organ
SM	Smarta
Sostdc1	sclerostin domain-containing-1
STAT	signal transducer and activator of transcription
T7EI	T7 endonuclease I
TCR	T cell receptor
TCF1	T cell factor 1
T _{fh}	T follicular helper cell
T _{fr}	follicular regulatory T cell
Thy-1.1	thymocyte antigen 1 isoform 1
TIGIT	T cell immunoreceptor with Ig and ITIM domains
TNF	tumor necrosis factor
T _{reg}	regulatory T cell
Wnt	wingless/int
WT	wildtype

II List of Figures

Figure 1	Schematic illustration of the lymph node structure.....	3
Figure 2	Schematic representation of a germinal center.....	5
Figure 3	T_{fh} cell dependence of the humoral immune response	6
Figure 4	Principle of adoptive transfer and lymphocyte activation	11
Figure 5	Principle of the CRISPR Cas9 system.....	13
Figure 6	Map of the eukaryotic expression vector pMSCV_IRES-GFP	15
Figure 7	Maps of the eukaryotic expression vectors pMSCV-U6-gRNA-PGK-PuroR-T2A-BFP and pMSCV-mAmetrine_U6-gRNA.....	17
Figure 8	Comparison of four different T_{fh} signature gene transcriptome analyses reveal 19 genes of interest	29
Figure 9	Early RANKL knock out does not affect T_{fh} cell development and B cell help during the immune effector phase.....	32
Figure 10	RANKL depletion affects memory T_{fh} cell numbers by phenotypical change of homing and migration markers	35
Figure 11	Early T cell-specific RANKL-depletion limits B cell differentiation and changes chemokine receptor expression in chronically inflamed lung tissue	38
Figure 12	Transcriptome analysis of T_{fh} cells of WT and RANKL KO mice reveals differentially expressed genes.....	40
Figure 13	Overexpression of T_{fh} cell signature genes has no effects on T_{fh} cell generation.....	44
Figure 14	Overexpression of retinoic acid receptor alpha (RAR α) influences T_{fh} and B_{GC} cell generation	47
Figure 15	Transgenic mouse strains and experimental set-up for CRISPR Cas9-based knock out in antigen-specific T cells.....	49
Figure 16	Verification of Cas9-induced knock out by T7EI assay or Sanger sequencing.....	51
Figure 17	CRISPR Cas9-induced knock out of Cd44 and Tigit in vitro shows strong downregulation of both molecules' surface expression	52
Figure 18	Cd40lg and Il21 KOs lead to decreased T_{fh} cells and reduced B cell helper capability	54
Figure 19	Inducible Cd40lg KO in vivo after initial T cell priming diminishes T_{fh} cell numbers.....	56
Figure 20	BFP ⁺ retrovirally infected cells were rapidly lost after transfer	58
Figure 21	Differential fluorophore immunogenicity and long-term stability of viral constructs encoding BFP, dsRed, GFP, and mAmetrine	60
Figure 22	A CRISPR Cas9-mediated knock out of eleven positively expressed T_{fh} signature genes does not affect T_{fh} cell number.....	64
Figure 23	Knock out of Sostdc1 does not affect transgenic T and B cells function or B cell helper capacity.....	68

III List of Tables

<i>Table 1</i>	<i>PCR primers and corresponding restriction enzymes for cloning of cDNA into eukaryotic expression vectors.....</i>	<i>16</i>
<i>Table 2</i>	<i>Oligos for the generation of sgRNAs</i>	<i>17</i>
<i>Table 3</i>	<i>Fluorochrome-labeled antibodies used for flow cytometry</i>	<i>25</i>
<i>Table 4</i>	<i>Screening of six downregulated T_{fh} cell signature genes for their role in T_{fh} cell generation</i>	<i>42</i>
<i>Table 5</i>	<i>Experimental conditions for the overexpression of T_{fh} signature genes</i>	<i>43</i>
<i>Table 6</i>	<i>Eleven positively expressed T_{fh} cell signature genes screened for their function in T_{fh} cell generation by CRISPR Cas9-mediated knock out.....</i>	<i>61</i>
<i>Table 7</i>	<i>Knock out of Bach2-regulated target genes showed knock out efficiencies of up to 90% ...</i>	<i>63</i>
<i>Table 8</i>	<i>Experimental groups for CRISPR-Cas9 mediated signature gene knock out</i>	<i>65</i>
<i>Table 9</i>	<i>Summary of the experimental conditions of investigated T_{fh} cell signature genes</i>	<i>71</i>

IV Abstract

T_{fh} cells are a CD4⁺ T cell subset that, together with cognate B cells, establishes the germinal center reaction. By providing unique signals for B cell help, T_{fh} cells support B cell differentiation into high-affinity plasma cells and long-lived memory B cells, thereby playing a crucial role during the humoral immune response.

Furthermore, exaggerated T_{fh} cell numbers are involved in autoimmune disorders, while diminished T_{fh} cell function causes immunodeficiency. Thus, identification and characterization of molecules involved in the generation and maintenance of T_{fh} cells are of high clinical interest.

A transcriptome analysis of T_{fh} and Non-T_{fh} cells revealed 19 signature genes with so far unknown function in T_{fh} cells. Retroviral infection of transgenic T cells allowed effective screening for these gene's function by means of genetic overexpression or CRISPR Cas9-mediated knock out. Additionally, adoptive transfer of modified cells enabled the tracking of antigen-specific, modified T cells *in vivo*.

The *Rara* gene, encoding for retinoic acid receptor α (RAR α), was found significantly downregulated in T_{fh} cells and positively influenced the humoral immune response upon overexpression, reflected in enhanced germinal center reactions. Thus, targeting RAR α might be a relevant target for treating allergic disorders and for enhancing vaccine efficacy. The remaining 18 genes did not directly affect T_{fh} cell biology, since targeting these genes did not affect unique T_{fh} cell function.

Nevertheless, screening for T_{fh} cell signature gene functions by means of genetic modification proved to be an efficient tool to gain novel insights into T_{fh} cell biology, especially given that the function of many selectively regulated T_{fh} cell molecules remains still unknown calling for further investigations.

V Zusammenfassung

T_{fh} Zellen stellen eine Subpopulation der CD4⁺ T-Zellen dar und sind gemeinsam mit kognaten B-Zellen Träger der Keimzentrumsreaktion. T_{fh} Zellen fördern dabei die Differenzierung von B-Zellen in hochaffine Plasmazellen und langlebige Gedächtnis-B Zellen durch die Bereitstellung hierfür essenzieller Signale. Dadurch spielen sie eine entscheidende Rolle in der humoralen Immunantwort. Darüber hinaus können verstärkte T_{fh} Zell-Reaktionen zur Entstehung von Autoimmunerkrankungen beitragen und verminderte T_{fh} Zell-Funktionen Immundefekte verursachen. Daher sind die Identifizierung und Charakterisierung von Molekülen, die an der Entstehung und Aufrechterhaltung dieser T Zell-Untergruppe beteiligt sind, von hohem klinischem Interesse.

Eine Transkriptomanalyse von T_{fh} und Nicht-T_{fh} Zellen ergab 19 T_{fh} Zell-Signaturgene mit bisher unbekannter Funktion für diese Zellpopulation. Ein effektives Screening der Funktion dieser Signaturgene wurde mittels retroviraler Infektion transgener T-Zellen zur Signaturgen-Überexpression oder einem CRISPR Cas9-vermitteltem *knock out* ermöglicht. Ein adoptiver Transfer modifizierter Zellen erlaubte die Verfolgung antigenspezifischer modifizierter T-Zellen *in vivo*.

Das Gen *Rara* kodiert für den Retinsäurerezeptor- α (RAR α) und wurde als in T_{fh} Zellen signifikant herunterreguliert gefunden. Eine Überexpression des *Rara*-Gens zeigte einen positiven Einfluss auf die humorale Immunantwort und äußerte sich in verstärkten Keimzentrumsreaktionen. Somit könnte eine Einflussnahme auf RAR α ein relevantes Ziel zur Therapie allergischer Erkrankungen sein oder zur Erhöhung der Effizienz von Impfungen beitragen. Die Untersuchung der 18 weiteren, in diesem Projekt identifizierten Signaturgene zeigte keinen direkten Einfluss auf die T_{fh} Zell-Regulation; die weiteren identifizierten Gene scheinen daher redundante oder nicht essenzielle Funktionen in T_{fh} Zellen aufzuweisen.

Das Screening der Funktion von T_{fh} Zell-Signaturgenen durch genetische Modifikation von T-Zellen stellt sich als ein effizientes Werkzeug heraus, um mehr Einblick in die Biologie von T_{fh} Zellen zu erhalten, insbesondere im Hinblick auf die nach wie vor unklare Funktion vieler essenziell an der humoralen Immunantwort, und im Besonderen an der T_{fh} Zell-Regulation beteiligter Moleküle, die weiterer wissenschaftlicher Auseinandersetzung bedürfen.

1 Introduction

Follicular T helper cells (T_{fh}) belong to the cluster of differentiation 4 positive ($CD4^+$) T cell family and are specialized in B cell help within germinal center (GC) reactions. Due to their unique function in the provision of essential signals for B cell proliferation and differentiation, T_{fh} cells are the key cell subset leading to the generation of high-affinity plasma cells (PC) and long-lived memory B (B_{mem}) cells. Therefore, T_{fh} cells exhibit a crucial role within the humoral immune response and thereby represent a target of high clinical relevance. While immune-deficient patients and vaccination strategies profit from enhanced T_{fh} cell functions, excessive T_{fh} cell responses have been shown in autoimmune disorders and allergies. Increasing our understanding on the mechanisms underlying T_{fh} cell generation and maintenance is therefore of high relevance. Identifying so far unknown molecules essential in these processes is the focus of this project.

1.1 T_{fh} cell-dependent GC reactions and the humoral immune response

Long-term immunity is achieved by long-lived PC and B_{mem} cells, which are reactivated upon repeated encounter with harmful substances and pathogens. The subsequent antibody-mediated humoral immune response leads to the neutralization of toxins, complement activation, antibody-dependent cellular cytotoxicity, and phagocytosis via opsonization (L. L. Lu *et al.*, 2018). Longevity of B cells and the generation of high-affinity antibodies, however, is strongly dependent on cognate interaction with a specific subset of T cells, so called T_{fh} cells, that takes place in secondary lymphoid organs (SLOs; Akkaya *et al.*, 2020; Good-Jacobson & Shlomchik, 2010).

Generally, mature but naïve $CD4^+$ T cells leave the thymus and circulate between blood and secondary lymphoid organs (i.e. the spleen, lymph nodes, and mucosa-associated lymphoid tissues; Qi *et al.*, 2014). When naïve T cells recognize their specific antigen via T cell receptor (TCR): peptide-major histocompatibility complex (pMHC)-interaction presented by antigen-presenting cells (APCs), T cells become activated. Besides the recognition of antigen by the TCR, activation by co-stimulatory signals is necessary. T cells are further influenced by cytokines that are released in

the surrounding microenvironment. This so-called priming leads to clonal expansion and the upregulation of various surface molecules as well as intracellular changes, encouraging CD4⁺ T cell-differentiation into various subtypes with corresponding effector functions (J.-R. Hwang *et al.*, 2020; Zhu & Paul, 2008). Activated T cells either migrate as effector cells to the site of inflammation or remain within secondary lymphatic organs to provide B cell assistance. Main CD4⁺ T helper subsets are Th₁, Th₂, Th₁₇; and T_{fh} cells as well as regulatory T cells (T_{reg}; Hilligan & Ronchese, 2020; J.-R. Hwang *et al.*, 2020; Kumar *et al.*, 2018; Qi *et al.*, 2014; Tomura *et al.*, 2010; Zhu & Paul, 2008).

Priming of naïve T cells takes place in secondary lymphoid organs which are highly organized structures divided into T and B cell zones. The lymph node as a characteristic secondary lymphoid organ, has a cortex containing B cell zones (Figure 1, yellow areas), in which B cells and stromal cells, particularly follicular dendritic cells (FDCs), form B cell follicles (Figure 1, dark yellow areas). FDCs are specialized in capturing immune complexes and in presenting them to B cells. T cell zones surround these B cell follicles in paracortical areas, similarly containing dendritic cells (DCs) as well as fibroblastic reticular cells (FRC) (Figure 1, green areas). The organization of the lymph node structure is supported by stromal cell-secreted chemokines which ensures the segregation of T and B cells in their distinct niches via expression of the corresponding chemokine receptors. Production of C-C-chemokine ligand 19 (CCL19) and CCL21 by FRCs and DCs directs C-C-chemokine receptor type 7 positive (CCR7⁺) naïve T cells into the T cell zones. Similarly, stromal cells and FDCs in the B cell follicles secrete C-X-C motif chemokine 13 (CXCL13) to attract C-X-C chemokine receptor type 5 positive (CXCR5⁺) naïve B cells (Förster *et al.*, 1996; Grant *et al.*, 2020; Qi *et al.*, 2014).

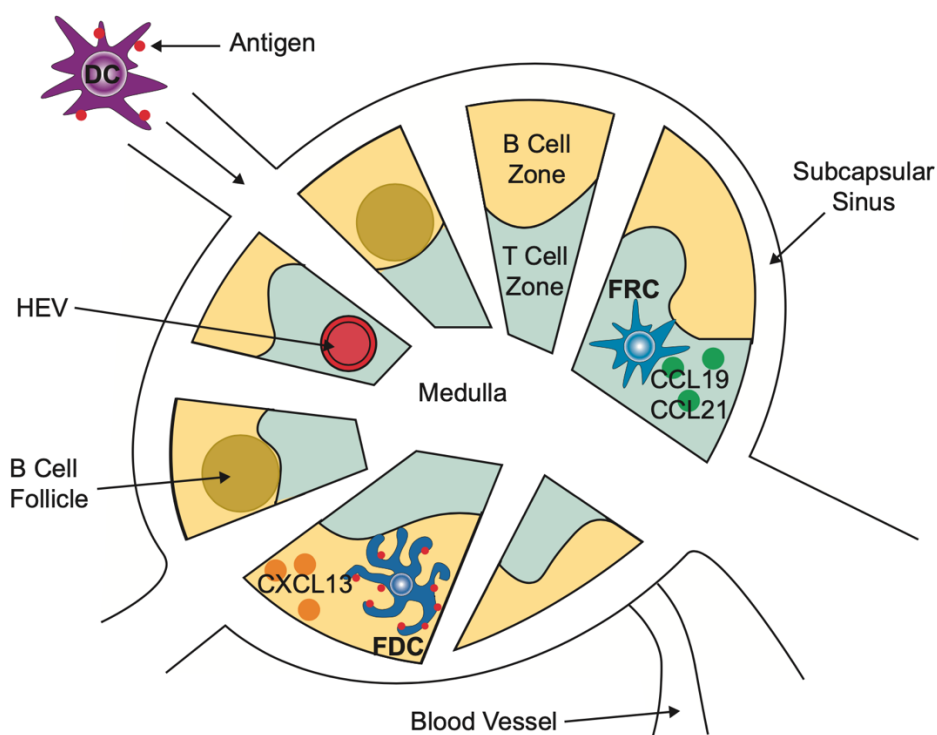


Figure 1 Schematic illustration of the lymph node structure

Naïve T and B cells circulate through blood and lymphatic vessels and enter the lymph node either via afferent lymphatic vessels or high endothelial venules (HEV). Lymph node stromal cells such as follicular dendritic cells (FDCs) in B cell zones (yellow) and fibroblastic reticular cells (FRCs) in T cell zones (green) organize lymph node structures by secretion of chemokines (CXCL13 and CCL19/CCL21, respectively). DCs and FDCs additionally serve as antigen-presenting cells (antigen depicted in red). (Figure adapted and modified from Murphy & Weaver, 2016)

Naïve CD4⁺ T cells recognize their specific antigen presented by DCs (Hilligan & Ronchese, 2020) and, depending on appropriate signaling in their microenvironment, differentiate into pre-T_{fh} cells followed by migration towards the border between the T cell zone and the B cell zone (T/B border; Haynes *et al.*, 2007; Takaharu Okada *et al.*, 2005; Qi *et al.*, 2014).

Like naïve T cells, naïve B cells circulate throughout the organism and become activated within SLOs upon encountering their cognate antigen in form of immune complexes presented by DCs, subcapsular sinus macrophages, and FDCs (Akkaya *et al.*, 2020; Heath *et al.*, 2019; Phan *et al.*, 2009). B cell receptor (BCR) signaling then triggers the upregulation of distinct molecules and promotes B cell migration towards the T/B border (Takaharu Okada *et al.*, 2005).

Here, the so-called cognate interaction, i.e. the first interaction of activated T and B cells recognizing the same antigen, is accomplished. Subsequently, some of these

cells form so-called primary foci, within which activated B cells proliferate and provide a first humoral immune response via the generation of plasmablasts. This B cell subpopulation is highly proliferative and secretes low-affinity antibodies as an early defense against invading pathogens (Allen, Okada, & Cyster, 2007; McHeyzer-Williams *et al.*, 2012). Other B cells however migrate, together with their cognate T_{fh} cells, into B cell follicles which thereupon turn into secondary lymphoid follicles – the germinal centers (Allen, Okada, Tang, *et al.*, 2007; De Silva & Klein, 2015; McHeyzer-Williams *et al.*, 2012).

GCs are highly organized microstructures within the SLO, structured into three areas by stromal cell-secreted chemokines: The outermost mantle zone is comprised of naive B cells, the light zone below contains antigen-presenting FDCs and T_{fh} cells, and in the innermost dark zone extensive B cell proliferation and BCR diversification occurs via somatic hypermutation (SHM) and class switch recombination (Figure 2; De Silva & Klein, 2015). Germinal center B cells (B_{GC}) leave the dark zone towards the light zone after SHM and class switch recombination and are again scanned by FDCs testing their modified BCR affinity. If the BCR-antigen binding capacity is lost, B_{GC} apoptosis is induced (negative selection). Otherwise, B_{GC} cells take up the specific antigen to subsequently present it to T_{fh} cells (Allen, Okada, & Cyster, 2007; De Silva & Klein, 2015; McHeyzer-Williams *et al.*, 2012). T_{fh} cells positively stimulated this way in turn provide help signals to B cells, leading to a positive B cell selection. This interaction is crucial for B_{GC} and T_{fh} cell maintenance and determines B cell fate (Gitlin *et al.*, 2014; Shulman *et al.*, 2013).

Upon the germinal center B_{GC}: T_{fh} cell interaction, B_{GC} cells either migrate back into the dark zone to further increase antigen affinity by SHM (cyclic reentry model). Alternatively, B_{GC} cells exit the germinal center in order to differentiate into long-lived antibody-producing PCs or B_{mem} cells (Allen, Okada, Tang, *et al.*, 2007; De Silva & Klein, 2015; McHeyzer-Williams *et al.*, 2012), ideally resulting in life-long protection against distinct pathogens.

T follicular regulatory cells (T_{fr}) cells, which also reside in the light zone, share phenotypic similarities to T_{fh} cells and are associated with the negative regulation of the magnitude of the germinal center reaction. Recently, the presence of T_{fr} cells has been shown to promote selection of high-affinity antibody-secreting B cells (Linterman *et al.*, 2011; Figure 2 and 3).

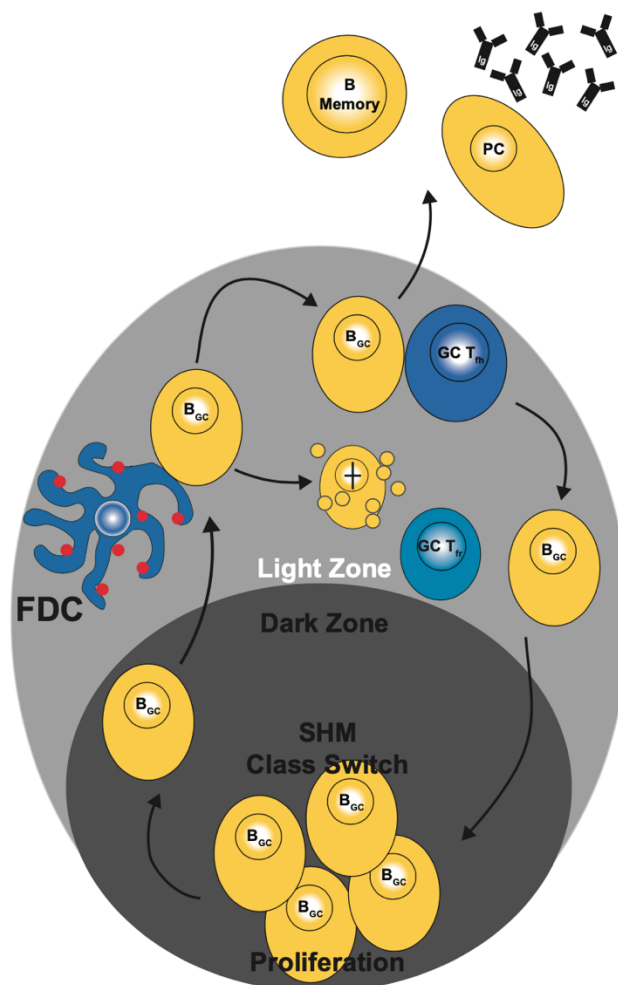


Figure 2 Schematic representation of a germinal center

GCs are highly organized microstructures with a dark zone (dark grey) containing B_{GC} cells (yellow) and a light zone (light grey) containing FDCs (blue), GC T_{fr} cells (bright blue), GC T_{fh} cells (dark blue) and B_{GC} cells. In the dark zone, extensive B cell proliferation, somatic hypermutation (SHM) and class switch recombination occurs. Subsequently, B_{GC} cells migrate to the light zone for uptake of antigens (red) provided by FDCs and antigen presentation to GC T_{fh} cells. B cells presenting antigen that lack affinity to T_{fh} cells undergo apoptosis. B cells presenting antigen with sufficient T_{fh} cell-recognition either exit the GC to differentiate into memory B cells or long-lived plasma cells (PC) or re-enter the dark zone to undergo further SHM. GC T_{fr} cells negatively regulate the GC response.

1.2 T_{fh} cell generation and maintenance

T_{fh} cell differentiation is a complex but crucial step in germinal center formation. The multi-step process involves interactions with DCs and B cells and ultimately leads to the generation of high-affinity long-lived PCs and B_{mem} cells.

While most effector T cell subsets and the necessity of T cells for successful antibody production have been known for decades, the responsible T_{fh} cells were not identified

as a distinct T cell subset until the early 2000s (Breitfeld *et al.*, 2000). Furthermore, the identification of Bcl-6 as the T_{fh} cell master transcription factor established them as a segregated T cell population (Crotty, 2019; Johnston *et al.*, 2009; Nurieva, Chung, Hwang, *et al.*, 2009; Yu *et al.*, 2009). In addition to Bcl-6, T_{fh} cells characteristically express the chemokine receptor CXCR5 and Programmed cell death protein 1 (PD-1), as well as other key molecules such as Inducible T cell costimulator (ICOS) and a member of the tumor necrosis factor (TNF) superfamily CD40 Ligand (CD40L). Furthermore, T_{fh} cells characteristically secrete interleukin (IL) cytokines (IL-4 and IL-21) that mediate B cell survival and differentiation. How T_{fh} cell differentiation proceeds in detail and which molecules are known to play a role in its maintenance will be described in further detail in the following chapter.

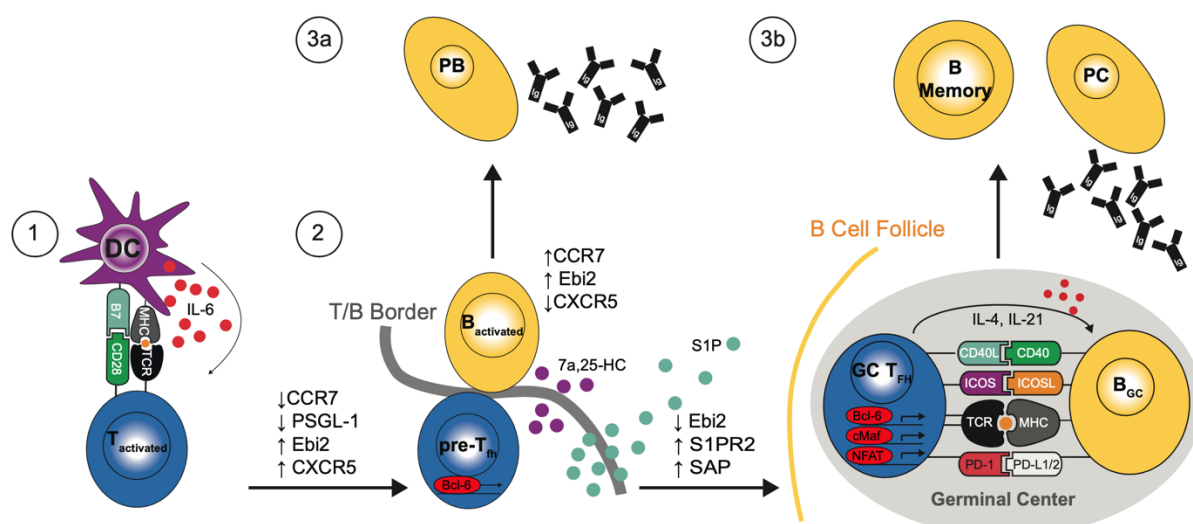


Figure 3 T_{fh} cell dependence of the humoral immune response

1) Upon priming of naive CD4⁺ T cells by DCs and co-stimulatory molecules (CD28–B7), additional IL-6 cytokine signaling determines the early fate of the T_{fh} cell. This is accompanied by activation of Bcl-6 and other molecular changes. **2)** Downregulation of CCR7 and PSGL-1 as well as upregulation of Ebi2 and CXCR5 enables migration to the T/B border. In parallel, activated B cells (*B_{activated}*) migrate towards the T/B border by upregulation of CCR7 and Ebi2 and downregulation of CXCR5. Upon initial contact with cognate B cells the pre-T_{fh} cell phenotype is stabilized. Subsequently, activated B cells either **3a)** differentiate directly into short-lived plasmablasts (PB) and secrete low-affinity antibodies for an initial immune response, or **3b)** migrate together with T_{fh} cells into B cell follicles to initiate a germinal center (GC) response. Migration is enabled by downregulation of Ebi2 and upregulation of S1PR2. The Ebi2 ligand 7 α ,25-dihydroxycholesterol (7 α ,25-HC) is highly abundant at the T/B border, while S1P, the ligand for S1PR2, is established as a negative concentration gradient from the perimeter to the center of the B cell follicle. T_{fh} cells subsequently differentiate into full T_{fh} cells expressing multiple transcription factors such as Bcl-6, c-Maf, and NFAT. Fully differentiated T_{fh} cells express molecules essential for repeated interaction with B cells (ICOS, PD-1), B cell help (CD40L), and secrete the cytokines IL-4 and IL-21. This interaction

provides both, B_{GC} cells and T_{fh} cells with survival signals and supports B cell differentiation into memory B cells (B_{Memory}) and long-lived plasma cells (PC) secreting high-affinity antibodies.

In addition to the initial activation of naïve CD4⁺ T cells by TCR: pMHC interaction, co-stimulation of CD28 by B7 molecules (CD80/ CD86) expressed on DCs is essential for full activation (Weber *et al.*, 2015). Following sufficient activation, the cell fate decision towards T_{fh} cells is influenced by TCR signaling strength and the interplay of diverse factors (Bartleson *et al.*, 2020). Sustained antigen stimulation (Deenick *et al.*, 2010) and enhanced IL-6 signaling induce expression of the T_{fh} master transcription factor Bcl-6 and initiate T_{fh} cell programming (Vinuesa *et al.*, 2016). In contrast, Interleukin-2 receptor alpha chain (IL2Ra) signaling suppresses T_{fh} cell differentiation (Ballesteros-Tato *et al.*, 2012; Johnston *et al.*, 2012; Nurieva *et al.*, 2012). Subsequently, other molecules essential for T_{fh} cell development, such as IL-21, are being upregulated. The cytokines IL-6 and IL-21 signal through Signal Transducer and Activator of Transcription 3 (STAT3), further enhancing Bcl-6 expression by direct binding to its gene's promoter region (Diehl *et al.*, 2012; Dienz *et al.*, 2009). Besides Bcl-6 and STAT3, there are other known transcription factors positively influencing early T_{fh} cell differentiation, including TCF1, LEF1, and Ascl2 (Vinuesa *et al.*, 2016). The interplay of these various factors leads to the upregulation of CXCR5, the receptor for CXCL13, and Epstein-Barr virus-induced G protein coupled receptor 2 (Ebi2). 7 α ,25-dihydroxycholesterol (7 α ,25-HC), the ligand for Ebi2, is highly abundant at the outer and interfollicular regions, enabling correct localization at the T/B border (Baptista *et al.*, 2019; J. Li *et al.*, 2016; Moriyama *et al.*, 2014). Besides, CCR7 and selectin P ligand (PSGL-1), which are both receptors for CCL19 and CCL21, are downregulated. In parallel, activated cognate B cells upregulate CCR7 and Ebi2 and downregulate CXCR5 (Gatto & Brink, 2013; Reif *et al.*, 2002). According to chemokine gradients created by stromal cells, changes in chemokine receptor expression enable migration towards the T/B border and the initiation of the first interaction between cognate T and B cells. T cells at this stage are referred to as pre-T_{fh} cells, which already express their signature molecules CXCR5 and PD-1 (Webb & Linterman, 2017; Figure 3 part 2). Stable and long-lived interaction between cognate T and B cells at the T/B border is supported by signaling lymphocyte activation molecule (SLAM) family receptors Ly108, CD84 and SLAM-associated protein (SAP; Cannons *et al.*, 2010; Takaharu Okada *et al.*, 2005; Qi *et al.*, 2008).

Supported by bystander B cells, ICOS and PD-1 signaling enables T cell migration into follicles (Shi *et al.*, 2018; Xu *et al.*, 2013). This migration goes along with Ebi2 downregulation (Suan *et al.*, 2015) and upregulation of sphingosine-1-phosphate receptor 2 (S1PR2, Moriyama *et al.*, 2014). S1PR2 ligand S1P is a lipid signaling molecule that negatively regulates S1PR2⁺ cell migration. By the establishment of a negative periphery-to-center concentration gradient within the B cell follicle, the combination of S1P gradient and S1PR2 upregulation promotes B_{GC} cell and T_{fh} cell migration into the center of follicles (J. A. Green & Cyster, 2012). Within follicles, signaling between T and B cells leads to final differentiation into GC T_{fh} cells and B_{GC} cells and the initiation of the GC response (Stebegg *et al.*, 2018).

T_{fh} cells migrate between neighboring GCs and the follicle, scanning B_{GC} cells by short, rapid contact (Allen, Okada, Tang, *et al.*, 2007; Shulman *et al.*, 2013). At this stage, GC T_{fh} cells exhibit the highest CXCR5 and PD-1 expression (Haynes *et al.*, 2007). Continuous antigen stimulation and interaction with B cell-expressed ligands is essential to stabilize short T/B contacts and to support B cell survival and proliferation (Shulman *et al.*, 2014). Only B cells with high receptor affinity to specific antigens take up and subsequently present antigens on MHC class II molecules, thereby receiving the required T cell help (Depoil *et al.*, 2005; Shulman *et al.*, 2014). Expression of T_{fh} cell transcription factors Bcl-6, c-MAF, and NFAT coordinate the expression of other essential molecules, such as SAP and ICOS (Elgueta *et al.*, 2009; Joyce Hu *et al.*, 2013; Weber *et al.*, 2015), finally leading to IL-4 and IL-21 secretion from T cells and high expression of CD40L (Bauquet *et al.*, 2009; Deenick *et al.*, 2010; Hiramatsu *et al.*, 2010; Rolf *et al.*, 2010; Shulman *et al.*, 2014; Figure 3 part 3b). CD40L is one the most important molecules within T/B interaction and within GCs, and it acts as a limiting factor for B_{GC} cell competition and thereby determines B_{GC} cell fate. CD40- CD40L signaling results in a CD40-ICOS-L-ICOS-CD40L intra- and intercellular positive-feedback loop which prolongs cognate T/B interaction and enhances T_{fh} cell-delivered B cell help (Wan *et al.*, 2019). Moreover, secreted cytokines not only provide the signal for antibody isotype switching and somatic hypermutation, IL-21 is also involved in autocrine T_{fh} cell maintenance (Bélanger & Crotty, 2016; Ozaki *et al.*, 2002; Spolski & Leonard, 2008; Vogelzang *et al.*, 2008).

To prevent excessive humoral immune responses, various negative regulatory mechanisms exist. These include the inhibitory molecules cytotoxic T-lymphocyte-associated Protein 4 (CTLA-4), B- and T-lymphocyte attenuator (BTLA), and Ephrin

1B receptor (P. Lu *et al.*, 2017; Sage *et al.*, 2014). Furthermore, cytokine-mediated, transcription factor-mediated, and metabolic regulatory mechanisms exist, which are effective at all stages of the T_{fh} cell life cycle (Dong *et al.*, 2020).

1.3 Clinical relevance of T_{fh} cells

Diverse molecules responsible for maintaining the T_{fh} cell phenotype and thus the GC response are known to date. Due to limited access to the relevant human tissues and the lack of manipulability of human cells *in vivo*, most data on GC reactions are obtained from murine model systems. Fortunately, human and murine T_{fh} cells are comparable in their hallmark features such as surface markers and gene expression profiles, suggesting a robust evolutionary conservation of T_{fh} cell physiology (Ueno *et al.*, 2015).

The importance of T_{fh} cell regulatory pathways is highlighted by patients suffering from ineffective or exaggerated humoral immune response, leading to immunodeficiency or autoimmune diseases, respectively. In a subset of these patients, dysregulations of distinct molecules or polymorphisms within genes encoding essential T_{fh} cell molecules were found. Deficiency of ICOS for example, one of the key molecules in T_{fh} activation, is responsible for the development of common variable immunodeficiency caused by impaired GC responses (Grimbacher *et al.*, 2003). CD40L, SAP, and STAT3 signaling are also essential for a fully developed germinal center response and have been shown in patients suffering from hyper-IgM syndrome (Aruffo *et al.*, 1993), X-linked lymphoproliferative disease (Qi *et al.*, 2008), and hyper-IgE syndrome (Ma *et al.*, 2012), respectively. Besides, integrin LFA-1 (Meli *et al.*, 2016), and miRNAs (R. Hu *et al.*, 2014; Kang *et al.*, 2013; Pratama *et al.*, 2015; Ripamonti *et al.*, 2017; Zeiträg *et al.*, 2020) only recently proved to be crucial in the maintenance of the T_{fh} cell phenotype.

While the absence of these regulatory molecules causes immunodeficiencies, excessive T_{fh} cell responses show the opposite effect: Overly responsive T_{fh} cells result in a lack of B cell competition for T cell help, thereby supporting clones with low or self-reactive receptor affinity leading to autoimmunity (Ueno *et al.*, 2015). Conclusively, autoimmune diseases such as systemic lupus erythematosus, Sjögren's

syndrome, or rheumatoid arthritis were previously shown to involve T_{fh} dysregulation (Liu *et al.*, 2012; Pontarini *et al.*, 2020; Simpson *et al.*, 2010).

1.4 Identification of T_{fh} cell signature genes by genetic modification of antigen-specific T cells

Signature genes are genes that are strongly expressed in particular cell types and significantly contribute to their function. In order to uncover new molecules essential for T_{fh} cell generation and maintenance, and due to the scarcity of relevant human tissue and unavailability of robust protocols for the generation of T_{fh} cells *in vitro* (Gao *et al.*, 2020; K. T. Lu *et al.*, 2011), this study adopted a mouse model. Importantly, the use of transgenic mouse models allows for the genetic modification of antigen-specific T cells and the functional investigation of modifying factors.

1.4.1 The adoptive transfer of genetically modified transgenic T cells

Under physiological conditions, only a small number of T cells exhibit a TCR specific for a given antigen. Therefore, detection of antigen-specific T cells *in vivo* is difficult to perform. To facilitate their detection, their frequency was increased using an adoptive transfer system employing transgenic donor animals. In the particular system used in this study, mice were modified to express the so-called Smarta TCR, which specifically recognizes a peptide derived from lymphocytic choriomeningitis virus glycoprotein 1 (GP1, so-called *Smarta* mice). Moreover, these animals carry the congenic surface marker thymocyte antigen 1 isoform 1 (Thy-1.1), enabling their detection in Thy-1.1-negative recipient animals (Figure 4A). In addition, adoptive transfer of transgenic B cells was performed in a subset of experiments. These carried the congenic marker CD45.1 and exhibited BCR specificity towards the hapten nitrophenol (NP; *B1-8i* mice). Upon isolation from donor animals, T and B cells were transferred into recipient animals. Due to expression of congenic markers in transgenic donor cells (Thy-1.1 for T cells and CD45.1 for B cells), these were readily distinguishable from endogenous wildtype (*C57BL/6* mice) recipient T and B cell populations positive for Thy-1.2⁺ and CD45.2⁺, respectively (Figure 4B). A conjugate of Smarta peptide (GP₆₁₋₈₀; SM) and iodinated nitrophenol coupled to mouse serum albumin (NIP-SM-MSA) was used as an antigen to stimulate activation of transgenic T and B cells (Figure 4C).

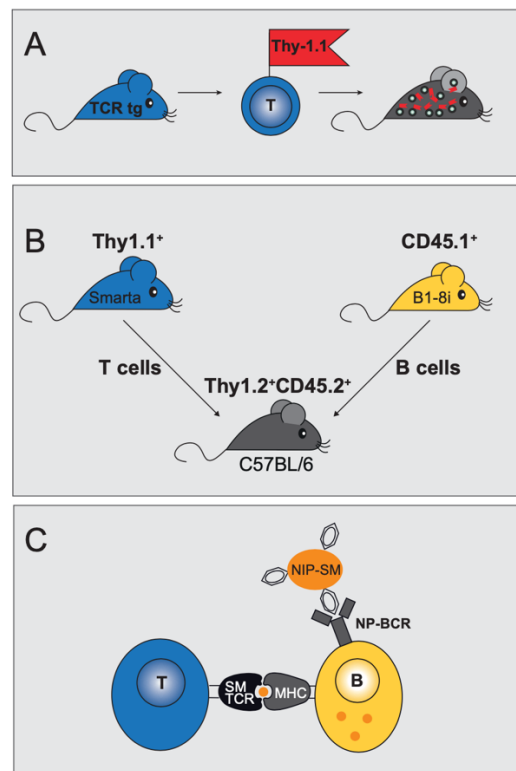


Figure 4 Principle of adoptive transfer and lymphocyte activation

A) T cells from TCR transgenic animals express the congenic surface marker *Thy-1.1*, allowing for the detection of these cells in recipient animals. B) *Thy-1.1*⁺ transgenic T cells from Smarta animals and *CD45.1*⁺ transgenic B cells from B1-8i mice were co-transferred into C57BL/6 WT recipient animals (*Thy-1.2*⁺ *CD45.2*⁺). C) An antigen conjugate consisting of Smarta peptide (SM) and iodinated nitrophenol (NIP) coupled to mouse serum albumin (NIP-SM-MSA) was used for activation of transgenic T and B cells.

1.4.2 Principle of the CRISPR Cas9 system

Genetic manipulation of cells allows the investigation of the function of specific molecules. One way to genetically modify cells is by use of the CRISPR Cas9 system, which provides fast and efficient knock out of pre-defined genes of interest.

The CRISPR (Clustered Regularly Interspaced Palindromic Repeat) Cas system was originally detected as a molecular mechanism employed during adaptive immunity in prokaryotes (Hille *et al.*, 2018). The past decade has seen a growing interest in this system as slight modifications enabled a simple and easy-to-use gene editing technology that was to date successfully adopted in biotechnology, agriculture and medicine (Doudna & Charpentier, 2014; Hille *et al.*, 2018).

Due to the requirement of only a single Cas enzyme type, Class 2 type II CRISPR Cas9 is one of the most widely used gene editing systems (Doudna & Charpentier, 2014; Hille *et al.*, 2018). Cas9 is a duplex-RNA-guided endonuclease that requires an RNA duplex, consisting of a CRISPR RNA (*crRNA*) and a transactivating *crRNA* (*tracrRNA*) for guidance to its target DNA sequence. The RNA-duplex can be engineered as a single-guide RNA (sgRNA) consisting of a DNA-targeting site (corresponds to *crRNA*, variable part; red sequence in Figure 5) located at the 5' end, and a Cas enzyme-binding site (corresponds to *tracrRNA*, constant part; green in Figure 5) located at the 3' end (Doudna & Charpentier, 2014). Another critical aspect for Cas9 guidance is the presence of a protospacer adjacent motif (PAM), usually consisting of 3 nucleotides (5'NGG) located adjacent to the *crRNA*-targeted sequence. Upon sgRNA binding within its central cleft, the Cas9 protein undergoes large conformational changes, establishing the so called sgRNA-bound surveillance complex. This complex scans DNA for target regions and upon recognition of DNA sequences complementary to sgRNA and PAM, a local unwinding of the DNA is established. Base-pairing of sgRNA and DNA promote additional conformational changes within the Cas9 enzyme which stabilize the hybridization of RNA with double-stranded DNA - the so-called R-loop formation - and subsequent DNA cleavage via Cas9's two nuclease domains (HNH and RuvC-like). The HNH domain cleaves the DNA strand complementary to the sgRNA whereas the RuvC-like domain cleaves the opposite strand (Doudna & Charpentier, 2014; Hille *et al.*, 2018). Cas9-mediated cleavage of DNA thereby leads to the introduction of DNA double-strand breaks (DSBs).

There are two known DSB repair mechanisms –nonhomologous end-joining (NHEJ) and the homology directed repair (HDR). Whereas the HDR requires exogenously delivered or endogenous DNA templates that are usually available during specific cell cycle phases only, NHEJ establishes religation of broken strands with little or no homology. Since NHEJ is the repair mechanism mainly used for simple religation of broken double strands, religated strands often contain insertional or deletional mutations of variable length, thereby inducing frameshift changes often leading to the knock out of genes coded on the religated strands (Figure 5; Boyle, 2008; El Khoury *et al.*, 2018; Sander & Joung, 2014).

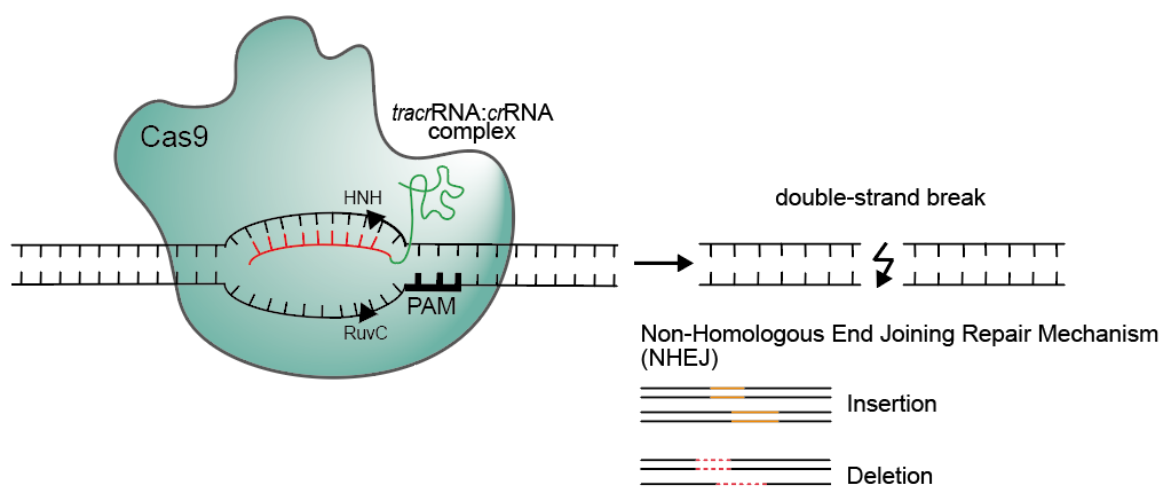


Figure 5 Principle of the CRISPR Cas9 system

Cas9 cleavage is guided by an RNA complex comprised of tracrRNA: crRNA on a single guide RNA strand (sgRNA) and the presence of a protospacer adjacent motif (PAM) sequence. Upon recognition of a DNA sequence complementary to the sgRNA, a double-strand DNA break is induced by cleavage with Cas9's two endonuclease domains HNH and RuvC. The non-homologous end joining repair mechanism leads to insertion-deletion mutations and thereby frameshifts, resulting in the knock out of the sgRNA-targeted genes of interest on the re-ligated DNA strands (figure adapted and modified from Doudna and Charpentier, 2014).

1.5 Objectives

Due to the crucial role of T_{fh} cells in the generation of an effective and long-lasting antibody-mediated humoral immune response, a better understanding of T_{fh} cells is of high clinical interest. In this context, achieving both, the generation of protective antibodies, e.g. in the context of vaccinations, as well as the suppression or elimination of harmful autoreactive antibodies in autoimmune diseases or allergies are important approaches.

Due to the accessibility and the simplicity of manipulating murine cells by use of the CRISPR Cas9 system or viral overexpression, the unavailability of similar human cell population *in vitro*, and the comparability of murine and human T_{fh} cells, the following data were generated by using a transgenic mouse model.

The aim of this work was to define so far unknown molecules crucially involved in the generation and maintenance of T_{fh} cells. By means of transcriptome analysis of murine samples, potential targets were defined and their function for the development and maintenance of T_{fh} cells were investigated by genetic manipulation (i.e., overexpression and knock out of target genes) in transgenic T cells.

2 Methods

2.1 Mice

For adoptive transfer experiments, mice transgenic for the Glycoprotein (GP)₆₁₋₈₀ TCR (below referred to as *Smarta*-TCR; Oxenius *et al.*, 1998) were crossed with *B6.PL* mice (*Jackson Laboratory*) to obtain expression of the congenic marker Thymocyte antigen 1 isoform 1 (Thy-1.1). Animals transgenic for both, the *Smarta*-TCR and Thy-1.1, are in the following referred to as *Smarta* mice. To generate an inducible system, *Smarta* animals were crossed to *CreER^{T2}* mice (Seibler *et al.*, 2003) where indicated. This introduced a tamoxifen-inducible CreER fusion protein gene ubiquitously expressed under the Rosa26 promoter.

To study the function of the molecule RANKL, *Smarta.CreER^{T2}* mice were additionally crossed to *RANKL^{fl/fl}* mice (Xiong *et al.*, 2011). These animals harbor a *Tnfsf11* allele encoding for RANKL flanked by loxP sites. By additional mating with *Smarta.CreER^{T2}* animals, a tamoxifen-inducible knock out of the RANKL gene is achieved (below referred to as *Smarta.CreER^{T2}/RANKL^{fl/fl}*). Since fewer cytotoxic side effects under tamoxifen treatment were observed in heterozygous *CreER^{T2}* animals (this study), *CreER^{T2}*-heterozygous animals were used for both *Smarta.CreER^{T2}* and *Smarta.CreER^{T2}/RANKL^{fl/fl}* strains in later studies. For CRISPR/Cas9-mediated knock outs, Cas9-GFP transgenic mice (Chu, Weber, *et al.*, 2016) were crossed to *Smarta* animals. For knock outs at defined timepoints, Cas9-GFP transgenic mice were crossed to *Smarta.CreER^{T2}* mice.

To investigate effects on B cells, BCR knockin animals specific for the hapten nitrophenol (NP) were used (*B1-8i*; Sonoda *et al.*, 1997). *B1-8i* animals were additionally crossed to κ -light chain KO animals (Zou *et al.*, 1993) and *Ly-5.1* animals (*Jackson Laboratory*) to ensure NP specificity and to introduce expression of the congenic marker CD45.1 (subsequently animals transgenic for CD45.1 and NP-BCR are referred to as *B1-8i*).

Recipients were either *C57BL/6* animals (referred to as *wildtype*) or *CD28* KO animals (referred to as *B6.CD28 KO*, when crossed back to a *C57BL/6NCrl* background; Shahinian *et al.*, 1993). The latter were used in transgenic B cell-T cell co-transfer experiments, since CD28 is a co-stimulatory molecule essential for T_{fh} cell formation (Weber *et al.*, 2015). Because of the impaired generation of endogenous T_{fh} cells in

B6.CD28KO mice, effects on adoptively transferred *B1-8i* B cells can directly be attributed to co-transferred transgenic T cells. All used animals were crossed back to animals of a *C57BL/6NCrl* background. Animals were bred under specific pathogen-free conditions in the animal facility of the Federal Institute for Risk Assessment (Berlin) and breeding as well as experiments were performed according to German animal welfare protection laws and approved by the responsible local governmental authority (LAGeSo, Berlin). Mice were kept in individually ventilated cages under a 12/12h light/dark cycle. Food and water were supplied *ad libitum*. For all experiments, animals at an age of at least 6 weeks and of both sexes were used.

2.2 Cloning of plasmids for genetic manipulation of T cells

2.2.1 Cloning of overexpression plasmids

Genes of interest were amplified by polymerase chain reaction (PCR) from cDNA generated from sorted non-T_{fh} cells. For PCR, Q5 polymerase (*New England Biolabs*) and the protocol according to the manufacturer's instructions were used. Primers for amplification contained appropriate restriction sites for enzymes to clone the PCR product into the pMSCV-IRES-GFP vector (Fig. 6) used for overexpression (Table 1).

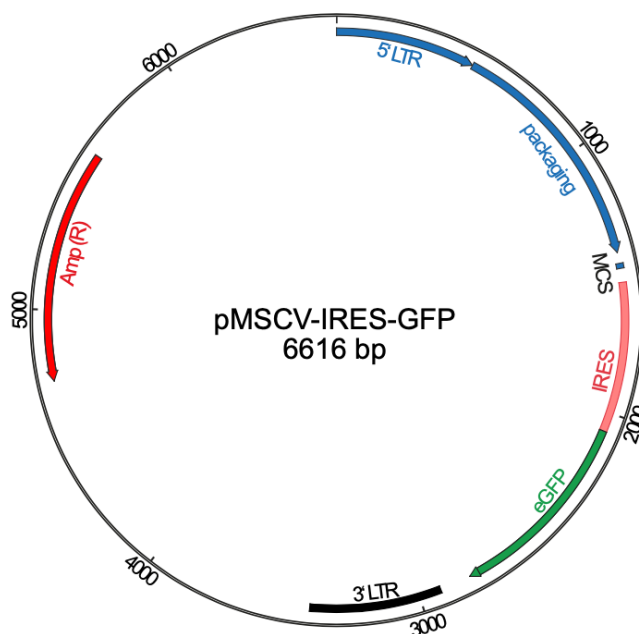


Figure 6 Map of the eukaryotic expression vector pMSCV_IRES-GFP

Scheme of the murine stem cell virus (MSCV) retroviral expression vector pMSCV-IRES-GFP consisting of 5' and 3' long terminal repeats (LTR, 5' LTR blue, 3' LTR black), packaging (blue), a multiple cloning site (MCS, blue) for

Methods

introduction of genes of interest, the fluorescence reporter eGFP (green) linked to an IRES site (light red), and ampicillin resistance (Amp^R), red).

Table 1 PCR primers and corresponding restriction enzymes for cloning of cDNA into eukaryotic expression vectors Table depicts genes of interest with corresponding primers for cDNA amplification. Primers include restriction sites for enzymes displayed in the right column. Identical or compatible restriction enzymes are used for digestion of the PCR product (insert) and vector.

Gene of interest	PCR primer	Restriction enzymes
Ccr2	5'-AATTAAGATCTGTTTCAGCTGCCTGCAAAGAC-3'	BglIII
	5'-AATTAAGCTCGAGCAAAGCTGCTCCCTCCTTCCC-3'	XhoI
Plac8	5'-AATTAAGATCTGCCACCATGGCTCAGGCACCAACAGTT-3'	BglIII
	5'-AATTAAGCTCGAGCTTAGAAAGCGTTCATGGCTCTCCTC-3'	XhoI
Fam129b	5'-AATTAAGGATCCGCCACCATGGGAGACGTAAGTCCAC-3'	BamHI
	5'-AATTAAGCTCGAGCCATGCTTAGAACTCCGTCTGCAC-3'	XhoI
Smad7	5'-AATTAAGATCTGCCACCATGTTTCAGGACCAACGATCTGC-3'	BglIII
	5'-AATTAAGCTCGAGACTACCGGCTGTTGAAGATGACC-3'	XhoI
Cish	5'-AATTAAGATCTGCCACCATGCCGGAGGGTACATTCCTAGTTC-3'	BglIII
	5'-AATTAAGCTCGAGGTCAGAGTTGGAAGGGGTACTGTCCG-3'	XhoI
Cxcr6	5'-AATTAAGGATCCGCCACCATGGATGATGGGCATCAAGAGTC-3'	BamHI
	5'-AATTAAGCTCGAGGTGGCAAGGCCTACTACAATTGGAA-3'	XhoI
Rara	5'-ATTAAGATCTCCCTCGCTTCGAGCAC-3'	BglIII
	5'-ATTAAGCTCGAGTCTGTCTGAGAGGACAAGCG-3'	XhoI
Klf2	5'-GGAAGATCTATGGCGCTCAGCGAGCCTA-3'	BglIII
	5'-GGAGTCGACACCCAGGCTACATGTGTCCG-3'	Sall

2.2.2 Cloning of sgRNAs for knock out of genes

SgRNAs were designed using the CrispRGold tool (<https://crisprgold.mdc-berlin.de>; MDC Berlin) This sgRNA design tool calculates off-target effects, specificity of the used sgRNA in different isoforms of the gene, and sgRNA intrinsic properties, such as GC content and folding energy to obtain an optimal sgRNA activity and specificity (see also Chu, Graf, *et al.*, 2016). Complementary oligonucleotides were ordered from Eurofins (Table 2) and annealed and phosphorylated by the T4 polynucleotide kinase according to the manufacturer's protocol (*New England Biolabs*). Resulting double-stranded oligonucleotides with 5' and 3' overhangs were cloned into the corresponding plasmid upon cleavage by the restriction enzyme BbsI (*New England Biolabs*). Initially, pMSCV-hU6-gRNA-PGK-Puro-T2A-BFP (left in Fig. 7; Chu, Graf, *et al.*, 2016) was

used as backbone plasmid. However, as BFP proved to be immunogenic, the plasmid was replaced by the pMSCV-mAmetrine_U6-gRNA plasmid (right in Fig. 7).

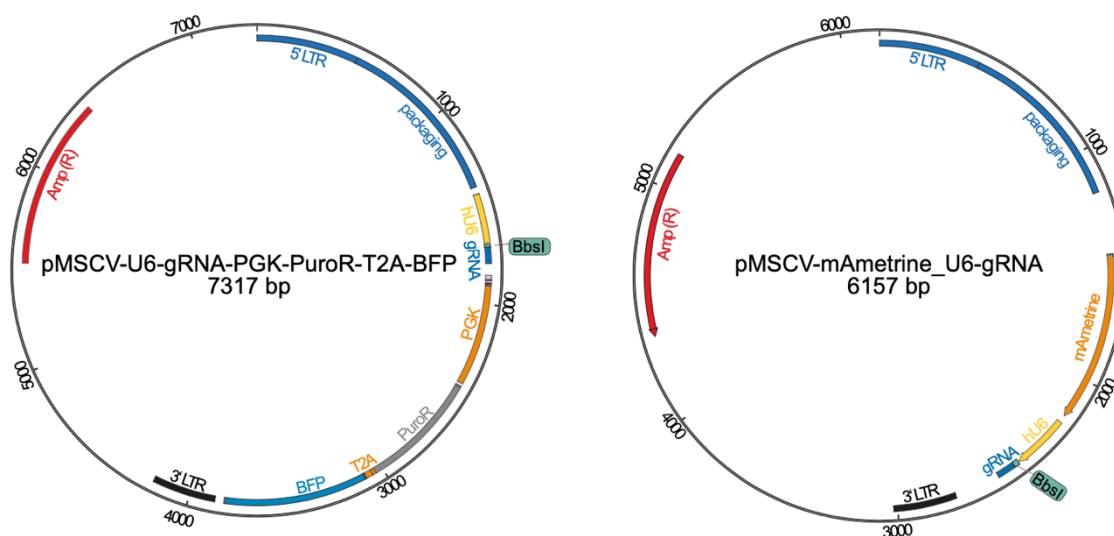


Figure 7 Maps of the eukaryotic expression vectors pMSCV-U6-gRNA-PGK-PuroR-T2A-BFP and pMSCV-mAmetrine_U6-gRNA

Scheme of the pMSCV retroviral expression vectors pMSCV-U6-gRNA-PGK-PuroR-T2A-BFP (left) and pMSCV-mAmetrine_U6-gRNA (right). Both plasmids contain 5' LTR (blue) and 3' LTR (black), packaging (blue), human U6 promoter (hU6, yellow), a BbsI restriction site for introduction of annealed oligos (green), the constant part of the sgRNA (gRNA, blue) and Amp (R). pMSCV-U6-gRNA-PGK-PuroR-T2A-BFP includes BFP as fluorescence reporter (blue) whereas pMSCV-mAmetrine_U6-gRNA includes mAmetrine (orange). pMSCV-U6-gRNA-PGK-PuroR-T2A-BFP additionally contains a phosphoglycerate kinase 1 promoter (PGK, orange), a puromycin resistance (PuroR, grey) and a T2A sequence (orange) in front of the BFP.

Table 2 Oligos for the generation of sgRNAs

Complementary oligos annealed and phosphorylated to generate double-stranded DNA for cloning into the eukaryotic expression vector used for CRISPR-Cas9-mediated knock outs.

Gene of interest	Oligos
Padi4	5'-CACCGCAAACCTGCCGTCCCGGTACA-3'
	5'-AAACTGTACCGGGACGGCAGTTTGC-3'
Sostdc1	5'-CACCGGCCGTCCGAAATGTATTTGG-3'
	5'-AAACCCAAATACATTTTCGGACGGCC-3'
Tigit	5'-CACCGTGCAAGCCTTACCTGTAGCG-3'
	5'-AAACCGCTACAGGTAAGGCTTGAC-3'
Fam43a	5'-CACCGCAGCTCATGCCGGTATACCC-3'
	5'-AAACGGGTATACCGGCATGAGCTGC-3'
Rgs16	5'-CACCGGAGCCAAAGAGTTCAAGACG-3'
	5'-AAACCGTCTTGAAGCTTTGGCTCC-3'
Angptl2	5'-CACCGAGACGGAGGCATCGTGAGCG-3'

	5'-AAACCGCTCACGATGCCTCCGTCTC-3'
Rnf157	5'-CACCGGACCGTGCACTACAAGCGAG-3'
	5'-AAACCTCGTTGTAGTGACGGTCC-3'
Dhrs3	5'-ACCGTTCAGCATACGTGGCAAAA-3'
	5'-AAACTTTTGCCACGTATGCTGGAAC-3'
Hmox1	5'-CACCGCTTCCAGGGCCGTGTAGATA-3'
	5'-AAACTATCTACACGGCCCTGGAAGC-3'
Trpm6	5'-CACCGAGTCTCACCTGACTAAATTG-3'
	5'-AAACCAATTTAGTCAGGTGAGACTC-3'
S100a11	5'-AAACTCACAAGGTATCTGTCCCAC-3'
	5'-CACCGTGGGACAGATACCTTTGTGA-3'
CD40L	5'-CACCGCATCTCCTCACAGTTCAGCA-3'
	5'-AAACTGCTGAACTGTGAGGAGATGC-3'
CD44	5'-CACCGTATGGTAACCGGTCCATCGA-3'
	5'-AAACTCGATGGACCGTTACCATAC-3'
Bcl6	5'-CACCGACCTTAATCGCCTCCGGAGT-3'
	5'-AAACTCCGGAGGCGATTAAGGTC-3'
IL21	5'-CACCGTAAGGTGACGAAGTCTAATC-3'
	5'-AAACGATTAGACTTCGTACCTTAC-3'

2.2.3 Generation of plasmids for genetic manipulation of target cells

Inserts and vectors were digested with appropriate restriction enzymes. Digestion was followed by gel purification using the Gel Extraction Kit (*Qiagen*). Afterwards, products were ligated by using the Quick Ligation Kit (*New England Biolabs*), followed by heat-shock transformation into Top10 competent *E. coli* (produced according to Hanahan *et al.*, 1991). Plasmids were isolated and purified with a Plasmid Mini Kit (*Qiagen*). To verify that the correct insert was contained, test digestion and subsequent Sanger sequencing (carried out at the sequencing core facility of the *Robert Koch Institute* or *Eurofins*) was performed. Additionally, plasmids were isolated using Plasmid Midi or Maxi kits (*Qiagen*) to obtain higher amounts of plasmid DNA.

2.3 Retroviral infection

2.3.1 HEK cell cultures and transfection by calcium phosphate precipitation

Human Embryonic Kidney (HEK) 293T cells were used as packaging cell line for virus particle generation. Cells were cultured in DMEM (*Gibco*) containing 10% Fetal Calf Serum (FCS), 50 μ M β -Mercaptoethanol (β -ME) and 100 μ g/ml penicillin/streptomycin at 37°C (5% CO₂). Cells were detached with trypsin/EDTA and seeded 12-18h before transfection to achieve a confluency of \approx 70%.

As transfection method, calcium phosphate precipitation was used. To this end, the previously generated pMSCV-plasmids were combined with the pECO (encoding for ecotropic envelope proteins) and pCGP plasmids (encoding for *gag* and *pol*, i.e. core structural proteins and protease/transcriptase/integrase, respectively). Equal volumes of a phosphate buffer (2x Hanks' balanced salt solution [50 mM HEPES, 10 mM KCl, 12 mM dextrose, 280 mM NaCl, 1.5 mM Na₂HPO₄, pH 7.05]) were added dropwise to the simultaneously aerated DNA-CaCl₂ (1.25 M) solution. For transfection, the resulting precipitates were then distributed on HEK cells for 4 h. Afterwards, HEK cells were washed with phosphate buffered saline (PBS) and medium was refreshed. Cell culture medium containing retroviral particles was harvested 24 and 48h later (filtered [0.45 μ m] and supplemented with HEPES [10 mM, pH 7.05]). Viral supernatants were shock frozen in liquid nitrogen and stored at -80°C until use.

2.3.2 Retroviral transduction of transgenic T cells

Spleens from the TCR-transgenic donor mice were dissected and prepared under sterile conditions. Spleens were first minced and passed through a 212 μ m sieve to obtain a single cell suspension. After lysis of erythrocytes (ACK-lysis buffer [final composition: 155 mM NH₄Cl, 10 mM KHCO₃, 0.1 mM EDTA, pH 7.2-7.4]) cells were dissolved in ViaCount solution, counted on an EasyCyte capillary flow cytometer (*Millipore*), seeded, and stimulated with *Smarta* peptide (GP₆₁₋₈₀; final concentration 1 μ g/ml). Cells were cultured in RPMI 1640 medium (*Gibco*) supplemented with 10% FCS, penicillin/streptomycin, 1% pyruvate, 1% non-essential amino acids and 50 μ M β -ME and maintained in an incubator (37°C, 5% CO₂, 95% humidity). 24 h after activation, cells were infected with the retroviral supernatant in a centrifugation step at

400 x g and 32°C for 90 min. To increase transduction rate, 8 µg/ml of polybrene was added. Afterwards, cells were washed and cultivated for at least another 40 h before used for the adoptive transfer.

2.3.2.1 *In vitro* polarization of Th₂ subsets

For *in vitro* polarization of Th subsets, TCR-transgenic cells were prepared and cultured under sterile conditions as described above. In addition to stimulation with *Smarta* peptide (GP₆₁₋₈₀; final concentration 1 µg/ml), recombinant IL-4 (10 ng/ml) and blocking antibodies against α-IL-12 (clone C17.8; 5 µg/ml) and α-IFNγ (clone AN18.17.24; 10 µg/ml) were added to the medium to induce Th₂ polarization. To achieve complete polarization, the above-mentioned blocking antibodies were kept in the culture medium over the whole course of the culture.

2.4 Mouse models

2.4.1 Adoptive transfer

For naïve CD4⁺ T cells, 1.25x10⁵ splenic transgenic cells were adoptively transferred by intravenous tail base injection into recipient mice. For pre-activated and retrovirally infected cells, 2.5x10⁵ transgenic cells were transferred. To additionally investigate effects on B cells, co-transfer with transgenic *B1-8i* cells was performed in a subset of experiments. In those experiments, four times as many B cells as compared to T cells were transferred.

Frequency of TCR transgenic T cells (CD4⁺Thy-1.1⁺Vα2-TCR⁺Vβ8-TCR⁺) and transgenic follicular B cells (CD19⁺Ac146⁺CD21^{lo}CD23^{hi}) were determined by flow cytometry. If the cells had not been sorted for fluorescent markers before, cells were first counted with the EasyCyte capillary flow cytometer (*Millipore*).

2.4.2 Immunization methods

2.4.2.1 Subcutaneous immunization

For subcutaneous (s.c.) immunization, animals received 20 µg cognate antigen in Complete Freund's Adjuvant (CFA; *Sigma Aldrich*) or Incomplete Freund's Adjuvant (IFA; *Sigma Aldrich*) at the tail base. A conjugate of *Smarta* peptide (GP₆₁₋₈₀; SM) and nitrophenol (NIP) coupled to mouse serum albumin (NIP-SM-MSA) was used as antigen. In experiments with pre-activated cells, immunization was performed immediately after adoptive transfer. In experiments with naïve cells, immunization was carried out 24 h after the transfer.

2.4.2.2 Intranasal immunization

To study T and B cell interaction in inflamed tissue, an airway inflammation model was used. First, after adoptive transfer at least 4 h were granted for the distribution of the transferred cells throughout the recipients' organism. Subsequently, animals were first anaesthetized by intraperitoneal (i.p.) administration of ketamine (75 mg/kg) and xylazine (4 mg/kg) dissolved in 100 µl PBS, followed by intranasal immunization with 10 µg of cognate antigen and 5 µg LPS. A conjugate of *Smarta* peptide (GP₆₁₋₈₀; SM) and nitrophenol (NIP) coupled to mouse serum albumin (NIP-SM-MSA) was used as antigen. Further immunizations were carried out on days 1, 10 and 13 after transfer.

2.4.3 Tamoxifen administration

For inducible knock outs, *Smarta.CreERT²* animals were used to generate T cells for transfer. CreER^{T2} recombinase activity was induced by i.p. administration of 1.5 mg tamoxifen (*Sigma Aldrich*) per animal dissolved in ethanol and sunflower oil (Feil *et al.*, 2009).

2.4.4 Lymphocyte isolation out of tissue

2.4.4.1 Lymphocyte isolation of draining lymph nodes

After isolation of draining lymph nodes, these were cleared of excess tissue under a binocular and transferred into medium (RPMI 1640 medium, *Gibco*; supplemented with 10% FCS and 33 µg/ml DNase I) via a 70 µm sieve to achieve single cell suspension. After another passage through a 70 µm sieve, cells were dissolved in ViaCount solution and counted by EasyCyte capillary flow cytometer (*Millipore*), before being resuspended at a defined cell concentration in either medium for restimulation or in FACS-PBS (PBS supplemented with 0.25% BSA and 0.1% NaN₃) for flow cytometry.

2.4.4.2 Lymphocyte isolation of lung tissue

Mice were sacrificed by intraperitoneal injection of 60 mg/kg ketamine and 60 mg/kg xylazine followed by blood withdrawal via lung perfusion. After removal of the draining lymph nodes (preparation see chapter 2.4.4.1), lungs were minced using forceps and transferred into medium (RPMI 1640 medium, *Gibco*; supplemented with 10% FCS, 0.5% BSA, 33 µg/ml DNase I and 0.5 mg/ml collagenase D). The tissue was then further minced using gentleMACS™ Dissociator (*Miltenyi Biotec*) followed by collagenase digestion at 37°C for 25 min. After addition of 10 mM EDTA, tissue was incubated at 37°C for 5 min. Again, GentleMACS™ Dissociator was used, and cell suspension was finally passed through a 70 µm sieve to obtain single cell suspensions. Cells were counted using a EasyCyte capillary flow cytometer (*Millipore*) and resuspended at a defined cell concentration either in medium for restimulation or in FACS-PBS for analysis by flow cytometry.

2.5 Fluorescence-activated cell sorting

To obtain and analyze cell populations enriched with defined surface molecules or fluorescent markers, tissue-harvested mixed cell populations were sorted and separated by fluorescence-activated cell sorting (FACS). For cell sorting, either the FACSAria II Flow sorter (*BD Biosciences*) or the SH800S Cell Sorter (*Sony*) was used according to the guidelines published in 2017 (Cossarizza *et al.*, 2017).

2.5.1 Sort of T_{fh} and non-T_{fh} cells for transcriptome analysis

For separating T_{fh} from non-T_{fh} cells, inguinal lymph nodes were prepared as described above (section 2.4.4.1). To enrich transgenic T cells (Thy-1.1⁺), magnetic activated cell sort (MACS) was carried out first. To this end, isolated cells were incubated with anti-Thy-1.1 MicroBeads (*Miltenyi Biotec*) and then separated by a magnetic column. The enriched cell fraction was then stained by fluorochrome-coupled antibodies (Table 3) and FACS-sorted accordingly with a 70 µm nozzle into live⁺dump⁻ CD44⁺Thy- 1.1⁺CXCR5^{hi}PD- 1^{hi} (T_{fh} cells) and live⁺dump⁻ CD44⁺Thy- 1.1⁺ CXCR5⁻PD-1⁻ (non-T_{fh} cells).

2.5.2 Sort of fluorescence⁺ cells

In order to investigate effects on genetically modified cells *in vivo*, cells were sorted before the adoptive transfer according to their fluorescent protein expressed upon retroviral infection. Depending on the used transduction construct, transduction efficiencies of up to 60% for living cells were achieved. Due to the pre-activation with *Smarta* peptide (GP₆₁₋₈₀) and FACS-sorting 3 days after initiation of the culture, nearly all cells were CD4⁺ Thy-1.1⁺. If sorted cells were Th₂ pre-polarized, sorting was performed 4 days after initiation of the culture. Besides viability staining, no additional staining was applied.

2.5.3 Cell staining of surface molecules and intracellular staining

All flow cytometric analyses were performed using the multicolor BDTMLSR Fortessa (*BD Biosciences*) or BDTMSymphony (*BD Biosciences*) flow cytometers according to published guidelines (Cossarizza *et al.*, 2017). Surface staining was performed by adding a mixture of fluorochrome-conjugated antibodies. Before, Fc receptors were blocked by 100 µg/ml 2.4G2 (anti-CD16/32) to prevent unspecific binding. For biotin-labeled antibodies, secondary staining was performed with fluorochrome-conjugated streptavidin. Dead cells were excluded by positive staining with 4',6-diamidino-2-phenylindole (DAPI, 0.33 µM) or propidium iodide (PI, 0.33 µM). For intracellular

stainings, viability staining was performed for 25 min on ice using fluorophore-coupled succinimidyl esters (*Invitrogen*) according to published protocols (Perfetto *et al.*, 2006). For staining of transcription factors, a FoxP3 staining buffer set (*eBioscience*) was used. Otherwise, cells were fixed using 4% paraformaldehyde (PFA) and permeabilized using saponin buffer (5% (w/v) saponin in FACS-PBS).

2.5.3.1 Restimulation of isolated cells

For restimulation of isolated lymphocytes, cells were transferred into medium (RPMI 1640 medium, *Gibco*) supplemented with 10% FCS, penicillin/streptomycin, 1% pyruvate and 1% non-essential amino acids. Cells were restimulated with phorbol 12-myristate 13-acetate (PMA; 1 µg/ml) and ionomycin (10 ng/ml) or *Smarta* peptide (GP₆₁₋₈₀; 1 µg/ml) for 4h at 37°C (5% CO₂). After 1 h of incubation, 5 µg/ml Brefeldin A was added. After 4 h overall stimulation time, cells were further treated as described in 2.5.3.

For data analysis, FlowJo™ Software (*Treestar*) was used. Doublets were excluded via forward and sideward scatter characteristics. Subsequently, dead cells were gated out by excluding DAPI⁺ or PI⁺ cells. Transgenic T cells were further gated as CD8⁻B220⁻CD4⁺Thy-1.1⁺ and transgenic B cells as CD4⁻CD8⁻CD45.2⁻CD45.1⁺. Gates with numbers indicate percentages of cells within the displayed gate.

Methods

Table 3 Fluorochrome-labeled antibodies used for flow cytometry

Antigen, conjugated fluorochrome, and antibody clone for individual used antibodies. Commercially available conjugates were purchased from BioLegend, eBioscience and BD. Otherwise, antibodies were purified from hybridoma cultures and coupled to fluorochromes by standard protocols. The following fluorochromes were used: fluorescein isothiocyanate (FITC), Peridinin-Chlorophyll-Protein (PerCP), Phycoerythrin (PE), PE-Dazzle, PE-Cyanin 7 (PE-Cy7), Allophycocyanin (APC), Alexa Fluor 647 (A647), Alexa Fluor 700 (A700), APC-Cyanin 7 (APC-Cy7), Pacific Blue (PacB), Pacific Orange (PacO), Brilliant Violet 421 (BV421), Brilliant Violet 650 (BV650), Brilliant Violet 711 (BV711), Brilliant Violet 785 (BV785), biotin conjugated and secondary stained with fluorochrome-labeled streptavidin

Specificity	Fluorochrome	Clone
CD4	BV711, BV785	RM4-5
CD8a	PacB, BV711, BV785	53-6.7
CD19	BV711, BV785	6D5
CD21	FITC	7G6
CD23	PE	B3B4
CD25	PE, BV650	PC61
CD38	APC-Cy7, PacB	90
CD44	FITC	IM7.8.1
CD45.1	PerCP, PE-Cy7, Biotin	A20
CD45.2	A700	104
CD45R (B220)	APC-Cy7, PacB, BV711	RA3-6B2
CD62L	FITC, PerCP, A700	Mel-14
CD69	FITC, PE, A647	H1.2F3
CD90.1 (Thy-1.1)	PerCP, A647, A700, PacB	OX-7
CD138	PE, PacB	281-2
CD154 (CD40L)	PE	MR1
CD183 (CXCR3)	BV650	CXCR3-173
CD185 (CXCR5)	BV421, Biotin	L138D7
CD254 (RANKL)	PE, Biotin	IK22/5
CD278 (ICOS)	A647, PacB	MIC-2043
CD279 (PD-1)	PE, PE-Cy7, A647	J43, 29F.1A12
Tigit	A647	GIGD7
V α 2-TCR	FITC	B20.1
V β 8-TCR	Cy5	F23.1
B1-8i BCR	A647	Ac146
GL7	A647	GL7
Bcl-6	PE	K112-91
IgA	PE	mA6E1
IgD	A647	11-26c

IgE	FITC	R35-72
IgG1	PE-Dazzle	A85-1
IgG2a	APC-Cy7	RMG2a-62
IgG2b	A647	RMG2b-1
IgM	FITC, PacB	Bet-2
IL-21	A647	IL-21R-hu IgG

2.6 Next generation sequencing

T_{fh} and non-T_{fh} cells from inguinal lymph nodes were FACS-sorted for subsequent gene expression analysis. For RNA isolation, a RNeasy Micro Kit (*Qiagen, Hilden, Germany*) was used and RNA quality was determined by a 2100 Bioanalyzer (*Agilent Technologies, Santa Clara, CA, USA*). RNA-sequencing was then carried out in cooperation with the group of Mir-Farzin Mashreghi (Deutsches Rheuma-Forschungszentrum). A library was created using the Nextera XT Library Preparation Kit (*Illumina, San Diego, CA, USA*) or, for samples with high RNA content, the TruSeq® Stranded Total RNA Sample Preparation Kit (*Illumina*). Paired end sequencing with 2 x 75 nucleotides was performed on a NextSeq500 device (*Illumina*). Sequence reads were mapped to the mouse GRCm38/mm10 genome with TopHat2 (Kim *et al.*, 2013) in very-sensitive settings for Bowtie2 (Langmead & Salzberg, 2012). Gene expression was quantified using feature counts (Liao *et al.*, 2014) and DESeq2 (Love *et al.*, 2014). Gene expression between T_{fh} and non-T_{fh} cells, or T_{fh} cells of different groups was considered significant if the p-value was ≤ 0.05 and log₂ fold-change was > 0.37 (analyzed by Wald test in the DESeq2 package and corrected for multiple testing according to Benjamini & Hochberg, 1995).

2.7 Proof of Cas9 knock out efficiency

Cas9-mediated knock out efficiency was quantified in cultured Cas9-transgenic splenocytes (chapter 2.3.2) retrovirally transduced with corresponding plasmids. Since it has been shown that, depending on the quality of the used sgRNA, optimal knock out efficiency can only be detected after approximately 5 days (Yuen *et al.*, 2017), the cells were kept in culture for 5 days. Fluorescence⁺ retrovirally infected cells were then sorted and DNA was isolated using the DNeasy Blood & Tissue Kit (*Qiagen*).

2.7.1 T7 Endonuclease Assay

Target genes were amplified by PCR, for which Q5 polymerase (*New England Biolabs*) and the protocol according to the manufacturer's instructions were used. Subsequently, the PCR products of WT and KO DNA were mixed 1:1 and processed according to the manufacturer's instructions (T7 Endonuclease I, *New England Biolabs*). Finally, successful knock out was tested for via gel electrophoresis.

2.7.2 Sanger sequencing

Target genes were amplified using Q5 polymerase according to the manufacturer's instructions (*New England Biolabs*). PCR products were purified using the QIAquick Gel Extraction Kit (*Qiagen*) and cloned into the intermediate plasmid pJET1.2 (CloneJET PCR Cloning Kit, *Thermo Fisher Scientific Inc.*) according to the manufacturer's instructions. Plasmids were further prepared as described in chapter 2.2.3. and in order to make a quantitative statement about the KO efficiency, for each target gene at least 10 clones were picked and subjected to Sanger sequencing.

2.8 Statistics

GraphPad Prism (*GraphPad Software, Inc.*) was used for statistical analysis. Unless otherwise specified, if data were normally distributed (tested by Anderson-Darling test, D'Agostino-Pearson omnibus normality test, Shapiro-Wilk normality test and Kolmogorov-Smirnov normality test) unpaired t-test were performed (Welch's t-test for unequal variances). Otherwise, the Mann-Whitney U test was performed for non-parametric data. For the statistical analysis of more than two groups one-way ANOVA (for normally distributed data) or Kruskal-Wallis test was performed. Subsequently, the resulting p-values were corrected using the two-stage linear step-up procedure of Benjamini, Krieger and Yekutieli and Holm-Šídák. In bar graphs, individual animals are represented by symbols while bar length reflects the mean. p-values < 0.05 were considered significant (* p < 0.05, ** p < 0.01, *** p < 0.001, ns p > 0.05).

3 Results

3.1 Screening for new T_{fh} signature target genes

The aim of this thesis was the identification of new genes involved in the generation and maintenance of T_{fh} cells. To identify these so called T_{fh} signature genes, a transcriptome analysis of sorted T_{fh} and Non-T_{fh} cells utilizing a tail base immunization model and a chronic airway inflammation model was performed (Figure 8A, bright yellow and orange). The analysis revealed the 300 most specifically up- or downregulated genes in T_{fh} cells.

To constrain the analysis to setup- and mouse model-independent genes, these 300 candidate genes were further compared to two published transcriptome analyses generated from different mouse models, organs and immunization methods (Linterman *et al.*, 2011; X. Liu *et al.*, 2012, Figure 8A). This comparison revealed 221 of the 300 initial genes additionally present in at least one of the published transcriptome analyses. These 221 genes were then further screened for their reported function based on available literature (detailed analysis is depicted in Table 4 and 6, literature research via <https://www.uniprot.org>, <https://scholar.google.com>, <https://www.genecards.org>, and <https://pubmed.ncbi.nlm.nih.gov>). The 19 most promising genes (Figure 8B) were further investigated. Functional analysis was achieved by targeted overexpression or knock out of the respective genes and investigation of potential effects on T_{fh} cell populations *in vivo*. Specifically, genes with negative logFC were overexpressed (*Ccr2*, *Plac8*, *Fam129b*, *Smad7*, *Cish*, *Cxcr6* and *Rara*; cf. chapter 3.3.1 and 3.3.1.1), whereas genes with positive logFC were knocked out (*Padi4*, *Sostdc1*, *Tigit*, *Fam43a*, *Rgs16*, *Angptl2*, *Rnf157*, *Dhrs3*, *Hmox1*, *Trpm6*, *S100a11* and *Tnfsf11*; see chapters 3.2, 3.3.3, and 3.3.3.1).

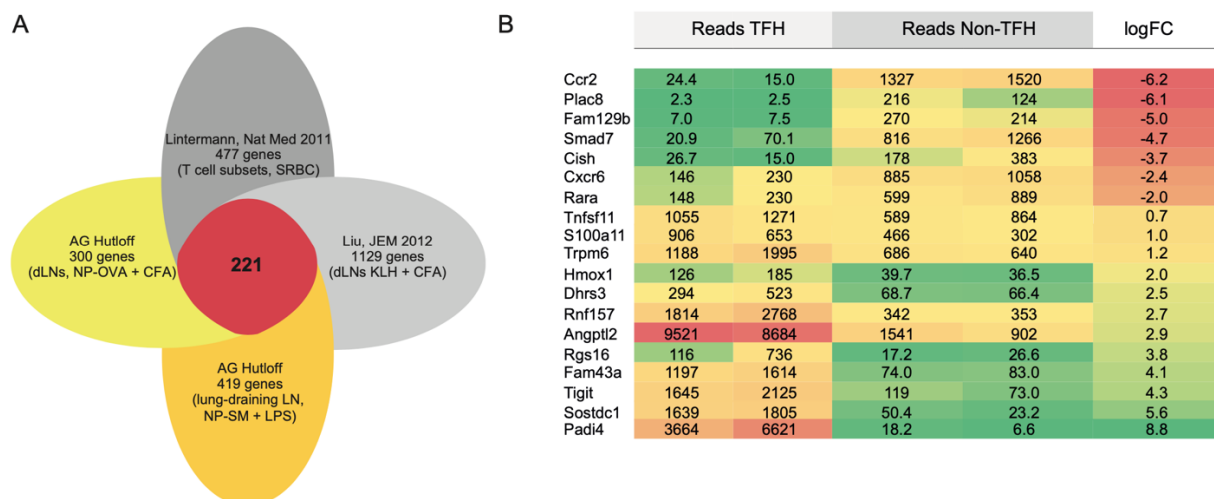


Figure 8 Comparison of four different T_{fh} signature gene transcriptome analyses reveal 19 genes of interest

A) Venn diagram of 300 genes up- or downregulated in T_{fh} cells compared to Non- T_{fh} cells (yellow: peptide-immunization with ovalbumin coupled to nitrophenol (NP-OVA) and CFA as adjuvant, subcutaneous immunization and analysis of draining lymph nodes (dLN); orange: airway inflammation, intranasal peptide-immunization with Smarta peptide coupled to nitrophenol (NP-SM) and LPS as adjuvant, analysis of lung and lung-draining lymph nodes) were compared to transcriptome data including other experimental setups, organs and immunization methods (Linterman et al., 2011 in dark grey for intraperitoneal injection of sheep red blood cells (SRBC), analysis of spleen; Liu et al., 2012 in bright grey for subcutaneous immunization with keyhole limpet hemocyanin (KLH) and CFA as adjuvant and subsequent analysis of dLN). The comparison revealed 221 genes at least occurring in one additional data set. (B) Table of the 19 most promising T_{fh} signature genes out of 221 differentially regulated T_{fh} cell genes identified in (A) adopted for subsequent analysis. Reads of T_{fh} and Non- T_{fh} as well as logarithmic fold change (logFC) are shown (Methods section 2.6 for a detailed description of the transcriptome analysis utilized in this study).

The protein-coding gene *Tnfsf11* had a significantly higher expression in T_{fh} cells (logFC 0.7) compared to non- T_{fh} cells. Although *Tnfsf11* was not the most differentially regulated gene within the group of 19 selected genes of interest, based on preliminary work from the Hutloff group and the published involvement of the encoded protein in the immune system, *Tnfsf11* was regarded a promising candidate and first subjected to the adopted experimental framework. To analyze the function of this gene and the corresponding protein, an inducible *Tnfsf11* knock out mouse was established.

3.2 The T_{fh} signature gene *Tnfsf11* is highly upregulated on T_{fh} cells but not involved in T_{fh} cell generation and maintenance

3.2.1 Early *Tnfsf11*-depletion does not alter T_{fh} cell and B_{GC} cell generation

The gene *Tnfsf11* encodes the protein Receptor Activator of NF- κ B Ligand (RANKL). RANKL belongs to the TNF cytokine family and is also known as TRANCE, CD245, OPGL, or ODF. In combination with its receptor RANK and the decoy receptor OPG, it was first described in the late 1990s (Anderson *et al.*, 1997; Wong *et al.*, 1997) and has since then been shown in multiple studies to play a major role in bone metabolism as well as the immune system (Leibbrandt & Penninger, 2010; Ono *et al.*, 2020).

Besides its pivotal role in lymph node development, RANKL is highly expressed on T cells upon TCR stimulation. Moreover, the expression of its receptor RANK on DCs is initiated by T cell/CD40L-induced stimulation (Anderson *et al.*, 1997). Thus, RANKL stimulation might promote T cell proliferation and T cell/DC interaction (Anderson *et al.*, 1997; Leibbrandt & Penninger, 2010; Mueller & Hess, 2012; Ono *et al.*, 2020). Moreover, RANKL/RANK signaling has been shown to contribute to autoimmune diseases such as systemic lupus erythematoses, rheumatoid arthritis, myasthenia gravis, and vitiligo, and enhanced RANK/RANKL signaling has been detected in various B cell lymphomata (Alankus *et al.*, 2020; Carmona-Fernandes *et al.*, 2011; Fonseca *et al.*, 2005; Jin *et al.*, 2016; Renton *et al.*, 2015).

A recent transcriptomic analysis of T_{fh} and Non-T_{fh} cells revealed an increased expression of *Tnfsf11* in T_{fh} cells and uncovered a link between *Tnfsf11* and *Bach2*, an antagonistic T_{fh} cell regulator (Lahmann *et al.*, 2019). Moreover, a significantly reduced number of transgenic T cells and T_{fh} cells in shRNA-mediated knock out experiments targeting RANKL *in vivo* was found (unpublished data). Thus, RANKL imposed as a likely candidate for the regulation of T_{fh} cell generation and maintenance.

Previous knock down of the T_{fh} signature gene was induced by shRNA, which inherently 1.) does not lead to complete absence of the targeted protein, 2.) poses the risk of unspecific targeting and hence unspecific knock down (Boettcher & McManus, 2015; D. D. Rao *et al.*, 2009), and 3.) is methodically constrained to constitutive knock down. To circumvent these limitations, *Smarta.CreER^{T2}/RANKL^{fl/fl}* mice were generated to allow for a specific and inducible knock out of floxed RANKL alleles. *Smarta.CreER^{T2}/RANKL^{fl/fl}* mice harbor the *Smarta*-specific TCR and ubiquitously

express estrogen receptor-dependent Cre recombinase (CreER^{T2}). Upon application of the estrogen-receptor agonist tamoxifen, cytosolic CreER^{T2} translocates into the nucleus and cleaves the floxed *Tnfsf11* gene, leading to its knock out. For control experiments, *Smarta.CreER^{T2}* wildtype animals were used (referred to as wt/wt below).

First, the contribution of RANKL to T_{fh} cell generation and the early phase of the immune response was investigated. To this end, transgenic donor animals were treated intraperitoneally with tamoxifen 11, 9, and 8 days before transfer of donor T cells to recipient animals in order to deplete RANKL in transferred cells. *Tnfsf11* knock out efficiency of the tamoxifen-treatment paradigm was verified in a fraction of donor cells cultured and stained for RANKL protein, revealing a near-complete knock out of the targeted gene in donor cells prior to transfer (mean fluorescence intensity (MFI) RANKL; wt/wt 2555, fl/fl 224; Figure 9A). T cells were co-transferred with *B1-8i* cells into recipient animals followed by s.c. immunization (NIP-SM-MSA in IFA) and i.p. tamoxifen administration 24 h after transfer. 8 days after transfer, draining LNs (dLN) were analyzed by flow cytometry (Figure 9A). An increased expression of the RANKL molecule on wt/wt T_{fh} cells compared to non-T_{fh} cells (MFI RANKL; non-T_{fh} 213.3 ± 22.85, T_{fh} 969.3 ± 102.4; mean ± SD; p = 0.0001) confirmed previous results from transcriptome analysis (cf. Figure 9B). However, knock out of RANKL prior to immune response did not have an effect on the proliferation of transgenic T cells (% Thy-1.1⁺; wt/wt 6.38 ± 1.75, fl/fl 6.16 ± 1.24; mean ± SD; p= 0.8011; Figure 9C), nor did it affect T_{fh} frequency as defined by CXCR5⁺ PD-1⁺ positives of all Thy-1.1⁺ cells (% T_{fh}; wt/wt 45.20 ± 5.83, fl/fl 40.44 ± 7.61; mean ± SD; p= 0.3007; Figure 9C and D). Moreover, early RANKL knock out did not affect the capacity of B cell help, and percentages of transgenic B cells (% CD45.1⁺; wt/wt 1.53 ± 0.37, fl/fl 1.47 ± 0.37; mean ± SD; p= 0.8029), B_{GC} cells (defined as CD38^{lo}GL7^{hi}; % of wt/wt 39.27 ± 7.45, fl/fl 40.26 ± 10.24; mean ± SD; p= 0.8519) and plasma cells (defined as CD19^{lo}CD138⁺; % of wt/wt 6.68 ± 3.27, fl/fl 8.70 ± 4.49; mean ± SD; p= 0.3914) were unaffected by RANKL knock out (Figure 9C and D).

Thus, RANKL did not contribute to early T_{fh} cell development and concomitant B cell help during the early immune response.

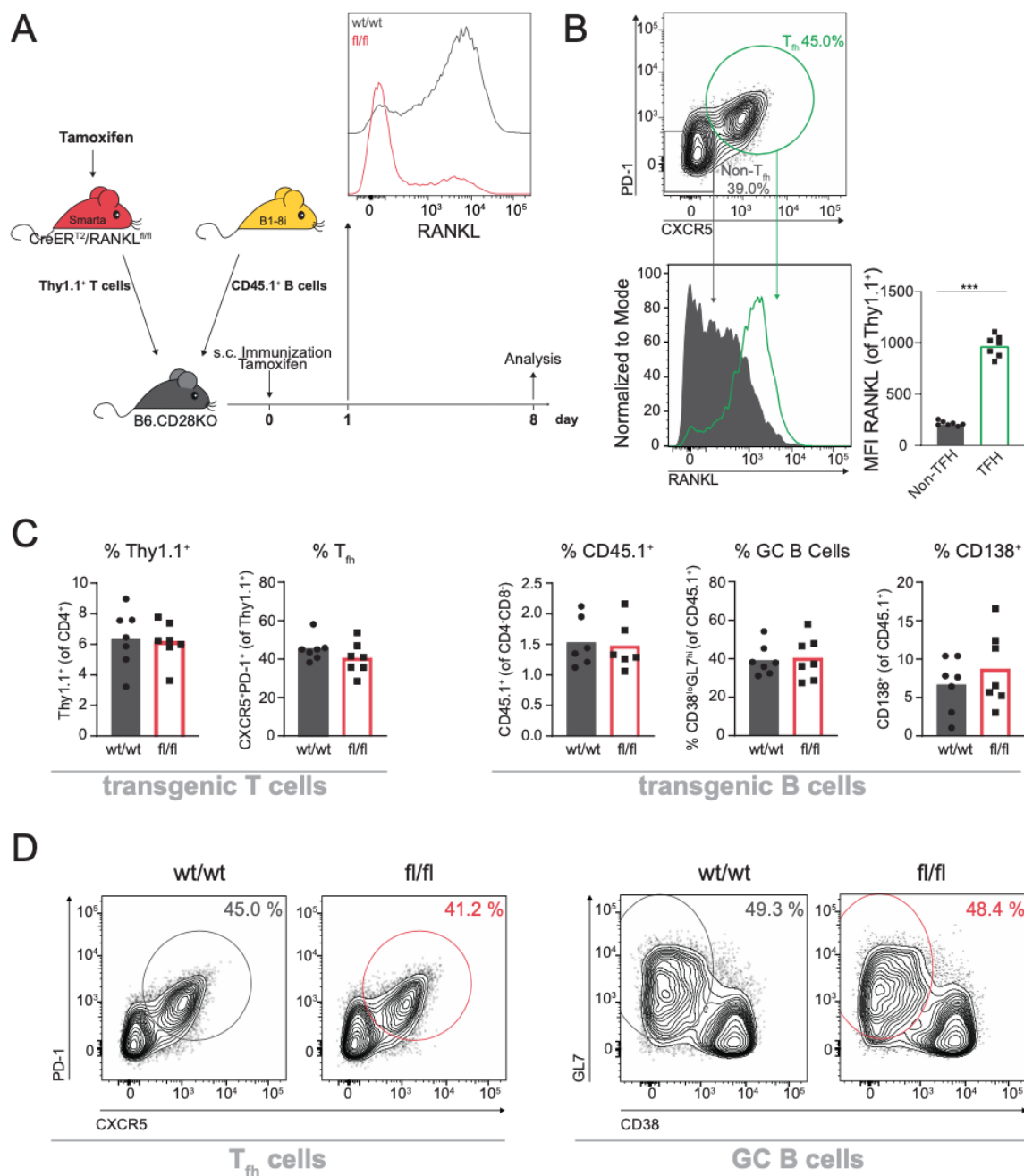


Figure 9 Early RANKL knock out does not affect T_{fh} cell development and B cell help during the immune effector phase

(A) Scheme of the experimental setup. Transgenic T cells of tamoxifen-treated *Smarta.CreERT²/RANKL^{fl/fl}* (*fl/fl*) mice or control mice (*Smarta.CreERT²*, referred to as *wt/wt*) were co-transferred with transgenic B cells from *B1-8i* mice into *B6.CD28 KO* recipients. Additionally, recipients were tail base-immunized and tamoxifen-treated. A fraction of transferred T cells was cultured for 24 h and analyzed by flow cytometry for verification of RANKL KO. Strong knock out of RANKL was selectively achieved in *fl/fl* animals with this protocol. (B) Representative contour plot of T_{fh} staining and histogram of RANKL in *wt/wt* animals. RANKL expression was significantly higher in T_{fh} cells compared to non- T_{fh} cells as assessed by analysis of RANKL MFI. (C) Percentage of marker-expressing transgenic T cells ($Thy-1.1^+$ and $CXCR5^+ PD-1^+$) and transgenic B cells ($CD45.1^+$, $CD38^{lo} GL7^{hi}$, and $CD19^+ CD138^+$) of all T/B cells in *wt/wt* compared to *fl/fl* mice (grey and red, respectively). (D) Contour plots of representative T_{fh} cell

Results

stainings (left, CXCR5⁺ PD-1⁺) and B_{GC} cell stainings (right, CD38⁺ GL7^{hi})⁺ in wt/wt compared to fl/fl animals (color code as in C). Bar graphs as overall group mean, markers as individual animals, comparison by unpaired t-test or Mann-Whitney-U-test, * p < 0.05, ** p < 0.01, *** p < 0.001, ns p > 0.05, 7 animals were analyzed for each group.

3.2.2 *Tnfsf11*-depletion in primed T cells affects memory T_{fh} cell maintenance in draining lymph nodes

Previous studies on RANKL had proposed a role of RANKL/RANK interaction during ongoing T cell activation and differentiation (Leibbrandt & Penninger, 2010). While for T cell priming the T cell: DC interaction via CD40L/CD40 seemed to be important (Anderson *et al.*, 1997), concomitant RANKL/RANK binding was hypothesized to enhance this interaction, thereby resulting in an altered cytokine expression and subsequent altered immune response (Leibbrandt & Penninger, 2010).

Since RANKL KO during early T cell activation and priming did not affect T_{fh} cell generation (Fig. 9), long-term effects of RANKL depletion on T_{fh} cell maintenance and memory T_{fh} cell generation were investigated in initiated T cells.

A clear separation of effector and memory cells in models with prolonged antigen presence, as in the s.c. tail base immunization paradigm with water-in-oil emulsion + Freund's Adjuvant used here, is difficult to achieve. However, a comparable experiment in our laboratory revealed a remaining fraction of ≈ 10% fraction of Ki-67⁺ transgenic cells in lymph nodes and spleen > d40, indicating a memory status (i.e. a resting state, data not shown) for the majority of cells according to proliferation, transcription and mobility criteria (Okhrimenko *et al.*, 2014). Therefore, an analysis at ≥ d40 was performed to analyze memory T_{fh} cells, which were defined as CXCR5⁺PD-1⁺. Since the vast majority of memory T_{fh} cells is located in spleen and dLN (Weber *et al.*, 2012), these organs were analyzed.

To do so, transgenic T cells and B cells from donor animals (*Smarta.CreER^{T2}/RANKL^{fl/fl}* or *Smarta.CreER^{T2}* and *B1-8i* animals, respectively) without prior tamoxifen treatment were co-transferred into *B6.CD28KO* recipients. Tail base immunization was performed 24 h after transfer and, to study the effect of RANKL deficiency after initial T cell priming, tamoxifen was administered three days after transfer. For analysis of memory T_{fh} cells, draining LNs and spleens were harvested at day 43 post-immunization and transgenic T cells were analyzed via flow cytometry (Figure 10A). Differences in the overall number of transgenic T cells (Thy-1.1⁺) were

neither detectable in dLNs nor spleens of wildtype versus KO animals (dLN: wt/wt 1.41 ± 1.07 , fl/fl 1.10 ± 0.81 , $p=0.4431$; spleen: wt/wt 1.12 ± 0.84 , fl/fl 0.85 ± 1.09 , $p=0.5594$; mean \pm SD; data not shown).

Memory T_{fh} cells (CXCR5⁺PD-1⁺) showed a significant $\approx 30\%$ reduction in cell frequency in dLNs of RANKL-depleted animals (% memory T_{fh} ; wt/wt 27.7 ± 10.65 , fl/fl 19.61 ± 2.98 ; mean \pm SD; $p=0.0498$). This effect was not observed in the spleen of RANKL KO animals where memory T_{fh} cell frequency trended towards higher values compared to control animals (% memory T_{fh} ; wt/wt 9.57 ± 6.86 , fl/fl 17.25 ± 10.29 , $p=0.1541$; mean \pm SD; Figure 10C).

In addition to the classic T_{fh} markers CXCR5 and PD-1, further markers associated with memory T cell status were investigated: CD44 as a marker for antigen-experienced T cells, CD62L and CD69 as markers for homing phenotypes, and CXCR3 as a marker for migratory behavior.

Firstly, as expected nearly all transgenic T cells expressed CD44 in both groups. Nevertheless, there was a downregulation of CD44 in the spleen of RANKL-depleted animals (% CD44⁺; wt/wt 98.31 ± 1.74 , fl/fl 94.14 ± 3.33 , $p=0.0125$; mean \pm SD).

Secondly, memory T_{fh} cells were characterized by the expression of residence-associated genes coding for CD62L and CD69 (Catron *et al.*, 2006; Künzli *et al.*, 2020; Pennock *et al.*, 2013), genes linked to memory cells tissue localization and retention (Weber *et al.*, 2012) enabling homing to secondary lymphoid organs and proliferation into effector cells upon antigen reencounter (Sallusto *et al.*, 2004). RANKL-depletion led to a significant upregulation of CD62L in dLN (% CD62L⁺; wt/wt 6.66 ± 2.03 , fl/fl 16.16 ± 6.19 , $p=0.0058$; mean \pm SD) while no differences in CD69 expression were detected (Figure 10C). Ongoing ICOS signaling is associated with maintenance and survival of T_{fh} memory cells (Künzli *et al.*, 2020; Latham *et al.*, 2020) but was not influenced by RANKL depletion (Figure 10C).

Finally, the impact of RANKL KO on the expression of the Th_1/Th_{17} -associated, especially splenic memory T_{fh} cell-related chemokine receptor CXCR3 was quantified (Asrir *et al.*, 2017). While no differences were observed in dLNs, CXCR3 expression was significantly reduced in spleens of RANKL KO animals (% CXCR3⁺; wt/wt 62.17 ± 10.10 , fl/fl 32.70 ± 20.35 , $p=0.0050$; mean \pm SD).

In summary, in contrast to the lack of an effect of RANKL KO on T_{fh} cell generation and the early immune phase, RANKL KO after T_{fh} cell priming reduced memory T_{fh} cell formation in lymph nodes. This was accompanied by higher lymph nodal expression

Results

of CD62L and lower splenic expression of the migration marker CXCR3 compared to wildtype littermates.

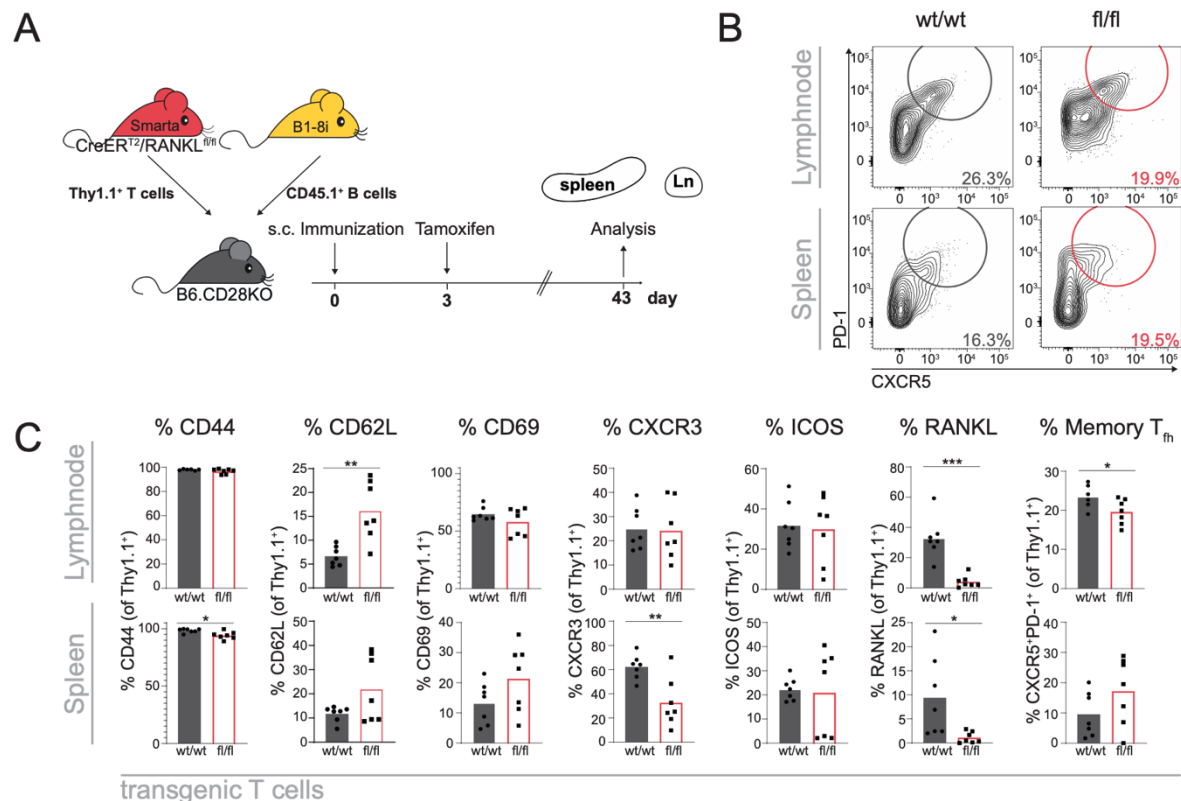


Figure 10 RANKL depletion affects memory T_{th} cell numbers by phenotypical change of homing and migration markers

(A) Scheme of the experimental setup. Transgenic T cells of KO animals (Smarta. $CreER^{T2}/RANKL^{fl/fl}$, subsequently fl/fl) and control animals (Smarta. $CreER^{T2}$, subsequently wt/wt) as well as transgenic B cells (B1-8i) were co-transferred into B6.CD28KO recipients. Animals received s.c. immunization 24 h post-transfer and tamoxifen-administration 3 days post-transfer. DLN and spleen were analyzed at day 43. (B) Contour-plots of representative memory T_{th} cells percentages (CXCR5⁺PD-1⁺) of wt/wt (grey) and fl/fl (red) mice in dLNs and spleen. (C) Marker expression of CD44, CD62L, CD69, CXCR3, ICOS, RANKL, and counts of memory T_{th} cells (wt/wt in grey, fl/fl in red) in dLN (upper panels) and spleen (lower panels). RANKL expression (% RANKL⁺) was significantly reduced in fl/fl mice compared to wt/wt (dLN: wt/wt 32.93 ± 13.6 , fl/fl 4.10 ± 4.03 , $p=0.0010$; spleen: wt/wt 9.41 ± 8.2 , fl/fl 1.13 ± 1.18 , $p=0.0383$; mean \pm SD). Bars provide mean values, symbols represent individual animals, 7 animals were analyzed for each group. Statistical testing with unpaired t-test or Mann-Whitney-U-test (* $p < 0.05$, ** $p < 0.01$, *** $p < 0.001$, ns $p > 0.05$).

3.2.3 T cell-specific *Tnfsf11*-depletion does not affect transgenic T and B cell migration behavior in inflamed lung tissue

T cell: B cell interaction not only occur in secondary lymphoid organs (SLOs), but also in inflamed tissue. In contrast to highly organized SLOs, tissue infiltrates rather form unstructured, loose aggregates characterized by the absence of FDCs or clearly separated T and B cell zones (Hutloff, 2018). Involved CD4⁺ T cells share T_{fh} cell features, such as PD-1, ICOS, CD40L, or IL-21 expression, but lack characteristic markers such as Bcl-6 and CXCR5 (D. A. Rao *et al.*, 2017; Vu Van *et al.*, 2016). These so called T_{fh}-like or peripheral T helper cells have the ability to efficiently promote B cell differentiation (Hutloff *et al.*, 2004; Manzo *et al.*, 2008; D. A. Rao *et al.*, 2017; Vu Van *et al.*, 2016) and were shown to contribute to chronic inflammation in autoimmune diseases or allergy (Bocharnikov *et al.*, 2019; Coquet *et al.*, 2015).

We have previously successfully established a chronic airway inflammation model that allowed the study of T cell: B cell cooperation in inflamed tissue. In this model, adoptive transfer of transgenic T and B cells into recipient mice was followed by repeated intranasal immunization (see also Methods section 2.4.2.2), enabling the characterization of T_{fh}-like and GC-like B cells in the inflamed lung in direct comparison to classical T_{fh} and B_{GC} cells in the lung-draining LN.

Interestingly, adopting the chronic airway inflammation model for transcriptome analysis of T cells in lung and lung-draining lymph node (Figure 8) had previously shown strong RANKL expression within the T_{fh} and T_{fh}-like population (data not shown). Moreover, several studies have reported an involvement of the RANKL/RANK axis in tissue inflammation (Bando *et al.*, 2018; Gregorczyk & Maślanka, 2020; Guerrini *et al.*, 2015; Loser *et al.*, 2006; Shimamura *et al.*, 2014). While an immunoregulatory function was attributed to RANKL/RANK signaling in most studies, Guerrini and colleagues (Guerrini *et al.*, 2015) and Gregorczyk and Maslanka (Gregorczyk & Maślanka, 2020) found opposing effects attributing a positive influence on the migratory behavior of pro-inflammatory T cell subsets in the central nervous system and in an allergy model, respectively. Thus, we aimed to further investigate the role of RANKL in chronic tissue inflammation.

To this end, tamoxifen-treated T cells of *Smarta.CreER^{T2}/RANKL^{fl/fl}* animals (fl/fl) or *Smarta.CreER^{T2}* animals (wt/wt) were co-transferred with transgenic B cells (*B1-8i*) into *C57BL/6* recipients (tamoxifen treatment similar to early immune phase scheme,

i.e. treatment of donor animals on day 14, 11 and 9 pre-transfer, tamoxifen treatment of recipients on transfer day, Figure 9). To evoke chronic airway inflammation, intranasal immunization with cognate antigen (NIP-SM-MSA + LPS) was performed according to the standard protocol (see below, for details also see Methods section 2.4.2.2) and lung and lung-dLN were dissected 17 days post-transfer (Figure 11A). RANKL depletion did not affect numbers of transgenic T cells in lung-dLNs (% Thy-1.1⁺, wt/wt 12.19 ± 7.67, fl/fl 11.91 ± 8.67, mean ± SD, p= 0.9553) or lungs compared to wt/wt controls (% Thy-1.1⁺, wt/wt 57.45 ± 11.65, fl/fl 59.28 ± 20.44, mean ± SD, p= 0.8524). Similarly, the frequency of transgenic B cells was unaffected in the knock out compared to the control condition (% CD45.1⁺, lung-dLN: wt/wt 0.78 ± 0.44, fl/fl 1.12 ± 0.65, p= 0.3411; lung: wt/wt 2.77 ± 0.57, fl/fl 2.35 ± 0.74, p= 0.3000, mean ± SD, Figure 11B).

Next, T_{fh} (CXCR5⁺PD-1⁺) and T_{fh}-like (PD-1^{hi}) cells were examined in lung-dLNs and lungs, respectively, but no differences in frequency were noted in fl/fl mice compared to wt/wt littermates (% T_{fh}: wt/wt 26.15 ± 7.61, fl/fl 30.00 ± 11.46, p= 0.5087; % T_{fh}-like: wt/wt 12.20 ± 1.62, fl/fl 16.75 ± 5.1, p= 0.1058, mean ± SD, Figure 11C upper part).

In parallel, the homing markers CD62L and CD69, as well as the lymphocyte migration marker CXCR3 were examined (Figure 11D). CD62L was lost during lung tissue preparation due to shedding during the 37°C incubation step, prohibiting analysis of CD62L in lung tissue. CXCR3 however was significantly upregulated in lung T cells of fl/fl mice (% CXCR3⁺; wt/wt 59.02 ± 9.37, fl/fl 74.33 ± 6.74; mean ± SD; p= 0.0281, Figure 11D). In dLNs, no phenotypic changes in CD62L and CD69 expression were observed in fl/fl compared to wt/wt animals.

Finally, B cell helper capacity was examined by quantification of B_{GC} cell (CD38^{lo}GL7^{hi}) and PC (CD19^{lo}CD138⁺) frequencies in lungs and lung-dLNs (Figure 11C lower part). While RANKL depletion did not affect B_{GC} cell frequency in lung-dLN and lung, PC frequencies were significantly reduced in lungs (% CD138⁺; wt/wt 35.9 ± 9.75, fl/fl 21.34 ± 9.32; mean ± SD, p=0.0245; Figure 11C).

In summary, T cell-specific RANKL depletion did not affect antigen-specific T and B cell migration during chronic airway inflammation. No phenotypic changes or effects on B cell help were found in lung-dLNs. In contrast, in lung tissue RANKL KO increased CXCR3 expression while PC generation was impaired.

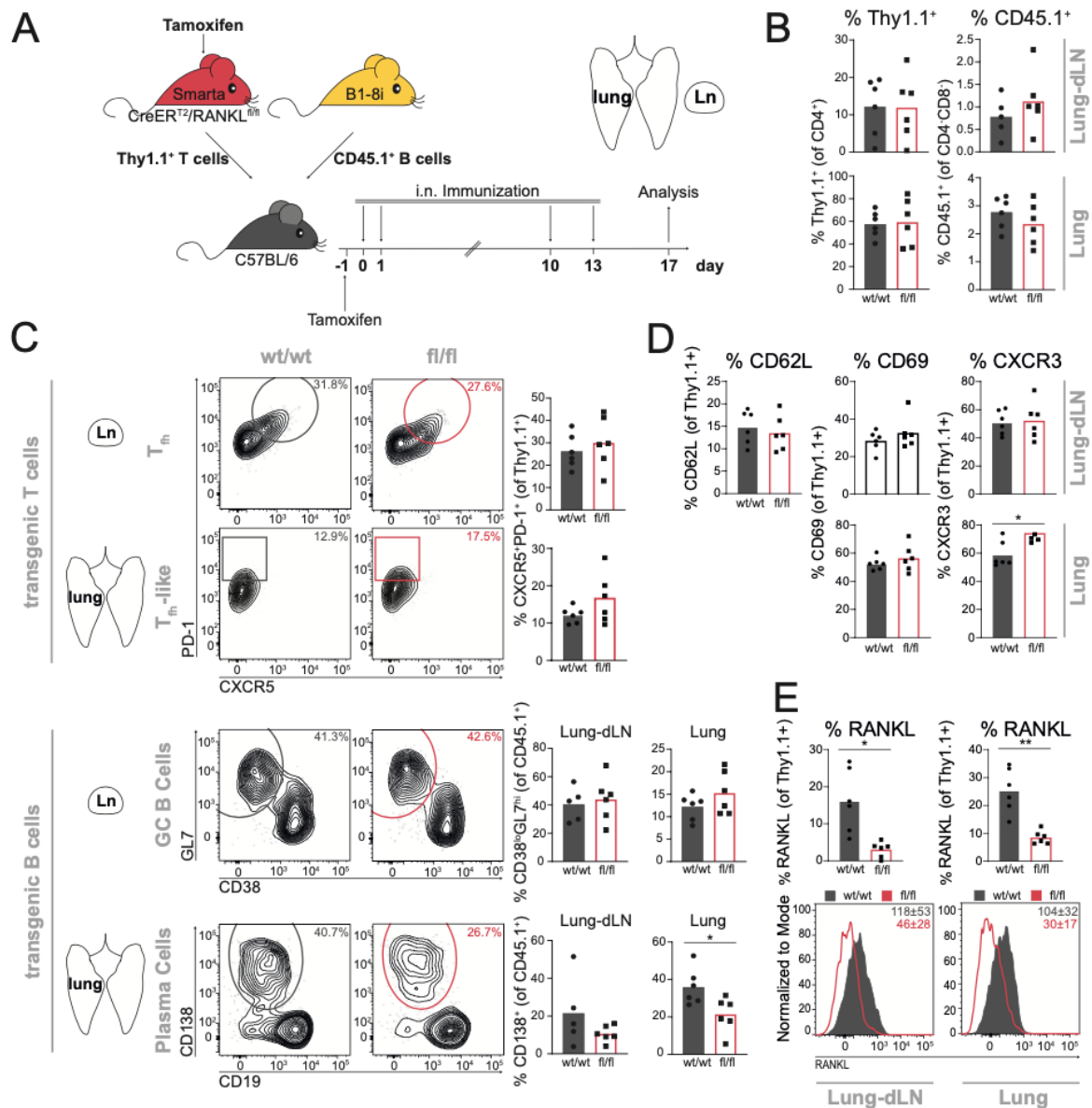


Figure 11 Early T cell-specific RANKL-depletion limits B cell differentiation and changes chemokine receptor expression in chronically inflamed lung tissue

(A) Schematic overview of the experimental setup. Tamoxifen-treated *Smarta.CreERT²/RANKL^{fl/fl}* (*fl/fl*) or *Smarta.CreERT²* wildtype (*wt/wt*) cells were co-transferred with transgenic B cells (*B1-8i*) into *C57BL/6* recipients followed by tamoxifen treatment (d-1). Intranasal immunization with NIP-SM-MSA + LPS was started one day post transfer (defined as day 0) and repeated 1, 10, and 13 days after transfer. Lungs and lung-dLNs were analyzed on day 17 post-transfer. (B) Frequencies of transgenic T cells (*Thy1.1⁺*, left panels) and transgenic B cells (*CD45.1⁺*, right panels) of lung-dLNs (top) and lungs (bottom; *wt/wt* in grey, *fl/fl* in red). (C) Top: Contour-plots of representative stainings of *T_{fh}* and *T_{fh}-like* cells of lung-dLNs and lungs, bar graphs visualize quantification. *T_{fh}*/*T_{fh}-like* cells were defined as *CXCR5⁺PD-1⁺* and *PD-1^{hi}*, respectively (upper part; *wt/wt* in grey, *fl/fl* in red). Bottom: Contour-plots of representative *B_{GC}* cell (*CD38^{lo}GL7^{hi}*) and *PC* (*CD19⁺CD138⁺*) stainings, quantification is displayed in bar graphs (*wt/wt* in grey, *fl/fl* in red). (D) Expression of *CD62L*, *CD69*, and *CXCR3* in T cells of dLNs and lungs (*wt/wt* in grey, *fl/fl* in red). (E) Percentage of *RANKL⁺* transgenic T cells in lung-dLNs and lungs (top) supported by representative histograms (bottom). Bars depict mean, symbols represent individual animals. 6 animals were analyzed per group.

Statistical analysis was performed using unpaired t-test or Mann-Whitney-U-test (* $p < 0.05$, ** $p < 0.01$, *** $p < 0.001$, ns $p > 0.05$).

3.2.4 Transcriptome analysis of *Tnfsf11*-depleted T_{fh} and non- T_{fh} cells reveals differentially regulated genes

In a final experiment, a transcriptome analysis of T_{fh} cells from RANKL KO and WT animals was performed to identify changes on the transcriptional level upon interference with RANKL in T_{fh} cells. *Smarta.CreER^{T2}/RANKL^{fl/fl}* (fl/fl) or *Smarta.CreER^{T2}* (wt/wt) cells were transferred into *B6.CD28KO* animals, followed by s.c. immunization. Pre-tests verified successful RANKL KO already 36h after tamoxifen administration (data not shown). Therefore, an analysis 36 h post-transfer was chosen to identify differential T_{fh} cell gene expression upon RANKL depletion at early stages. For transcriptome analysis, tamoxifen was administered 6 days after the transfer and 36h later, cell sorting of wt/wt and fl/fl cells into T_{fh} (CD44⁺Thy-1.1⁺CXCR5^{hi}PD-1^{hi}) and Non- T_{fh} (CD44⁺Thy-1.1⁺CXCR5⁻PD-1⁻) cells was performed (Figure 12A). To verify a successful RANKL KO for transcriptome analysis, one animal per group was analyzed the following day, revealing successful RANKL depletion (data not shown). Samples were prepared according to standard protocol (cf. Methods section 2.6) and gene expression was considered differentially regulated if the adjusted p-value was ≤ 0.05 (corrected according to Benjamini & Hochberg, 1995) and the log₂-fold change (log₂FC) was > 0.37 .

Out of $> 39,000$ analyzed genes (Figure 12B), 517 genes were found differentially regulated. Only relatively low fold changes in gene expression were identified in wt/wt T_{fh} and fl/fl T_{fh} cells (maximum log₂ FC of upregulated genes in fl/fl T_{fh} cells: -1.18; maximum log₂ FC of downregulated genes in fl/fl T_{fh} cells: 1.45, see Figure 12C Top50 regulated genes).

To investigate genes relevant for T_{fh} cells, these 517 genes were compared to the top 300 genes differentially regulated in T_{fh} versus non- T_{fh} cells (see chapter 3.1, Figure 8). This comparison revealed 11 genes identified in both data sets, 3 of which were expressed stronger in fl/fl T_{fh} cells and belonged to the 50 most intensely regulated genes (*Tubb2a*, *Atp1a3*, and *Dnase1l3*; Figure 12C). *Tubb2a* (log₂ FC 0.63) encodes for tubulin beta-2A chain, *Atp1a3* (log₂ FC 0.67) for sodium/potassium-transporting ATPase subunit alpha-3, and *Dnase1l3* (log₂ FC 0.80) for deoxyribonuclease1 (source UniProt: Q7TMM9, Q6PIC6 and P49183, respectively).

Results

After literature-based research revealing no apparent link to immunological processes, and only small variations in expression levels between RANKL KO and control animals for all identified genes, analysis of these genes was not pursued further.

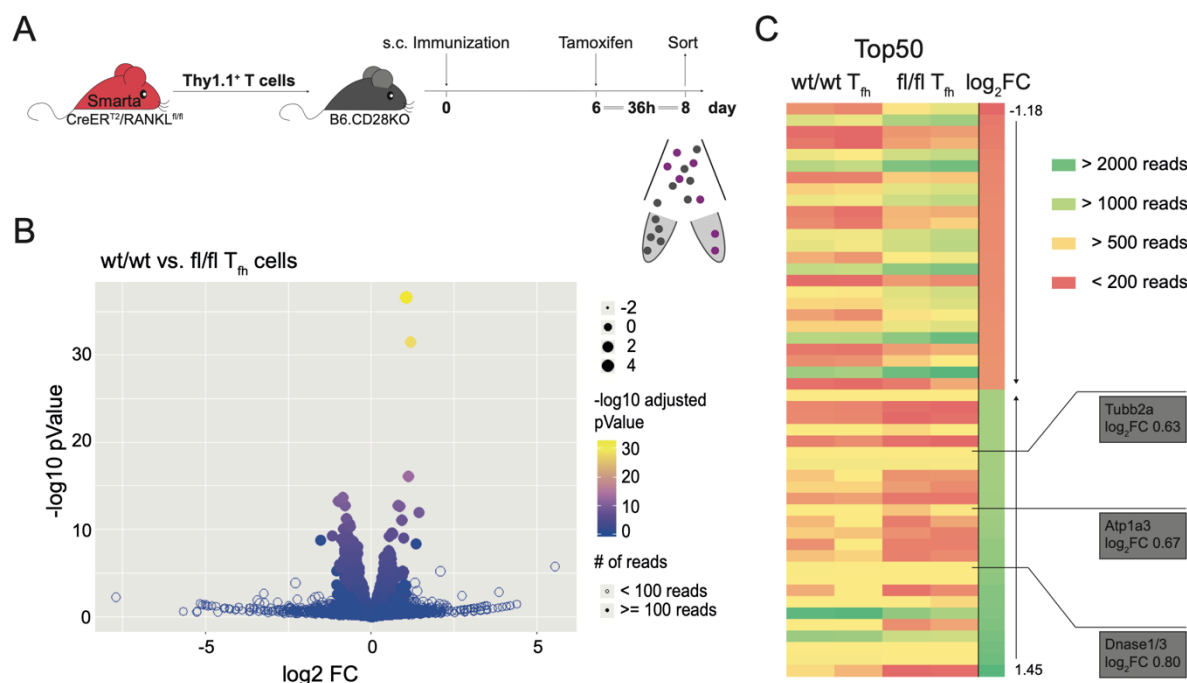


Figure 12 Transcriptome analysis of T_{fh} cells of WT and RANKL KO mice reveals differentially expressed genes

(A) Scheme of the experimental setup. T cells from *Smarta.CreER²/RANKL^{fl/fl}* (fl/fl) or *Smarta.CreER²* (wt/wt) were transferred into *B6.CD28KO* mice followed by s.c. immunization (NP-SM-MSA in IFA) on day 1 after transfer. Tamoxifen was administered 6 days post-transfer and sorting of T_{fh} ($CD44^+Thy-1.1^+CXCR5^{hi}PD-1^{hi}$) and non-T_{fh} cells ($CD44^+Thy-1.1^+CXCR5^+PD-1^+$) was performed 36h after tamoxifen administration. (B) Volcano plot of transcriptome data displaying $-\log_{10}$ p-values (color coded) over \log_2 FC changes, showing the most significantly regulated genes in yellow. (C) Heat map of the Top50 most up- or downregulated genes in fl/fl T_{fh} cells compared to wt/wt T_{fh} cells. Values were sorted according to the \log_2 FC value. Red \log_2 FC fields represent strongly downregulated genes and green fields represent strongly upregulated genes in fl/fl T_{fh} cells. The genes *Tubb2a*, *Atpa3* and *Dnase113* were significantly downregulated in fl/fl T_{fh} cells and present in the Top300 list of genes differentially expressed in T_{fh} vs. non-T_{fh} cells (Fig. 8).

In summary, T cell specific RANKL KO showed only minor effects on T_{fh} cells and their phenotype. Consistently, a complementary transcriptome analysis failed to provide suggestive information on the function of RANKL in T_{fh} cells.

In the following, further T_{fh} signature-genes identified by the transcriptome analysis (cf. Results section 3.1) other than the RANKL-encoding gene *Tnfrsf11* were investigated by genetic modification of transgenic T cells. Specifically, overexpression and CRISPR Cas9-mediated knock out of these genes were performed.

3.3 Screening for T_{fh} signature gene function by overexpression and CRISPR Cas9-mediated knock out in transgenic T cells

The identification of molecules with to date unknown function for T_{fh} cell generation and/or maintenance is of great therapeutic relevance, context-dependently enabling the promotion or inhibition of the humoral immune response.

Since a full functional characterization of the remaining 18 T_{fh} cell signature genes was beyond the scope of this study, a screening was carried out to address whether overexpression or knock out of each particular gene affected T_{fh} cell frequency. Subsequently, the function of T_{fh} cell-affecting genes was studied in detail.

Similar to the interference with the *Tnfrsf11* gene above, the adoptive transfer model of transgenic T cells was used for functional screening. However, in contrast to RANKL KO animals used above, retroviral infection was used for genetic modification of *Smarta* TCR-specific transgenic T cells. This allowed to circumvent complex and time-consuming mating and breeding of genetically modified animals for individual target genes and enabled quick, cost-effective, and efficient functional screening.

3.3.1 Overexpression of seven negatively regulated T_{fh} cell signature genes reveal a unique function of RAR α in T_{fh} cell generation

Seven genes were considered interesting candidates for playing a role in T_{fh} cell homeostasis based on previously reported function (Table 4) and hence were further investigated. Since these genes were strongly reduced in T_{fh} cells, their function was examined by use of an overexpression (OE) system. Based on published data (Table 4), six of those seven genes (*Ccr2*, *Plac8*, *Fam129b*, *Smad7*, *Cish*, and *Cxcr6*; Table 4) were investigated via overexpression in T cells and analysis of lymph nodes subsequent to adoptive transfer and s.c. immunization. In contrast, *Rara* overexpression was studied using the chronic airway inflammation model.

First, the seven target genes were amplified from non-T_{fh} cell-derived cDNA and cloned into eukaryotic expression vectors. Target gene expression was linked to GFP via an internal ribosomal entry site (IRES) site that allowed the isolation of cells successfully expressing target genes for subsequent transfer by means of fluorophore detection.

Results

Table 4 Screening of six downregulated T_{fh} cell signature genes for their role in T_{fh} cell generation

The genes depicted here have been selected for further screening based on their published function. Rara is not included in this table and is described in detail in section 3.3.1.1.

T_{fh} signature genes	Function	Literature
<i>C-C Motif Chemokine Receptor 2 (Ccr2)</i>	<ul style="list-style-type: none"> • corresponding ligand (CCL2) expressed on a variety of immune cells • recruitment of macrophages/monocytes & tissue localization of T cells; involved in several diseases, e.g. atherosclerosis • balance between Th_{17} and T_{reg} populations 	Bakos <i>et al.</i> , 2017; Kara <i>et al.</i> , 2015
<i>Placenta Associated 8 (Plac8)</i>	<ul style="list-style-type: none"> • identified as leukocyte inhibitory factor-regulated gene in murine uterus • involved in immune system, cell differentiation, apoptosis, and control of several diseases • defense against bacteria, involved in Th_2-mediated immune defense 	Jia <i>et al.</i> , 2018; Jimenez-Preitner <i>et al.</i> , 2011; Johnson <i>et al.</i> , 2012; Ledford <i>et al.</i> , 2007; Tibbitt <i>et al.</i> , 2019
<i>Family With Sequence Similarity 129 Member B (Fam129b)</i>	<ul style="list-style-type: none"> • protein structure shows essential features of a signaling molecule • cell-cell-connection, reorganization of cytoskeleton; migration/invasion of tumor cells • essential in wound healing 	S. Chen <i>et al.</i> , 2011; Ji <i>et al.</i> , 2016; Oishi <i>et al.</i> , 2012
<i>SMAD Family Member 7 (Smad7)</i>	<ul style="list-style-type: none"> • fine tuning of TGF-β signals, thereby generating the balance between pro- and anti-inflammatory conditions • upregulation inhibits TGF-β & enhances Th_1 and Th_2 cell differentiation 	Fantini <i>et al.</i> , 2004; Garo <i>et al.</i> , 2019; Gorelik <i>et al.</i> , 2000; Hauptelshofer <i>et al.</i> , 2019; Kleiter <i>et al.</i> , 2010; Tronccone <i>et al.</i> , 2018
<i>Cytokine inducible SH2-containing protein (Cish)</i>	<ul style="list-style-type: none"> • member of suppressors of cytokine signaling (SOCS) protein family • upregulated upon TCR signaling, involved in early T cell signaling, T helper cell differentiation/ functional characteristics • associated to allergies, malignant and infectious diseases 	Carow <i>et al.</i> , 2017; Guittard <i>et al.</i> , 2018; Periasamy <i>et al.</i> , 2011; Seyfarth <i>et al.</i> , 2018; X. O. Yang <i>et al.</i> , 2013
<i>C-X-C Motif Chemokine Receptor 6 (Cxcr6)</i>	<ul style="list-style-type: none"> • expressed on a variety of immune cells • in combination with its ligand CXCL16 essential for localization/activation of lymphocytes in non-lymphoid tissue • associated with Th_1-mediated diseases, e.g. arthritis/sarcoidosis 	Ashhurst <i>et al.</i> , 2019; Latta <i>et al.</i> , 2007; O'Connor <i>et al.</i> , 2012

The experimental sets are summarized in Table 5. In general, transgenic *Smarta*-TCR specific T cells were retrovirally infected (gene of interest–IRES–GFP vectors) and cultured for four days. Subsequently, fluorescence⁺ T cells were sorted and co-transferred into *B6.CD28KO* recipients in combination with transgenic *B1-8i* cells. Immediately after transfer, s.c. tail base immunization (NIP-SM-MSA in CFA or IFA) was performed. DLNs were analyzed on day 7 or 10 by flow cytometry (Table 5 & Figure 13A).

Additionally, in experiment 3, *Kruppel-like factor 2 (Klf2)* overexpression was used as a positive control, since this gene encodes for a transcription factor well-known as a negative regulator of T_{fh} cell differentiation (J.-Y. Lee *et al.*, 2015; Weber *et al.*, 2015).

Table 5 Experimental conditions for the overexpression of T_{fh} signature genes

Grouping, p-values, and experimental scheme for target gene overexpression. Detailed information for statistical analysis is given in the legend of figure 13. P-values indicate the significance value of the respective overexpression group compared to the corresponding empty vector control group. As recipients, *B6.CD28 KO* mice were used.

#	Overexpression of genes	corresponding p-values	Immunization	Day of analysis
1	<i>Plac8, Cish, Cxcr6</i>	Plac8: 0.99; Cish: 0.9691; Cxcr6: 0.4178	CFA	d7
2	<i>Fam129b, Smad7, Cish</i>	Fam129b: 1.0; Smad7: 0.8905; Cish: 0.99	IFA	d7
3	<i>Ccr2, Fam129b, Smad7, Cxcr6</i> (<i>Klf2</i>)	Ccr2: 0.99; Fam129b: 1.0; Smad7: 0.99; Cxcr6: 0.99; Klf2:0.26	IFA	d10

Overexpression of none of the six signature genes significantly affected T_{fh} cell generation (defined as CXCR5⁺PD-1⁺) compared to the empty vector control group (EV; % T_{fh} normalized to corresponding EV; EV 100 ± 40.32, Ccr2 82.44 ± 30.5, Plac8 96.48 ± 27.88, Fam129b 75.26 ± 11.92, Smad7 89.25 ± 24.49, Cish 113.1 ± 47.11, Cxcr6 111.7 ± 59.6, mean ± SD, p-values of the respective experiments are depicted in Table 5).

However, due to high variability among the recorded T_{fh} cell frequencies, also the expected negative effect of *Klf2* overexpression was not observed on the T_{fh} cell population (% T_{fh} normalized to corresponding EV; EV 100 ± 40.32, Klf2 54.16 ± 42.0; p=0.26). In summary, even though retrovirally induced overexpression represented an

efficient tool to screen for the function of distinct genes of interest, no significant effects on T_{fh} cells were detected and conclusively, none of these genes were further investigated.

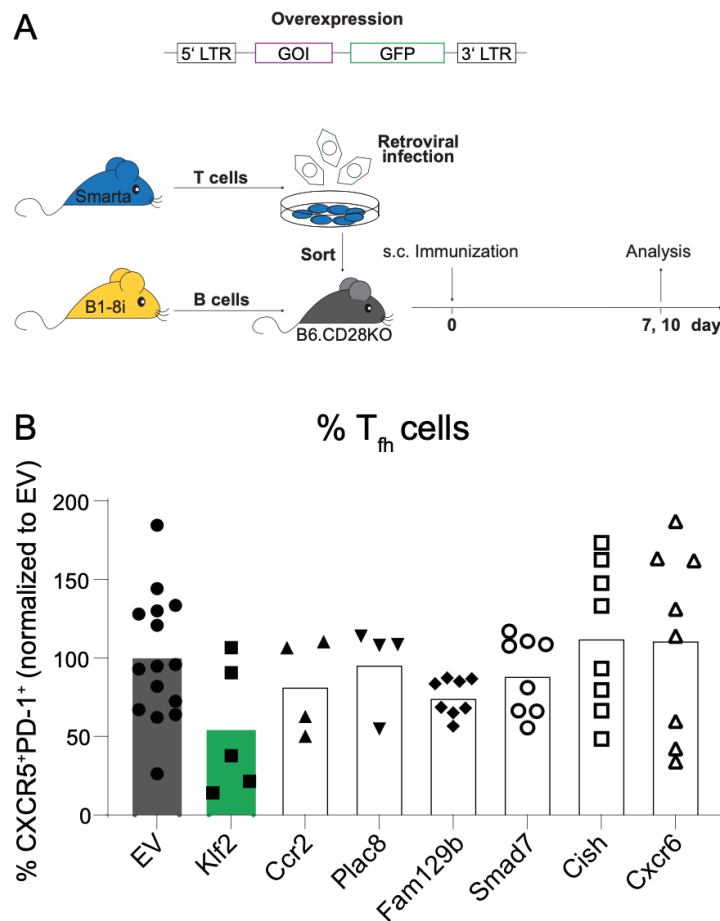


Figure 13 Overexpression of T_{fh} cell signature genes has no effects on T_{fh} cell generation

(A) Schematic overview of the experimental setup. Transgenic Smarta T cells were retrovirally infected with plasmid containing the gene of interest (GOI). GOI expression was linked to GFP via an IRES site and GFP⁺ cells were sorted and co-transferred (B1-8i) into B6.CD28KO recipients followed by s.c. immunization (NIP-SM-MSA in CFA or IFA). Analysis of dLN was performed at day 7 or day 10 (day 10 for additional B cells analysis). (B) Frequencies of T_{fh} cells (CXCR5⁺PD-1⁺) normalized to the corresponding empty vector control group (EV) for overexpression of GOIs. Results for individual GOIs contained in multiple experimental groups (cf. Table 5) were pooled. Bars indicate mean, symbols represent individual animals. For the statistical analysis of more than two groups one-way ANOVA or Kruskal-Wallis test was performed. Subsequently, the resulting p-values were corrected using the two-stage linear step-up procedure of Benjamini, Krieger and Yekutieli and Holm-Šidák (* $p < 0.05$, ** $p < 0.01$, *** $p < 0.001$, ns $p > 0.05$).

3.3.1.1 Nuclear retinoic acid receptor α promotes germinal center responses

Another T_{fh} signature gene, the retinoic acid receptor alpha ($RAR\alpha$; also known as vitamin A receptor), was analyzed in more detail. Vitamins and their metabolites fulfill essential functions in the control of the innate and adaptive immune system. The importance of vitamin A as an immune modulator has been known since the beginning of the 20th century, when it was reported as an anti-infectious agent (Bono *et al.*, 2016; H. N. Green & Mellanby, 1928; Hufnagl & Jensen-Jarolim, 2018). Vitamin A metabolites are stored in the liver and use-dependently hydrolyzed to release retinol into the circulation, where it binds to a variety of retinol binding proteins. Retinol can subsequently be metabolized further to retinoic acid (RA), with *all-trans* RA (ATRA), 13-*cis* RA, and 9-*cis* RA being the main isomers (Bono *et al.*, 2016; Goswami & Kaplan, 2016). RA is membrane permeable and initiates signaling via nuclear retinoic acid receptors (RAR) and retinoic x receptors (RXR), thereby e.g. leading to lymphocyte activation, proliferation, and homing (Scholz *et al.*, 2020). Interestingly, vitamin A metabolites have been shown by several studies to play a role in the pathophysiology of allergic responses like asthma, which was hypothesized to be related to an increased generation of vitamin A-mediated Th_2 responses (Matheu *et al.*, 2009). Even though conflicting statements on the effect of vitamin A on T cell reactions have been published (Hufnagl & Jensen-Jarolim, 2018; Schuster *et al.*, 2008; H. Yang *et al.*, 2020), the gene *Rara*, encoding the alpha form of the RAR receptor, $RAR\alpha$ (Nuclear retinoic acid receptor α), was identified as a strongly regulated gene by the transcriptome analysis of T_{fh} compared to Non- T_{fh} cells (cf. Fig. 8B; *Rara* was downregulated in T_{fh} cells, logFC -2.0). Due to the involvement of RA signaling in T cell development and allergic diseases like asthma as described above, the role of $RAR\alpha$ was investigated in the following in a chronic airway inflammation model, mimicking a chronic allergy-like respiratory inflammation.

To do so, transgenic *Smarta* TCR-specific T cells were first Th_2 -polarized (cf. Methods section 2.3.2.1) before retroviral infection with a plasmid coding for $RAR\alpha$ (IRES-GFP additionally included in the vector; see Scholz *et al.*, 2020). After five days in culture, sorted GFP⁺ T cells were co-transferred with *B1-8i* B cells into *B6.CD28KO* recipients and chronic airway inflammation was induced by intranasal immunization (NIP-SM-MSA + LPS). Due to the transfer of pre-polarized T cells and the focus on early T_{fh} cell

generation, analysis of lungs and lung-dLNs was performed 7 days after transfer (Figure 14A).

RAR α OE induced a significant 67% reduction in the numbers of transgenic T cells in the lung (% Thy-1.1⁺; EV 52.17 \pm 11.72, RAR α OE 16.95 \pm 5.70, mean \pm SD, p=0.0001) and a nearly significant reduction in lung-dLNs (EV 12.21 \pm 6.00, RAR α OE 7.76 \pm 1.53; p=0.0541; Figure 14B). Moreover, RAR α OE significantly increased frequencies of T_{fh} and T_{fh}-like cells in both lung-dLNs and lungs (% CXCR5⁺PD-1⁺; lung-dLN: EV 28.41 \pm 3.00, RAR α OE 39.96 \pm 8.04, p=0.0043; lung: EV 7.26 \pm 1.69, RAR α OE 15.93 \pm 4.46, mean \pm SD, p=0.0010; Figure 14B) which was accompanied by higher B_{GC} cell frequencies in the lung (% CD38^{lo}GL7^{hi}; lung: EV 47.46 \pm 9.43, RAR α OE 71.20 \pm 4.98, mean \pm SD, p=0.0001; Figure 14B).

Besides the frequency of transgenic T cells, T_{fh} cells and B_{GC} cells, additional markers of T cell function were examined: The T_{fh} cell antagonist CD25 (IL-2R α), the essential T_{fh} cell molecule ICOS, and the activation and homing marker CD69. In line with increased T_{fh} cell frequencies upon RAR α OE, CD25 expression in lung-dLNs was reduced (% CD25; lung-dLN: EV 7.01 \pm 1.64, RAR α OE 3.8 \pm 1.4; p=0.0013; mean \pm SD), accompanied by enhanced ICOS expression (% ICOS; lung-dLN: EV 11.06 \pm 3.09, RAR α OE 27.8 \pm 9.85, p= 0.0016; mean \pm SD). In addition, enhanced RAR α expression led to upregulation of CD69 in both lung-dLNs and lungs (% CD69; lung-dLN: EV 15.17 \pm 3.5, RAR α OE 35.15 \pm 9.25, p= 0.0003; lungs: EV 50.11 \pm 11.54, RAR α OE 66.69 \pm 16.64, p=0.0459; mean \pm SD, Figure 14C). This indicates that RAR α OE promoted T_{fh} cell activation and differentiation.

Since the production of allergen-specific antibodies is one of the key drivers in allergic reactions (Williams *et al.*, 2012) and 9-cis RA was shown to modulate the humoral immune response (Heine *et al.*, 2018), the generation of immunoglobulin subclasses in the lung was studied next. A 2-fold upregulation of IgE- and IgG1-producing B cells was found upon RAR α OE (% IgE: EV 0.69 \pm 0.43, RAR α OE 1.9 \pm 1.08, p=0.0037; % IgG1: EV 34.31 \pm 3.19, RAR α OE 62.01 \pm 3.75, p=0.0001; mean \pm SD), whereas IgG2b and IgM-producing B cells were decreased by RAR α OE (% IgG2b: EV 9.93 \pm 2.2, RAR α OE 1.97 \pm 0.43, p=0.0001; % IgM: EV 52.5 \pm 3.7, RAR α OE 40.41 \pm 3.76, p=0.0001; mean \pm SD; Figure 14E). Thus, enhanced RAR α signaling not only positively influenced the generation of T_{fh} cells, but also guided the humoral immune response towards a distinct direction.

Results

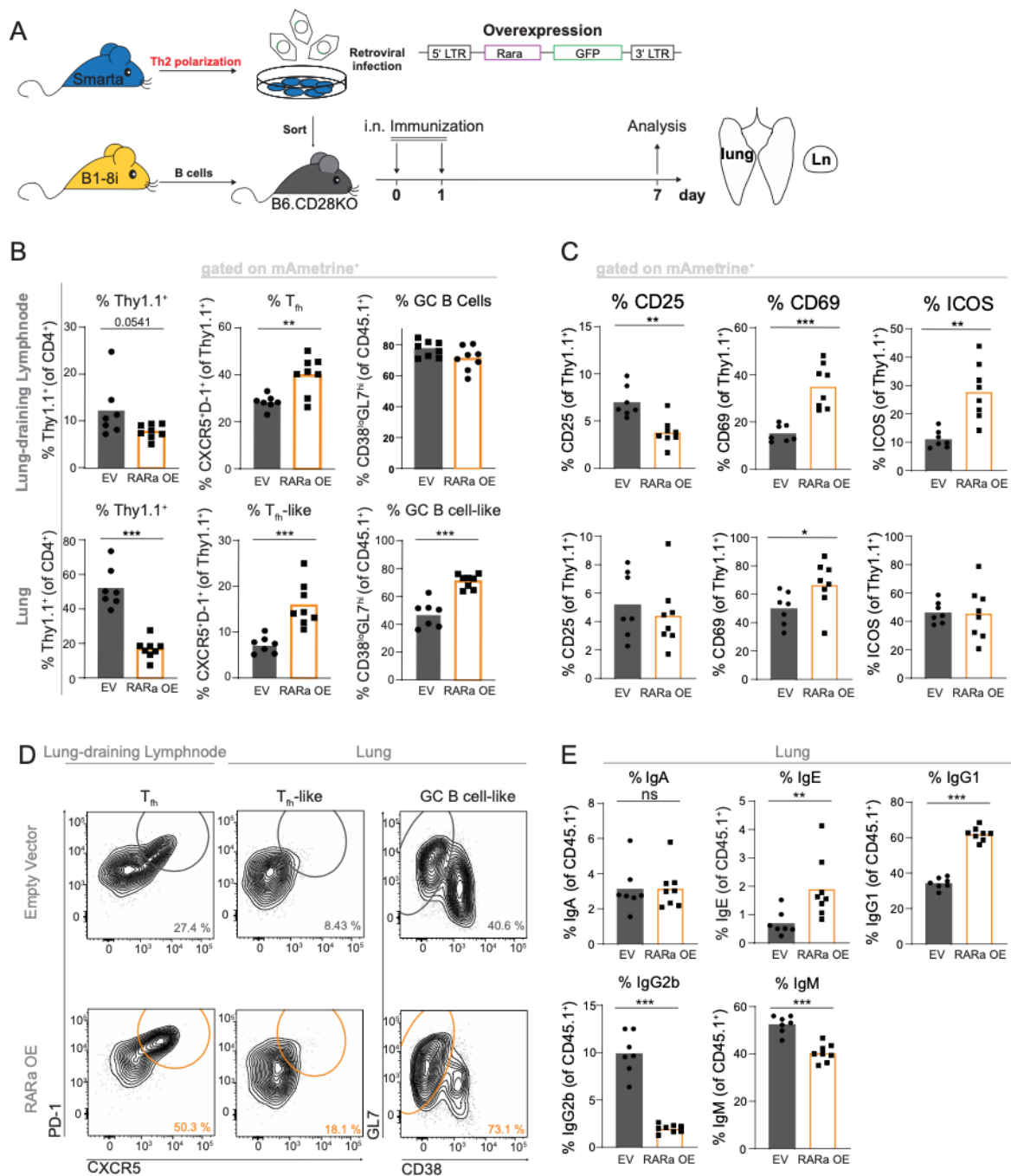


Figure 14 Overexpression of retinoic acid receptor alpha (RARa) influences T_{fh} and B_{GC} cell generation

(A) Schematic overview of the experimental setup. Th₂ pre-polarized transgenic Smarta T cells were infected with Rara-containing retroviruses (RARa OE) or empty vector controls (EV) and fluorescence⁺ T cells were sorted and co-transferred with B1-8i B cells into B6.CD28KO recipients. Animals received intranasal immunization (NIP-SM-MSA + LPS) on day 0 and 1 and analysis of lung-dLNs and lungs was performed on day 7 post-transfer. (B) Percentages of transgenic T cells (Thy-1.1⁺, left panels), T_{fh}/T_{fh-like} cells (CXCR5⁺PD-1⁺, middle panels) and B_{GC} cells/GC-like B cells (CD38^{lo}GL7^{hi}, right panels) in lung-dLNs (upper row) and lungs (lower row; EV in grey, RARa OE in orange). (C) Percentages of T_{fh} cell antagonist CD25⁻ (left), T cell activation marker ICOS⁻ (middle part), and activation and homing marker CD69-expressing T cells (right) in lung-dLNs (upper row) and lungs (lower row; EV in grey, RARa OE in orange). (D) Contour plots of representative T_{fh} (CXCR5⁺PD-1⁺) and B_{GC} cell (CD38^{lo}GL7^{hi})

Results

stainings in lung-draining LNs (left) and lungs (middle and right part) of EV- and RAR α OE-vector treated animals (EV in grey, RAR α OE in orange). (E) Percentages of B cells generating immunoglobulin subclasses IgA, IgE, IgG1 (top row, from left to right) and IgG2b and IgM (lower row, left and right, respectively) within lungs (EV in grey, RAR α OE in orange). Bar graphs depict mean, symbols represent individual animals. Statistical analysis was performed using unpaired t-test or Mann-Whitney-U-test (* $p < 0.05$, ** $p < 0.01$, *** $p < 0.001$, ns $p > 0.05$).

In summary, the comparison of different transcriptome data sets revealed signature genes differentially downregulated in T_{fh} cells. Overexpression of nuclear retinoic acid receptor α highly promoted the humoral immune response. On the contrary, none of the remaining six T_{fh} cell-suppressed genes showed a unique functional contribution to T_{fh} cell generation upon overexpression in our adoptive transfer model. However, the function of these genes and the encoded molecules should be investigated in more detail, as its marked downregulation within the T_{fh} cell population indicates a relevant function in T_{fh} generation or existence.

3.3.2 CRISPR Cas9-mediated knock out of eleven positively regulated T_{fh} cell signature genes in antigen-specific T cells

3.3.2.1 Establishment of an *in vivo* CRISPR Cas9-mediated knock out system

To knock out genes of interest in antigen-specific T cells in a fast and efficient manner, a CRISPR Cas9-based system was developed. Transfer of the comparatively large Cas9 enzyme into targeted cells is one of the major challenges related to effective GOI knock out using the CRISPR Cas9-system and was overcome by utilization of a newly generated Cas9-transgenic mouse line, kindly provided by Klaus Rajewsky (MDC Berlin). These mice harbor a gene cassette containing the Cas9 gene as well as an IRES-linked eGFP in the Rosa26 locus for constitutive Cas9 expression. These animals were crossed to Smarta TCR transgenic mice (top left in Figure 15). To additionally allow for a GOI knock out at defined timed points, *Smarta.CreER^{T2}xStopF-Cas9* animals were generated that additionally harbored 1.) a floxed stop-cassette upstream of the Cas9 gene that restricted the Cas9 gene transcription to the presence of Cre recombinase, and 2.) expressed Cre recombinase fused to a modified human estrogen receptor (CreER^{T2}). Binding of the estrogen-homologue tamoxifen to this receptor resulted in nuclear translocation of the fusion protein, thereby enabling Cre recombinase to excise the floxed stop-cassette, leading to the expression of the Cas9-IRES-eGFP sequence (bottom left in Figure 15).

T cells from both Cas9 mouse lines (*SmartaxCas9-GFP* and *Smarta.CreER^{T2}xStopF-Cas9*) were isolated and retrovirally infected with plasmids containing specifically designed sgRNA targeting genes of interest and the fluorescence reporter mAmetrine enabling selection for successfully infected T cells (right in Figure 15). T cells containing both, the Cas9 transgene and the retroviral sgRNA vector, were then identified by dual fluorophore (eGFP and mAmetrine) expression.

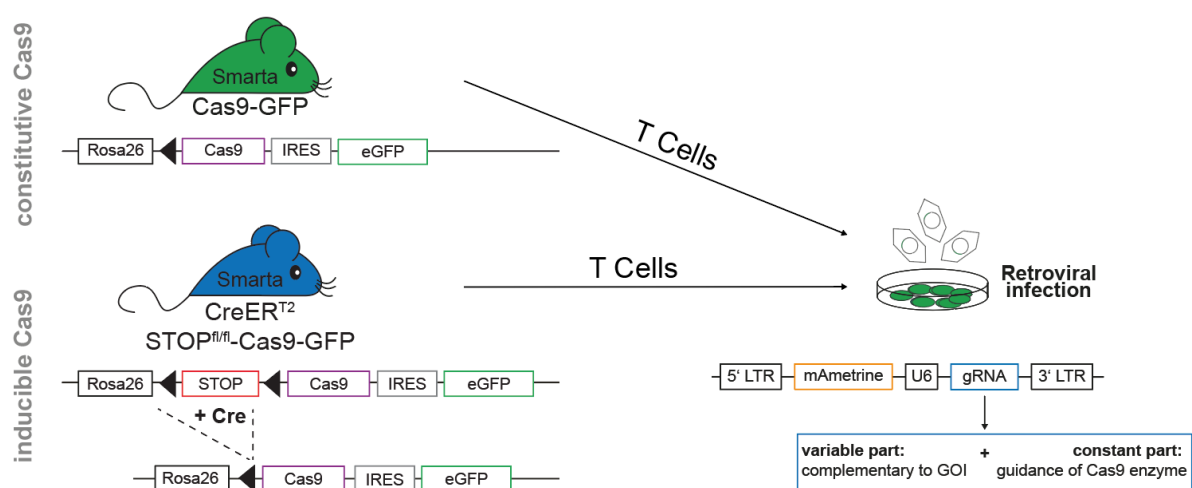


Figure 15 Transgenic mouse strains and experimental set-up for CRISPR Cas9-based knock out in antigen-specific T cells

For constitutive Cas9 expression, *SmartaxCas9-GFP* transgenic mice were used (top left). For conditional Cas9 expression, *Smarta.CreER^{T2}xStopF-Cas9* transgenic animals were treated with tamoxifen to induce Cas9-expression at distinct time points (bottom left). Isolated transgenic T cells were retrovirally infected with a plasmid containing mAmetrine as fluorescent reporter and a gRNA consisting of a variable part (designed to be complementary to the gene-of-interest) and a constant part (mandatory for Cas9 enzyme guidance; right).

3.3.2.2 Verification of knock out efficiency of genes of interest

The use of Cas9-transgenic animals has been shown to enable a knock out efficiency of up to 90% on both alleles for transfected cells (Chu, Graf, *et al.*, 2016). However, knock out or DNA modification efficiency (e.g. the introduction of specific point mutations) depend on base-pair composition of the designed sgRNA, PAM site position, DNA accessibility related to chromatin structure in euchromatin and heterochromatin, and nucleosome positioning (Isaac *et al.*, 2016; Jensen *et al.*, 2017; Sentmanat *et al.*, 2018). Therefore, it was mandatory to first quantify GOI knock out efficiency of the used sgRNA in order to correctly interpret the results in targeted cells. First, knock out of target genes was tested by the T7 Endonuclease I (T7EI) assay (Figure 16A and B). For this assay, retrovirally-infected fluorescence⁺ cells were sorted

and GOIs were amplified by PCR after DNA isolation from WT and KO animals. Then, amplicons were mixed 1:1, denatured and subsequently reannealed. During reannealing, DNA-heteroduplexes formed between both, WT DNA strands and strands containing introduced mutations. These imperfectly base-paired heteroduplexes characteristically form loops between both annealed DNA strands which were recognized and cleaved by T7 endonuclease I. After cleavage, DNA strands were denatured again and DNA fragments were analyzed by gel electrophoresis. In case of a successfully introduction of mutations, fragments of multiple lengths were detectable whereas single fragment length was detected in WT samples (grey box in Figure 16A).

The transcription factor Bach2 has previously been shown to act as a negative regulator of specific sets of T_{fh} cell signature genes, e.g. *Bcl6* and *Rgs16* (Lahmann et al., 2019). To quantify Cas9-mediated KO, KOs of *Bcl6* and *Rgs16* were performed and probed by the T7EI assay. In the respective knock out groups, two fragments were seen in mixed KO and WT samples after analysis by gel electrophoresis whereas only a single band was detectable in control groups, confirming successful Cas9-mediated KO of both genes (Figure 16B).

However, the T7EI assay inherently does not provide quantification of KO efficiency. This is due to the heterogeneity in abundance and length of mutated sequences as well as the formation of secondary structures (Sentmanat et al., 2018). Therefore, Sanger DNA sequencing was additionally performed to determine both, modification specificity and knock out efficiency introduced by Cas9. For the quantification of knock out efficiency by sequencing, Cas9-transgenic T cells were retrovirally infected and cultured *in vitro* for 5 days before double fluorophore-positive cells (GFP and mAmetrine; i.e. virally infected, Cas9-transgenic cells) were sorted and genomic DNA was isolated, amplified by PCR and cloned into a vector for sequencing. At least 10 clones per targeted gene were selected for subsequent Sanger sequencing. Figure 16C provides an example of Cas9-mediated IL-21 knock out. Three out of the five shown exemplary clones harbored a mutation in the targeted sequence, reflecting a knock out efficiency of 60%. Due to the qualitative and quantitative information on knock out constructs gained by Sanger DNA sequencing; this sequencing method was used subsequently to elucidate the specific modifications introduced by Cas9 for all knock outs of GOIs.

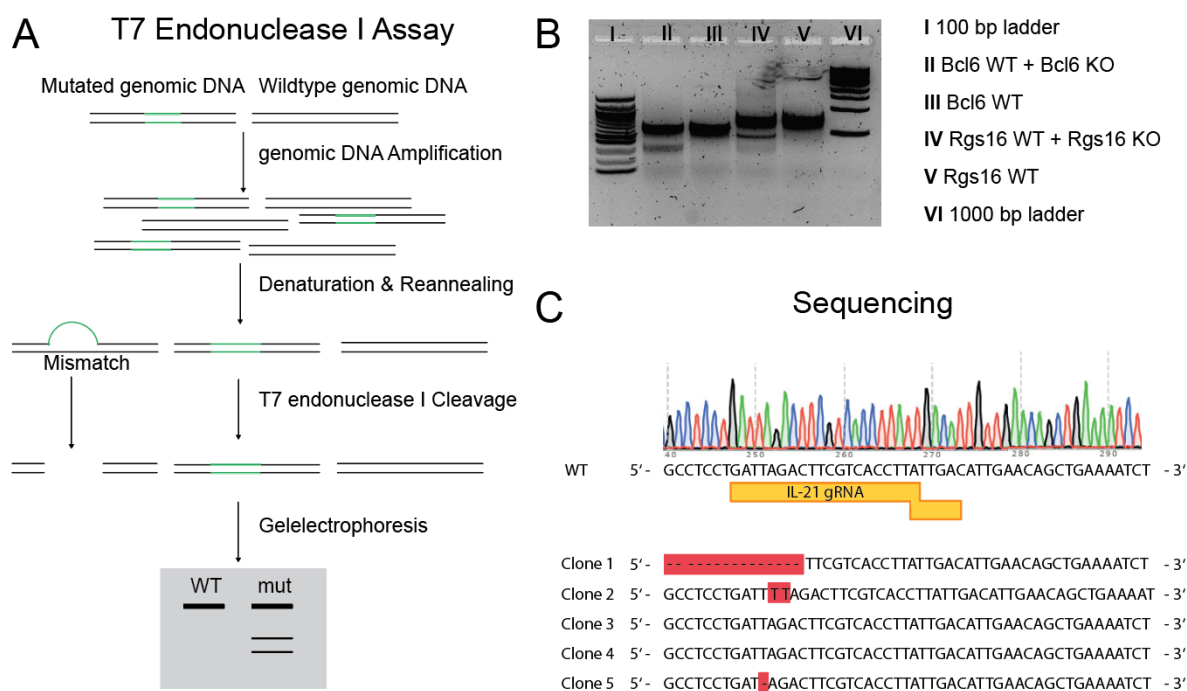


Figure 16 Verification of Cas9-induced knock out by T7EI assay or Sanger sequencing

(A) Principle of T7 Endonuclease I (T7EI) Assay. After amplification of genes of interest, amplicons are denatured and reannealed. Resulting mismatches are recognized by T7 endonuclease I, cleaved, and detected via gel electrophoresis. (B) Representative result of a T7EI assay used for knock out verification of *Bcl6* and *Rgs16*. Samples were mixed with the appropriate control and compared to wildtype (WT) DNA-only controls. (C) Representative example verifying the knock out efficiency by IL-21 gRNA (depicted in yellow) using Sanger sequencing. Sequences of analyzed clones were compared to WT sequence, Cas9-introduced mutations are depicted in red.

3.3.2.3 Proof of principle of successful knock out and functional effects on T_{fh} cell numbers *in vitro* and *in vivo*

3.3.2.3.1 Successful *in vitro* knock out of *Cd44* and *Tigit*

The experimental set-up was validated *in vitro* by the knock out of *Cd44* and *T cell Ig and ITIM domain (Tigit)*, two surface molecules highly expressed on T cells providing straightforward verifiability of knock out efficiency via surface staining. CD44 is a widely used marker for antigen-experienced T cells whose expression is upregulated and sustained upon TCR engagement (Baaten *et al.*, 2012). Besides, it was also shown to play an important role in various cellular processes like cell migration, adhesion, and as a co-receptor in signal transmission via cytoskeletal interactions (Huet *et al.*, 1989; Ponta *et al.*, 2003). TIGIT is known to be mainly expressed on

activated T cells and natural killer cells. In T cells, TIGIT inhibits T cell responses and plays a critical role as a negative regulator in autoimmune diseases (Lozano *et al.*, 2012; Mao *et al.*, 2017).

To induce *Cd44*- and *Tigit*-specific KO, Cas9-transgenic T cells were isolated and retrovirally infected with plasmids containing the target gene-complementary sgRNA. After 5 days in culture, cells were restimulated with phorbol-12-myristate 13-acetate (PMA)/Ionomycin and 12 h later surface expression of the respective molecules was analyzed via flow cytometry (Figure 17A). Expression of both molecules was almost completely abolished compared to the empty vector control groups (EV, only coding for BFP; MFI of CD44: EV 13275 ± 693.5 , CD44 KO 1144 ± 39.80 , $p = 0.0011$; MFI of TIGIT: EV 185.7 ± 24.44 , TIGIT KO 2.74 ± 2.60 , $p = 0.0055$, mean \pm SD), thus indicating near-complete knock out by the CRISPR/Cas9 system (Figure 17B).

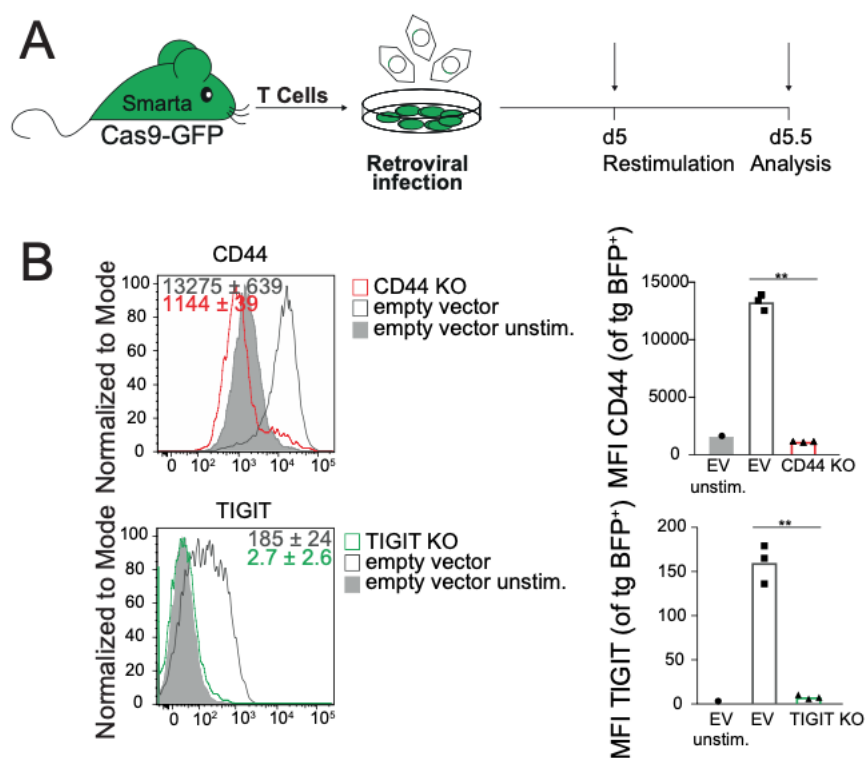


Figure 17 CRISPR Cas9-induced knock out of *Cd44* and *Tigit* in vitro shows strong downregulation of both molecules' surface expression

(A) Scheme of the experimental Setup. Cas9-transgenic T cells were retrovirally infected with plasmids containing a fluorescence reporter and the target gene-complementary sgRNA as described. For comparison, an empty vector control group (EV), only coding the reporter fluorophore, was used. After 5 days in culture, restimulation of T cells was performed and cell surface expression was analyzed by flow cytometry 12 h after restimulation. (B) Representative histograms and bar graphs displaying mean fluorescence intensity (MFI) of surface-expressed target proteins in knock outs and corresponding controls (unstimulated EV condition as solid filled grey bars, stimulated EV condition as empty grey bars, CD44 KO as red, TIGIT KO as green bars). Bars depict mean and

symbols represent individual replicates. For stimulated empty vector and the knock out groups, 3 replicates were recorded, the unstimulated empty vector control group represents a single measurement. Statistical analysis was performed using unpaired *t*-test (* $p < 0.05$, ** $p < 0.01$, *** $p < 0.001$, ns $p > 0.05$).

3.3.2.3.2 Constitutive *in vivo* knock out of *Cd40lg* and *Il21* diminishes T_{fh} cell help

T cell: B cell interaction establishes the so called ‘immunological synapse’, which is crucial for GC formation and the generation of an effective humoral immune response. For the formation of T cell: B cell synapse, several molecules play an important role (Papa & Vinuesa, 2018). First, CD40L is a type II membrane protein and member of the TNF ligand family that is highly expressed on activated $CD4^+$ T cells. Interaction with its B cell-expressed receptor CD40 not only promotes B cell survival and proliferation, but also critically regulates Ig class switching, GC differentiation, and the generation of PCs and B_{mem} cells (Bolduc *et al.*, 2010; Kawabe *et al.*, 1994; Weinstein *et al.*, 2016). Second, IL-21 is one of the main cytokines produced by T_{fh} cells and a key regulator of GCs. In combination with other cytokines like IL-4, it is essential for the maintenance of Bcl-6 expression in B_{GC} cells and its absence leads to defects in Ig affinity maturation and PC generation (Bélanger & Crotty, 2016; Weinstein *et al.*, 2016). In T_{fh} cells, IL-21 production is important for differentiation, however IL-6 and probably other cytokines adopt the IL-21 function in its absence (Deenick & Ma, 2011). Due to the essential contribution of CD40L and IL-21 to T_{fh} and B_{GC} cell function, both genes were interesting targets for the verification of the Cas9 system *in vivo* and the investigation of their functional effects on T cell: B cell interaction.

Cas9-transgenic T cells were isolated, retrovirally infected and cultured according to the above-described protocol. Double fluorophore-positive cells were sorted and co-transferred with *B1-8i* B cells into *B6.CD28KO* recipients followed by tail base immunization (NIP-SM-MSA in IFA). Antigen-specific T and B cells of dLN were analyzed via flow cytometry 10 days after the transfer (Figure 18A).

A significant reduction in the frequency of T_{fh} cells (defined as $CXCR5^+PD-1^+$) was observed in both knock out conditions compared to the EV controls (% T_{fh} ; EV 41.48 ± 7.63 , CD40L KO 14.21 ± 4.44 , IL-21 KO 26.68 ± 5.83 , $p=0.0003$ and $p=0.0138$, respectively, mean \pm SD). Whereas the number of T_{fh} cells generated in the CD40L KO condition was reduced by $> 50\%$, T_{fh} cells in the IL-21 KO condition were reduced by $\approx 35\%$, potentially confirming earlier findings of other cytokines substituting IL-21 functionally upon IL-21 loss. Accordingly, B_{GC} cells (defined as $CD38^{lo}GL7^{hi}$) were

almost completely absent in CD40L KO animals (B_{GC} cell counts; EV 115968 ± 44709 , CD40L KO 6218 ± 7727 , $p=0.0026$, mean \pm SD) while cell counts were decrease by IL-21 KO non-significantly (EV 115968 ± 44709 , IL-21 KO 63199 ± 38163 , $p=0.0997$, mean \pm SD), furthermore supporting the hypothesis of a compensatory rescue upon IL-21 KO (Figure 18B and C).

Collectively, the Cas9 system achieved significant knock out efficiencies of characteristic T_{fh} surface makers in both, *in vitro* and *in vivo* models, thereby enabling further functional investigation of these markers as well as novel signature genes in T_{fh} and B_{GC} cells.

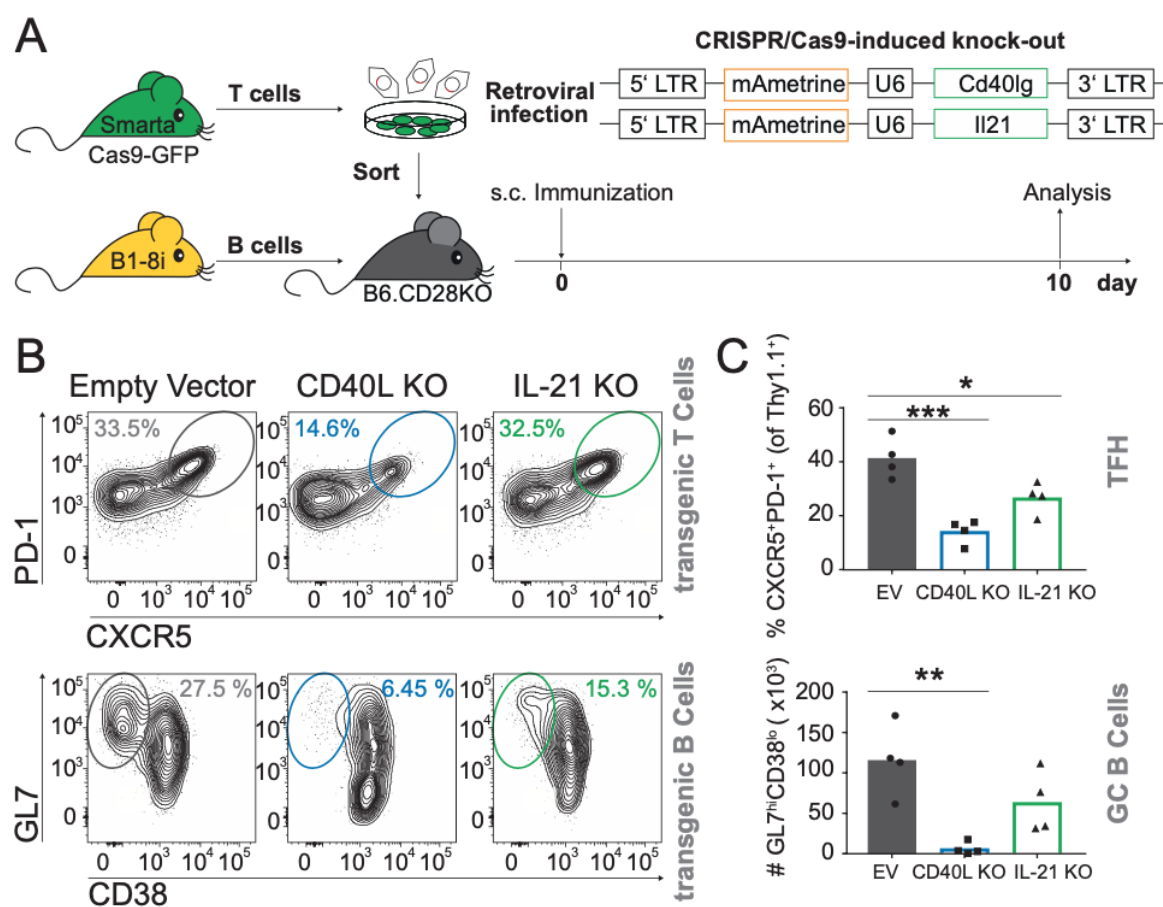


Figure 18 Cd40lg and Il21 KOs lead to decreased T_{fh} cells and reduced B cell helper capability

(A) Overview of the experimental setup. Cas9-transgenic T cells were retrovirally infected with plasmids containing mAmetrine as fluorescent reporter and either control sgRNA (empty vector control, EV) or sgRNA targeting Cd40lg and Il21. To study effects on B cells, infected T cells were co-transferred with transgenic B1-8i B cells into B6.CD28 KO recipient animals followed by tail base immunization (NIP-SM-MSA in IFA). Flow cytometric analysis of dLN was performed 10 days later. (B) Contour plots show representative stainings of T_{fh} cells (CXCR5⁺PD-1⁺ gated on transgenic fluorescence⁺ T cells, upper part) and B_{GC} cells (CD38^{lo}GL7^{hi} gated on transgenic B cells, lower part) for EV (grey), CD40L KO (blue), and IL-21 KO (green). (C) Percentages of T_{fh} cells (upper panel) and total number of B_{GC} cells (lower panel) gated on transgenic fluorescence⁺ T cells and transgenic B cells, respectively (color code

as in B). Bars depict mean, symbol represents individual animals. Statistical analysis was performed using One-way ANOVA (* $p < 0.05$, ** $p < 0.01$, *** $p < 0.001$, ns $p > 0.05$).

3.3.2.3.3 Verification of an inducible *in vivo* Cas9-mediated *Cd40lg* knock out

Especially for molecules suspected to play a role in T cell maintenance or memory phase, inducible knock out at defined time points is desirable. Therefore, *Smarta.CreER^{T2}xStopF-Cas9* animals were generated (for details see Methods section 3.3.2.1). To validate the functionality of the inducible KO system *in vivo*, a knock out of *Cd40lg* after initial priming of the CD4⁺ T cells was generated.

Cas9-transgenic T cells were retrovirally infected with a plasmid containing sgRNA against *Cd40lg* and mAmetrine and fluorescence⁺ T cells were transferred into *C57BL/6* recipient animals followed by tail base immunization (NIP-SM-MSA in IFA). Two days after transfer, animals were treated with tamoxifen (+TMX) or remained untreated (control group; w/o TMX) and antigen specific T cells of dLN were analyzed by flow cytometry 4 days after Cas9 induction (Figure 19A).

The percentage of CD40L expressing T cells was reduced by $\approx 75\%$ in tamoxifen treated animals (w/o TMX 91.65 ± 3.04 , + TMX 22.87 ± 4.96 , $p=0.0004$, mean \pm SD) and the percentage of T_{fh} cells (CXCR5⁺PD-1⁺) was reduced by $\approx 50\%$ compared to the untreated control group (wo TMX 41.60 ± 0.28 , + TMX 20.13 ± 5.67 , $p=0.0148$; Figure 19B), confirming results of the constitutive KO model (cf. section 3.3.2.3.2). Moreover, the reduction in T_{fh} cell counts by late CD40L KO provided that T_{fh} cell development not only depended on initial activation via CD40: CD40L interaction with dendritic cells. Instead, ongoing CD40L signaling was required for T_{fh} cell generation and maintenance.

However, to temporally resolve the involvement of CD40L and further molecules in T_{fh} cell activation, further experiments systematically varying the timepoint for tamoxifen administration will be needed, especially during memory phase as cells divide less frequently.

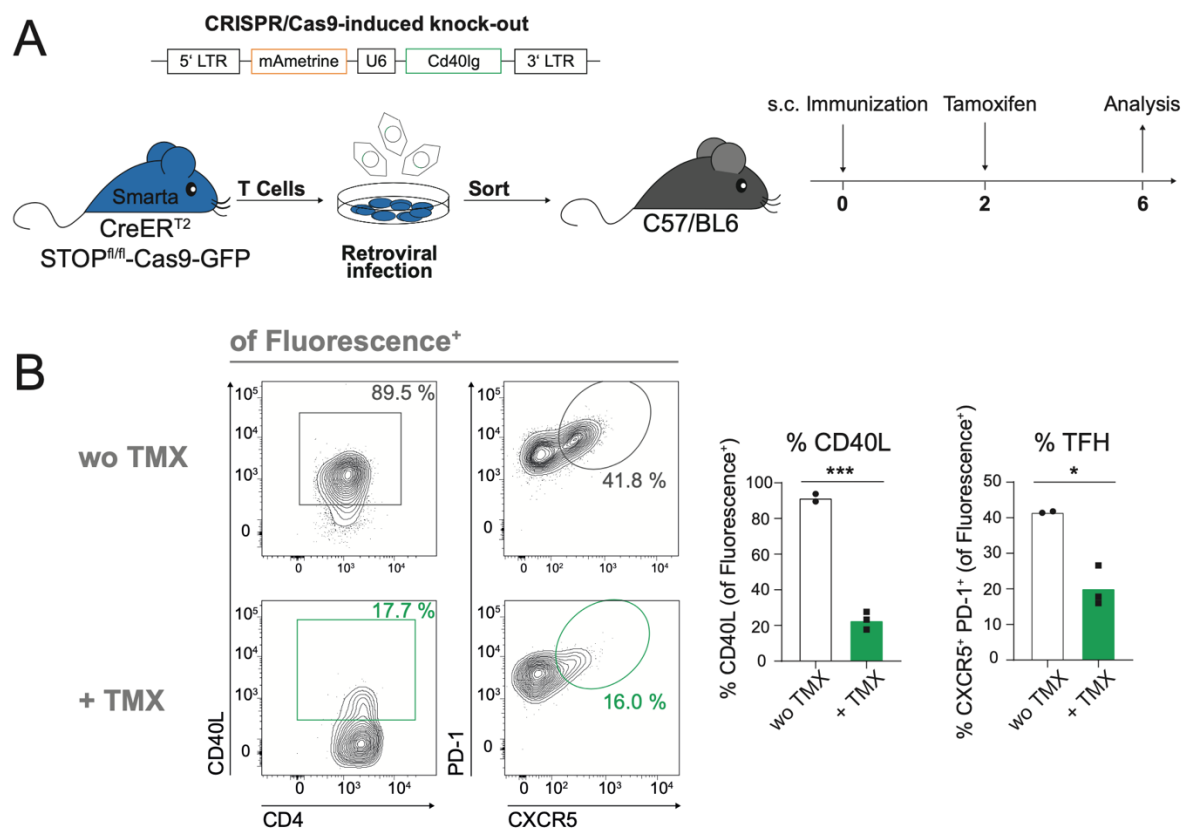


Figure 19 Inducible Cd40lg KO in vivo after initial T cell priming diminishes T_{fh} cell numbers

(A) Scheme of the experimental setup. Transgenic T cells from inducible Smarta.CreER^{T2}xStopF-Cas9 animals were retrovirally infected with plasmid containing mAmetrine as fluorescence reporter and sgRNA targeting Cd40lg. Sorted cells were transferred into C57BL/6 recipient animals that were tail base immunized (NIP-SM-MSA in IFA) and tamoxifen-treated 2 days post-transfer for Cas9 activation (+ TMX; w/o TMX control animals received no tamoxifen treatment). Flow cytometric analysis of antigen-specific T cells of dLNs was performed 6 days after the transfer. (B) Contour plots display representative CD40L and T_{fh} cell (CXCR5⁺ PD-1⁺) stainings with (+ TMX) and without tamoxifen (wo TMX) treatment. Cells were gated on transgenic marker (Thy-1.1⁺) and positive fluorescence markers (mAmetrine for retroviral infection and GFP for induced Cas9 expression, w/o TMX in grey, + TMX in green). (C) Percentages of CD40L⁺ T cells and T_{fh} cells of transgenic and fluorescence⁺ cells (color code as in B). Bars depict mean, symbols represent individual animals. 2 to 3 animals were used for each group. Statistical analysis was performed using unpaired t-test or Mann-Whitney-U-test (* $p < 0.05$, ** $p < 0.01$, *** $p < 0.001$, ns $p > 0.05$).

3.3.2.3.4 Fluorophore-dependent long-term stability of retrovirally infected cells

During Cas9-mediated target gene knock out in antigen-specific T cells *in vitro* and *in vivo*, the numbers of adoptively transferred transgenic T cells were found to decrease over time, especially when using a plasmid containing BFP as a fluorescence reporter for retroviral infection (data not shown). We hypothesized this to be potentially caused by harmful processing of cultured and transferred cells during the protocol, interfering with long-term T cell survival. Known critical steps affecting cell viability are the

mandatory activation of T cells, immunogenicity of fluorescent proteins, the process of retroviral infection *per se*, and mechanical stress during the sorting procedure due to the cell sorter's nozzle size as well as the adjusted sample and sheath pressure. Moreover, probe handling and the duration of the sorting procedure are known determinants impacting cell survival.

To confirm the observation of decreasing cell numbers and to exclude a suboptimal sorting procedure, an experiment elucidating expression kinetics was performed. *Smarta* transgenic T cells were retrovirally infected with a plasmid containing BFP as fluorescence marker only. Afterwards, unsorted cells were transferred into *C57BL/6* recipients that were subsequently immunized (NIP-SM-MSA in IFA). The frequency of all transgenic T cells (Thy-1.1⁺) and of BFP-expressing transgenic T cells was analyzed in draining LNs 6 and 13 days post-transfer by flow cytometry (Figure 20A). Similar to the previous observation, numbers of transgenic T cells diminished over time and on day 13 only 20% of the T cells observed on day 6 were detectable (% Thy-1.1⁺; day 6 1.15 ± 0.04 , day 13 0.19 ± 0.07 , mean \pm SD, $p = 0.0001$). This effect was even more prominent if solely BFP⁺ cells were analyzed, which on day 13 decreased to $\approx 5\%$ of those observed on day 6 (% BFP⁺ of Thy-1.1⁺; day 6 39.83 ± 5.1 , day 13 1.88 ± 0.08 , mean \pm SD; $p = 0.0002$, Figure 20B). Thus, transferred T cells decreased over time, with BFP⁺ cells showing even lower long-term stability post-transfer. Since cells were not sorted prior to transfer, FACS-sorting itself did not seem to be a major determinant of the loss of transferred cells.

In addition, the relatively low number of retrovirally infected cells 6 days after transfer ($\approx 40\%$; % BFP⁺ of Thy-1.1⁺) compared to a rate of 95% achieved using sorting, indicated that sorting prior to transfer was mandatory to enable the investigation of a homogeneous, genetically modified cell population.

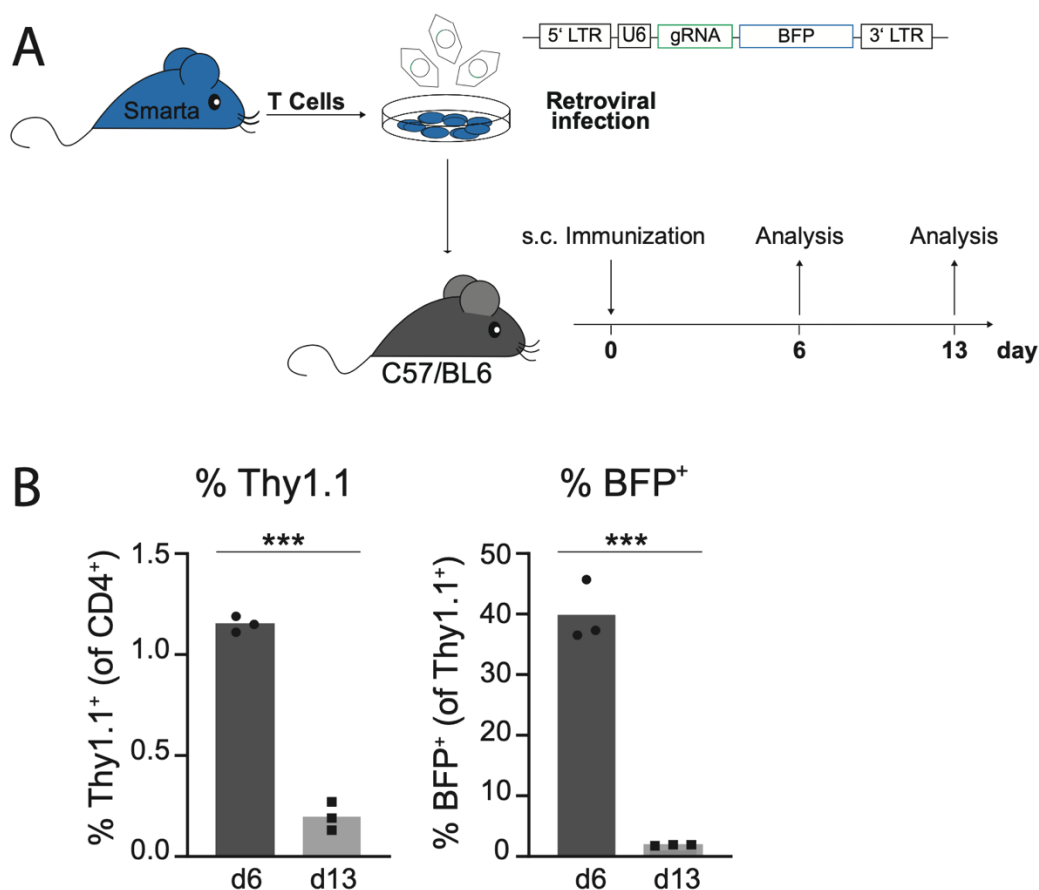


Figure 20 BFP⁺ retrovirally infected cells were rapidly lost after transfer

(A) Scheme of the experimental setup. Smarta transgenic T cells were retrovirally infected with a plasmid coding for the BFP fluorophore only. Cells were transferred into C57BL/6 recipient animals without sorting followed by tail base immunization (NIP-SM-MSA in IFA). Cells of draining LNs were analyzed at day 6 and day 13 post-transfer via flow cytometry. (B) Percentages of Thy-1.1⁺ and BFP⁺ transgenic T cells at day 6 (dark grey) and day 13 (light grey). Bars depict mean, symbols represent individual animals. 3 animals were analyzed per group. Statistical analysis was performed using unpaired t-test or Mann-Whitney-U-test (* $p < 0.05$, ** $p < 0.01$, *** $p < 0.001$, ns $p > 0.05$)

Since BFP as a surrogate marker for successful transfection turned out to be lost faster than transferred cells on average, it seemed unsuitable for long-term monitoring of genetically modified cells. Therefore, alternative fluorescence reporters were investigated.

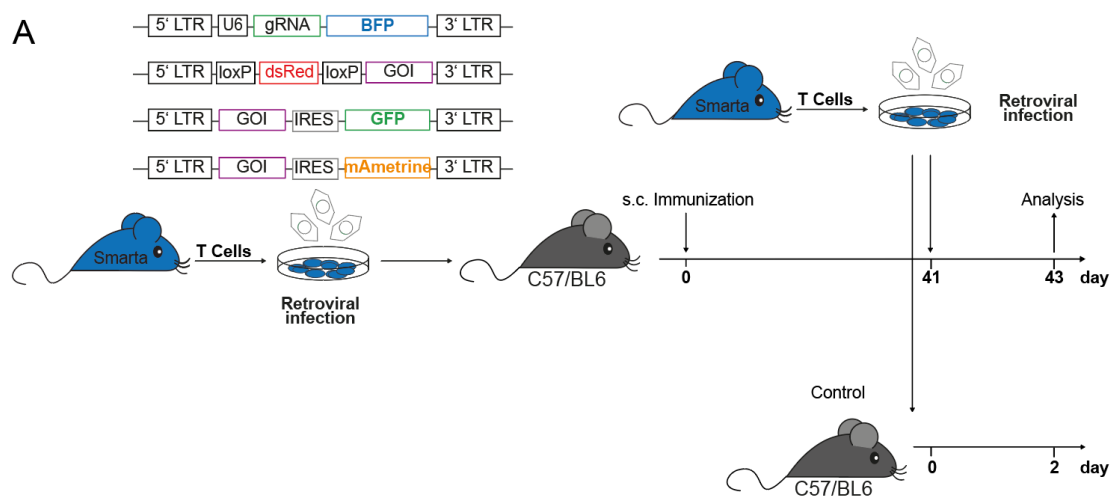
Transgenic T cells were retrovirally infected with plasmids containing BFP, dsRed, GFP, or mAmetrine as fluorescence reporter. As for BFP, unsorted cells were directly transferred into C57BL/6 recipients followed by tail base immunization (NIP-SM-MSA in IFA). Additionally, to test whether antibody-dependent cellular cytotoxicity was involved in the loss of fluorophore-expressing transgenic cells, animals received retrovirally infected cells again at day 41. As control, retrovirally infected cells were

transferred into so far untreated *C57BL/6* animals. Spleens of both, retransferred (transfer at day 0 and 41) and control animals (transfer at day 41 only) were analyzed 2 days after day 41-transfers by flow cytometry (Figure 21A). As for testing BFP stability before, frequencies of transgenic T cells were normalized and compared to their respective control groups (Ctl).

Surprisingly, three out of four tested fluorescence reporters showed variable degrees of rejection over time. As expected, BFP⁺ T cells were almost completely abolished following a second transfer in comparison to the control group (% BFP⁺Thy-1.1⁺; Ctl 100 ± 2.86, 2nd transfer 1.88 ± 0.82, p=0.0001, mean ± SD). Furthermore, only 30–40% of the cells positive for dsRed or mAmetrine were found in the double-retransferred animals compared to the respective single-transferred controls (% dsRed⁺Thy-1.1⁺: Ctl 100 ± 1.70, 2nd transfer 38.42 ± 1.20, p=0.0001; % mAmetrine⁺Thy-1.1⁺: Ctl 100 ± 1.50, 2nd transfer 27.74 ± 7.42, p=0.0001, mean ± SD). In contrast, GFP-transfected cell counts turned out to be stable over time and did not show immunogenicity, leading to only non-significantly, minimally reduced cell numbers following retransfer (% GFP⁺Thy-1.1⁺; Ctl 100 ± 1.50, 2nd transfer 92.5 ± 7.89, mean ± SD, p= 0.2428; Figure 21B). In summary, GFP was found to be the only marker exhibiting long-term stability, whereas BFP turned out to be most immunogenic marker tested.

In the experiments above, transgenic Cas9 expression was linked to expression of GFP. Therefore, viruses coding for GFP as a reporter for viral infection could not be used in conjunction with Cas9-transgenic cells. Since the fluorophore mAmetrine has successfully been used for overexpression experiments over at least 17 days (data not shown) by the Hutloff laboratory, and since the following experiments investigated the T cell effector phase, BFP was replaced by mAmetrine in viral constructs.

Results



B

normalized to corresponding Ctl

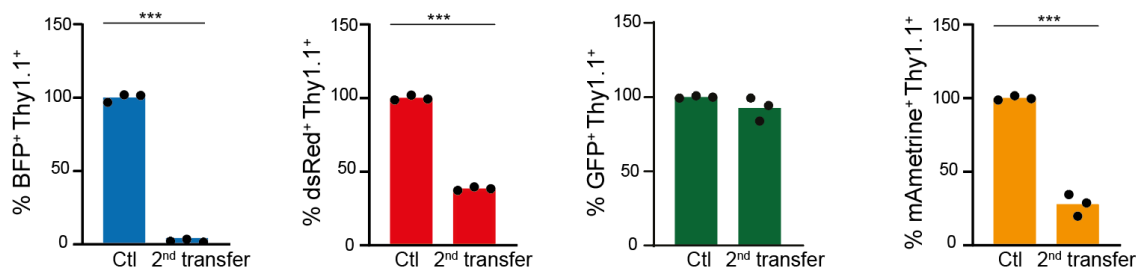


Figure 21 Differential fluorophore immunogenicity and long-term stability of viral constructs encoding BFP, dsRed, GFP, and mAmetrine

(A) Schematic overview of the experimental setup. Transgenic T cells from Smarta animals were retrovirally infected with plasmid containing either BFP, dsRed, GFP, or mAmetrine as fluorescence marker. Upon transfer into C57BL/6 mice, tail base immunization was performed (NIP-SM-MSA in IFA). At day 41, a retransfer of retrovirally infected cells was performed. For control, retrovirally infected cells were transferred into untreated control C57BL/6 animals. Splens of all animals were analyzed 2 days after the last transfer via flow cytometry.

(B) Frequencies of fluorescence⁺ T cells in control animals and retransferred animals normalized to the corresponding control group receiving only a single transfer. For each group, 3 animals were analyzed. Bars depict mean, symbols represent individual animals. Statistical analysis was performed using unpaired t-test or Mann-Whitney-U-test (* $p < 0.05$, ** $p < 0.01$, *** $p < 0.001$, ns $p > 0.05$).

3.3.3 Functional screening of eleven T_{fh} signature genes by CRISPR Cas9-mediated knock out

After the successful establishment of CRISPR Cas9-mediated target gene knock out *in vitro* (Fig. 17) and *in vivo* (Fig. 18 and Fig. 19) as well as the determination of the long-term stability of transfected cells *in vivo* (Figure 21), the function of molecules encoded by positively expressed T_{fh} signature genes (Fig. 8B) was analyzed by CRISPR Cas9-mediated knock out. Eleven genes were selected based on either

Results

published immune cell-related or so far unreported function (Table 6). Of note, Bach2 is a negative regulatory transcription factor crucially involved in T_{fh} cell maintenance (Lahmann *et al.*, 2019), and conclusively six of the eleven identified genes (*Bcl-6*, *Rgs16*, *Rnf157*, *Hmox1*, *Trpm6*, and *S100a11*) were already reported to be regulated by Bach2 (bold in Table 6).

Table 6 Eleven positively expressed T_{fh} cell signature genes screened for their function in T_{fh} cell generation by CRISPR Cas9-mediated knock out.

The provided genes have been selected from the unbiased T_{fh} signature gene transcriptome (Fig. 8) for further screening based on their reported function or so far unknown function. Genes given in bold font were additionally evaluated due to their known regulation by the T_{fh} cell transcription factor Bach2.

T _{fh} Signature Gene	Reported functions	Literature
<i>Peptidyl arginine deaminase (Padi4)</i>	<ul style="list-style-type: none"> • protein citrullination • generation of neutrophilic extracellular traps (NETs) • involved in pathology of rheumatoid arthritis • gene regulation via citrullination of transcription factors/ histones 	Li <i>et al.</i> , 2010 Y. Liu <i>et al.</i> , 2018 Sharma <i>et al.</i> , 2012 Suzuki <i>et al.</i> , 2016
<i>Sclerostin domain-containing-1 (Sostdc1)</i>	<ul style="list-style-type: none"> • antagonist of BMP/Wnt signaling • maturation of NK cells 	Laurikkala <i>et al.</i> , 2003 Millan <i>et al.</i> , 2019
<i>T cell immunoglobulin and ITIM domain (Tigit)</i>	<ul style="list-style-type: none"> • immunosuppressive effects (induction of anti-inflammatory cytokines, inhibition of NK cell cytotoxicity) • expressed on activated T cells, negative regulator of autoimmune diseases 	D. J. Lee, 2020 Lozano <i>et al.</i> , 2012 L. Mao <i>et al.</i> , 2017
<i>Family With Sequence Similarity 43 Member A (Fam43a)</i>	<ul style="list-style-type: none"> • expressed in variety of tissues (brain, cerebellum, spinal cord) • SNP found nearby Fam43 associated with autism, schizophrenia and learning difficulties; SNPS in genetic region associated with mental retardation 	Baron-Cohen <i>et al.</i> , 2014 Mulle <i>et al.</i> , 2010 Sagar <i>et al.</i> , 2013 Willatt <i>et al.</i> , 2005
<i>Regulator Of G Protein Signaling 16 (Rgs16)</i>	<ul style="list-style-type: none"> • belongs to regulators of G protein signaling (RGS) superfamily, negatively regulates G protein activity • associated with T cell trafficking and homeostasis • IL-17-mediated upregulation in T_{fh} cells promotes ability of T_{fh} to form conjugates with B cells 	(Beadling <i>et al.</i> , 1999; Ding <i>et al.</i> , 2013; I.-Y. Hwang <i>et al.</i> , 2017; Shankar <i>et al.</i> , 2012)
<i>Angiopoietin-like protein 2 (Angptl2)</i>	<ul style="list-style-type: none"> • pivotal roles in various inflammatory diseases • required for maximal B cell activation and proliferation 	Amadatsu <i>et al.</i> , 2016 Bolger-Munro <i>et al.</i> , 2019 Tatsuya Okada <i>et al.</i> , 2010

Results

	<ul style="list-style-type: none"> • pro-inflammatory, circulating levels of ANGPTL2 in various chronic inflammatory diseases and associated with poor prognosis of cardiovascular diseases, diabetes, chronic kidney disease, and various types of cancers 	Sasaki <i>et al.</i> , 2015 Thorin-Trescases & Thorin, 2017 Yugami <i>et al.</i> , 2016
Ring Finger Protein 157 (Rnf157)	<ul style="list-style-type: none"> • regulates important aspects of neuronal development • associated with cell cycle suppression and autophagy 	Dogan <i>et al.</i> , 2017 Kosacka <i>et al.</i> , 2018 Matz <i>et al.</i> , 2015
<i>Dehydrogenase/Reductase 3 (Dhrs3)</i>	<ul style="list-style-type: none"> • involved in the biosynthesis of all-trans-retinoic acid, cell adhesion, cell differentiation, and morphology 	Baldeón Rojas <i>et al.</i> , 2016 Haeseleer & Palczewski, 2000
Heme Oxygenase 1 (Hmox1)	<ul style="list-style-type: none"> • mediates cellular heme catabolism • suppression of CD4⁺ T cell activation, regulation of lineage-related cytokines and transcription factors to participate in the Th/T_{reg}-mediated immune response • related to pathogenesis of Alzheimer disease (AD) and other aging-related neurodegenerative disorders 	Schipper, 2011
Transient Receptor Potential Cation Channel Subfamily M Member 6 (Trpm6)	<ul style="list-style-type: none"> • regulation of Mg²⁺-homeostasis • TRPM6 deficiency lethal in embryonic mice 	Brandao <i>et al.</i> , 2013 Perraud <i>et al.</i> , 2004
S100 Calcium Binding Protein A11 (S100a11)	<ul style="list-style-type: none"> • member of the EF-hand Ca²⁺-binding family, activated by increased Ca²⁺ concentrations, interference with Ca²⁺-signaling pathways by binding to and regulation of target proteins • associated with protein phosphorylation, cell growth, motility, and cell survival • regulated by Th₂ cytokines 	Heizmann, 2019 Howell <i>et al.</i> , 2008 Santamaria-Kisiel <i>et al.</i> , 2006

Knock out efficiencies were again determined by Sanger sequencing (see Methods chapter 2.7.2), reporting KO efficiencies of 67 - 90% (Table 7). However, as shown in Figure 22, even a seemingly low knock out efficiency of 67% (e.g. for KO of Bcl-6) proved to be sufficient to cause strong biological effects.

Results

Table 7 Knock out of *Bach2*-regulated target genes showed knock out efficiencies of up to 90%

Retrovirally infected cells were sorted 5 days after the start of the *in vitro* culture. Upon DNA isolation and amplification of target genes via PCR, amplicons were cloned into intermediate plasmids and at least 10 clones per target gene were selected for Sanger sequencing in order to verify the knock out efficiency. Results showed an efficiency of 67 to 91%.

Target	Analyzed Sequences	Efficiency
Bcl-6	12	67%
Rgs16	11	91%
Rnf157	11	91%
Hmox1	11	91%
Trpm6	12	67%
S100a11	11	91%

For practical reasons, the analysis of the eleven target genes (*Padi4*, *Sostdc1*, *Tigit*, *Fam43a*, *Rgs16*, *Angptl2*, *Rnf157*, *Dhrs3*, *Hmox1*, *Trpm6*, *S100a11*) was performed in several independent experiments (experimental combinations summarized in Table 8). Cas9-transgenic T cells were retrovirally infected with plasmids containing target gene-specific sgRNAs and mAmetrine and cultured for four days (Fig. 22A). Fluorescence⁺ cells were subsequently sorted, followed by adoptive transfer into recipient animals. Transgenic *B1-8i* cells were co-transferred into *B6.CD28KO* recipients for the analysis of effects on B cells in a subset of experiments (see below and Table 8). Otherwise, *C57BL/6* animals were used as recipients. In both cases, the transfer was immediately followed by s.c. tail base immunization (NIP-SM-MSA in IFA or CFA). Analysis of dLNs was performed either 6 days post-transfer to test the knocked out genes' effect on T_{fh} cell generation, or 7 or 10 days post transfer to simultaneously test effects on B_{GC} cells. Since Bcl-6 is the T_{fh} cell master transcription factor (Johnston *et al.*, 2009; Nurieva, Chung, Martinez, *et al.*, 2009; Yu *et al.*, 2009), *Bcl6* knock out was included into one of the experimental sets as a positive control, anticipating a strong suppressive effect of Bcl-6 KO on the T_{fh} cell population.

Knock out of none of the investigated genes significantly affected the generation of T_{fh} cells (Fig. 22B), since no differences in T_{fh} cell percentages were found compared to the respective empty vector controls (% T_{fh} cells normalized to EV; EV 99.57 ±

29.47, Padi4 116.3 ± 26.87 , Sostdc1 91.16 ± 31.33 , Tigit 101.3 ± 20.41 , Fam43a 101.0 ± 26.50 , Rgs16 98.08 ± 44.20 , Angptl2 122.3 ± 41.74 , Rnf157 122.2 ± 26.57 , Dhrr3 95.14 ± 26.07 , Hmox1 104.90 ± 32.80 , Trpm6 72.45 ± 13.84 , S100a11 106.7 ± 53.67 ; mean \pm SD, p-values of the respective experiments are depicted in table 8). As expected however, the *Bcl6* KO positive control showed a significant reduction in the percentage of T_{fh} cells (*Bcl6* 9.14 ± 3.73 , mean \pm SD, $p=0.0040$ compared to EV), providing evidence for the efficiency of the Cas9 mediated KO *per se*.

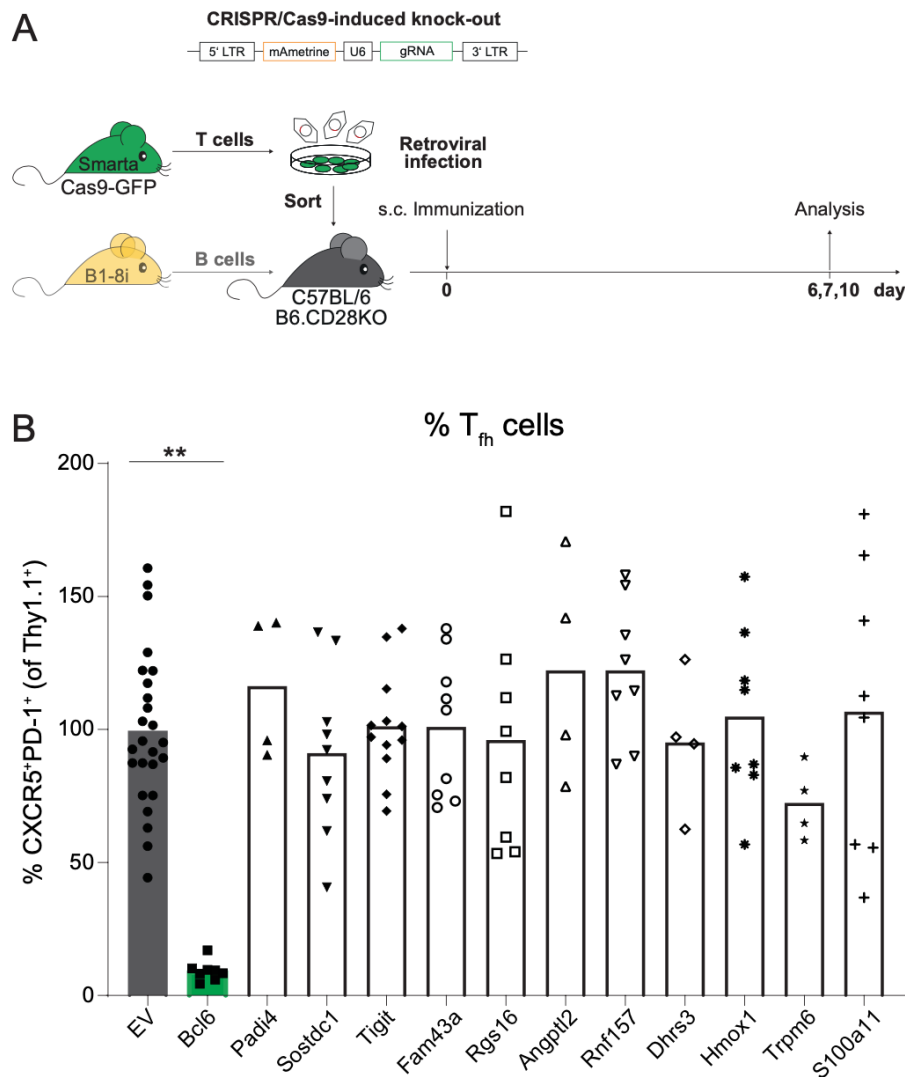


Figure 22 A CRISPR Cas9-mediated knock out of eleven positively expressed T_{fh} signature genes does not affect T_{fh} cell number

(A) Overview of the experimental setup. Cas9-transgenic T cells were retrovirally infected with plasmids containing sgRNA targeting the respective GOI. Fluorescence⁺ cells were sorted and transferred into C57BL/6 recipient animals when the effects on B cells were not investigated, or co-transferred with transgenic B1-8i cells into B6.CD28KO animals for the concomitant analysis of B cells (see Table 8 or experimental grouping). Upon transfer, s.c. tail base immunization was performed with NIP-SM-MSA in IFA or CFA. Subsequently, draining lymph nodes were analyzed by flow cytometry 6, 7, or 10 days post-transfer. (B) Frequencies of T_{fh} cells (CXCR5⁺PD-1⁺) in the

Results

different knock out conditions were normalized to counts in empty vector (EV) controls included in each experimental group. Results are shown pooled for individual genes. Bars depict mean, symbols represent individual animals. For the comparison of two groups, unpaired *t*-test was performed for statistical analysis. For the analysis of more than two groups a one-way ANOVA or Kruskal-Wallis test was performed. Subsequently, the resulting *p*-values were corrected using the two-stage linear step-up procedure of Benjamini, Krieger and Yekutieli and Holm-Šidák (* *p* < 0.05, ** *p* < 0.01, *** *p* < 0.001, ns *p* > 0.05).

Table 8 Experimental groups for CRISPR-Cas9 mediated signature gene knock out

The table depicts the experimental grouping for knock out experiment, *p*-values and experimental scheme. Knocked out genes in individual experiment groups as well the recipient animals, used adjuvant, and day of analysis are provided. *P*-values compare knock out groups to the corresponding intra-experimental empty vector control groups. Detailed information for statistical analysis is provided in figure legend 22.

#	Knocked out genes	P-values	Recipients	Immunization	Day of analysis
1	<i>Bcl6</i> , <i>Rgs16</i> , <i>Rnf157</i> , <i>Hmox1</i> , <i>S100a11</i>	<i>Bcl6</i> : 0.004; <i>Rgs16</i> : 0.3424; <i>Rnf157</i> : 0.9999; <i>Hmox1</i> : 0.9999; <i>S100a11</i> : 0.5361	<i>C57BL/6</i>	CFA	d6
2	<i>Bcl6</i> , <i>Rgs16</i> , <i>Rnf157</i> , <i>Hmox1</i> , <i>Trpm6</i> , <i>S100a11</i>	<i>Bcl6</i> : 0.004; <i>Rgs16</i> : 0.5230; <i>Rnf157</i> : 0.4494; <i>Hmox1</i> : 0.7179; <i>Trpm6</i> : 0.9999; <i>S100a11</i> : 0.4402	<i>C57BL/6</i>	CFA	d6
3	<i>Tigit</i>	<i>Tigit</i> : 0.9488	<i>C57BL/6</i>	CFA	d6
4	<i>Padi4</i> , <i>Sostdc1</i>	<i>Padi4</i> : 0.9109; <i>Sostdc1</i> : 0.6891	<i>B6.CD28KO</i>	IFA	d7
5	<i>Tigit</i> , <i>Fam43a</i> , <i>Angptl2</i> , <i>Dhrs3</i>	<i>Tigit</i> : 0.9999; <i>Fam43a</i> : 0.9898; <i>Angptl2</i> : 0.6079; <i>Dhrs3</i> : 0.9969	<i>B6.CD28KO</i>	IFA	d7
6	<i>Sostdc1</i> , <i>Fam43a</i> , <i>Tigit</i>	<i>Sostdc1</i> : 0.7035; <i>Fam43a</i> : 0.9818; <i>Tigit</i> :0.9949	<i>B6.CD28KO</i>	IFA	d10

To investigate whether knock out of signature genes affected B cell helper capability or altered T cell phenotypes, the most promising gene - *Sclerostin domain-containing-1* (*Sostdc1*) - was identified based on available literature and studied in more detail below.

3.3.3.1 The cell signaling regulator *Sostdc1* is highly upregulated in T_{fh} cells but not involved in T_{fh} cell generation or maintenance

Although screening for signature gene function via Cas9-mediated knock out did not significantly affect T_{fh} cell frequencies, a more detailed analysis of T_{fh} cell phenotype and function was performed at the example of one of the most highly upregulated T_{fh} cell genes - *Sclerostin domain-containing-1* (*Sostdc1*; cf. Figure 8B, logFC 5.6). *Sostdc1* encodes a secreted protein of the sclerostin family also known as Ectodin, USAG-1, or WISE (Hu *et al.*, 2019). Besides its negative regulation of the bone morphogenic protein (BMP) and wingless/int (Wnt) signaling, making it a pivotal regulator of developmental processes, SOSTDC1 has been shown to serve as an inhibitor of cancer progression (Bartolomé *et al.*, 2020; Cui *et al.*, 2019; Laurikkala *et al.*, 2003; Millan *et al.*, 2019; Zhou *et al.*, 2017). Since SOSTDC1 has moreover been shown to be a critical regulator in NK cell maturation and cytotoxicity (Millan *et al.*, 2019), we tested whether it also played a role in T_{fh} and B cell regulation.

To this end, Cas9-transgenic T cells were retrovirally infected with plasmid coding for *Sostdc1*-targeting sgRNA (SOSTDC1 KO) or empty control vectors (EV), sorted for GFP⁺mAmetrine⁺ T cells, and co-transferred with transgenic *B1-8i* cells into *B6.CD28KO* recipients (tail base immunization with NIP-SM-MSA in IFA after transfer). Draining LNs were analyzed 10 days post-transfer (Figure 23A).

In addition to unaffected T_{fh} cell counts in the SOSTDC1 KO compared to the EV condition (% T_{fh}; EV 44.30 ± 16.78, SOSTDC1 KO 50.78 ± 8.33, mean ± SD, p=0.4715; Figure 23D, also cf. Fig. 22B), SOSTDC1-knock out did not affect the number of transgenic T cells (% Thy-1.1⁺; EV 0.93 ± 0.54, SOSTDC1 KO 1.77 ± 1.01, mean ± SD, p=0.1426) or transgenic B cells (% CD45.1⁺; EV 0.98 ± 0.36, SOSTDC1 0.85 ± 0.20; mean ± SD, p=0.4881; data not shown).

Additionally, KO of SOSTDC1 did not alter expression of the T cell activation markers TIGIT, ICOS, and CD69 (% TIGIT⁺: EV 31.54 ± 10.95, SOSTDC1 KO 37.24 ± 4.97, p=0.3202; % ICOS⁺: EV 16.48 ± 3.96, SOSTDC1 KO 16.52 ± 3.99, p=0.9877; % CD69⁺: EV 10.30 ± 1.20, SOSTDC1 KO 13.24 ± 2.64, p=0.0952, mean ± SD, Fig. 23B and C).

Besides the analysis of phenotypic changes (i.e. T cell activation), T_{fh} cell-derived B cell helper capacity was examined via analysis of CD40L and IL-21 expression. Additionally, percentages of B_{GC} cells (CD38^{lo}GL7^{hi}) and PCs (CD19^{lo}CD138⁺) were quantified. Although T_{fh} cells of the SOSTDC1 KO group showed an increased

CD40L/IL-21 double-positive cell fraction (% CD40L/IL-21; EV 41.28 ± 7.75 , SOSTDC1 KO 52.58 ± 5.8 , mean \pm SD, $p=0.0312$), this was not reflected in changes in B cell populations, as no differences in the fraction of B_{GC} cells (% B_{GC} cells; EV 22.31 ± 16.28 , SOSTDC1 KO 26.84 ± 11.68 , mean \pm SD, $p=0.6165$) or PCs were detected (% PC; EV 2.64 ± 1.75 , SOSTDC1 KO 3.82 ± 0.87 , mean \pm SD, $p=0.2040$; Figure 23E).

To further examine the potential function of SOSTDC1, immunoglobulin subclasses were quantified in the EV and SOSTDC1 KO condition, but no changes in immunoglobulin subclass composition were detected (% IgA: EV 6.18 ± 1.11 , SOSTDC1 KO 7.64 ± 1.13 , $p=0.0602$; % IgD: EV 81.85 ± 5.27 , SOSTDC1 KO 79.20 ± 2.68 , $p=0.2468$; % IgG1: EV 23.85 ± 5.52 , SOSTDC1 KO 28.20 ± 9.91 , $p=0.1775$; % IgG2a: EV 5.05 ± 0.63 , SOSTDC1 KO 5.24 ± 0.63 , $p=0.6403$; % IgG2b: EV 12.01 ± 4.66 , SOSTDC1 KO 14.52 ± 2.43 , $p=0.3072$; % IgM: EV 5.20 ± 2.50 , SOSTDC1 KO 6.08 ± 2.36 , $p=0.5648$; mean \pm SD; Figure 23F). Only a trend towards an increased IgA class switch was noted in the absence of SOSTDC1 (% IgA: EV 6.18 ± 1.11 , SOSTDC1 KO 7.64 ± 1.13 , mean \pm SD, $p=0.0602$).

Results

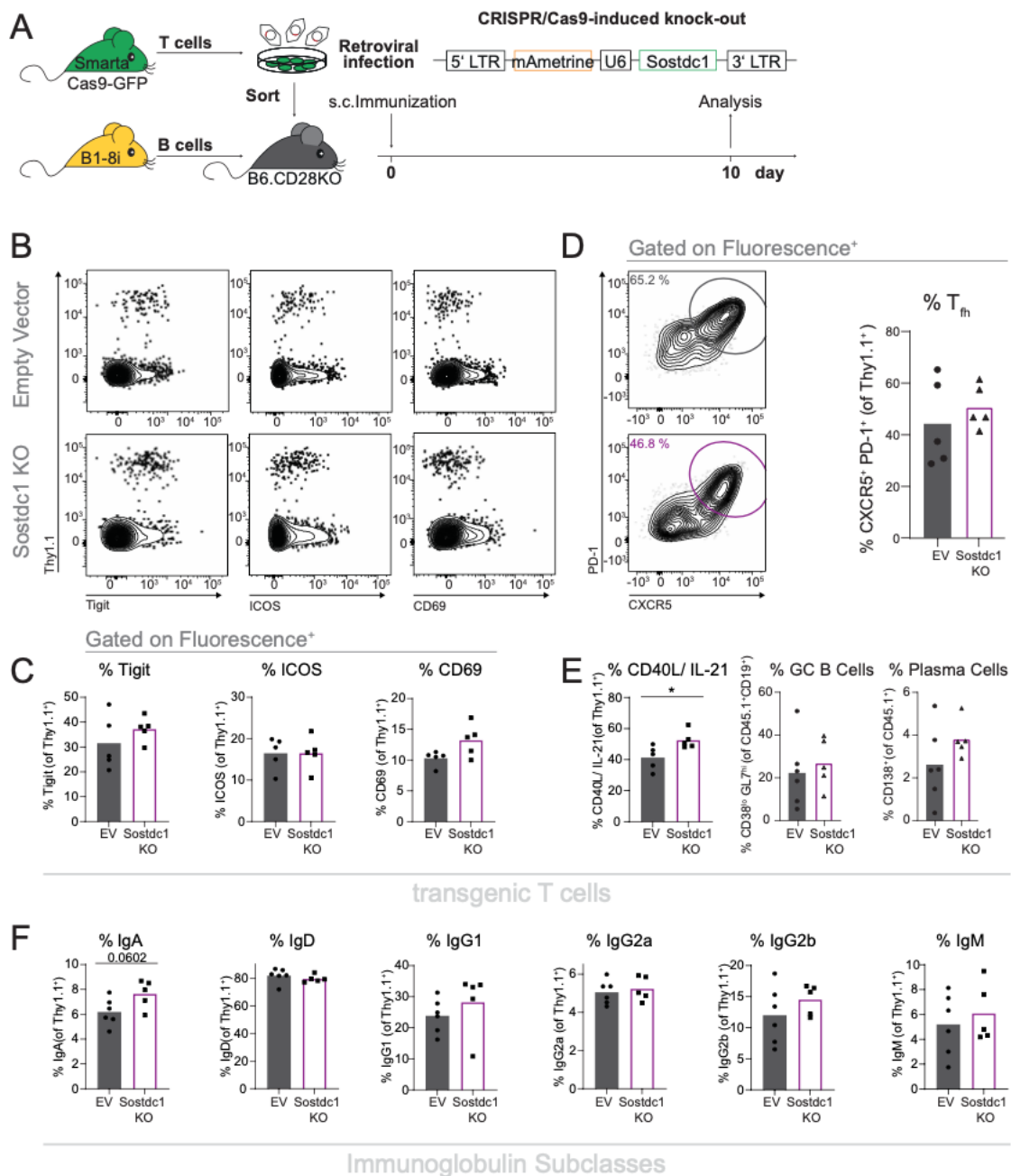


Figure 23 Knock out of *Sostdc1* does not affect transgenic T and B cells function or B cell helper capacity

(A) Overview of the experimental setup. SMxCas9-GFP transgenic T cells were retrovirally infected with a plasmid containing *Sostdc1* sgRNA (SOSTDC1 KO) and mAmetrine or an empty vector (EV, mAmetrine only). Sorted cells were co-transferred with transgenic B1-8i cells into B6.CD28KO recipients, which were tail base immunized (NIP-SM-MSA in IFA) after transfer. DLN were analyzed 10 days post-transfer via flow cytometry. (B) Representative contour plots (gated on CD4⁺ T cells) and (C) corresponding bar graphs for T cell activation markers TIGIT, ICOS, and CD69 gated on Thy-1.1⁺GFP⁺mAmetrine⁺CD4⁺ T cells (EV in grey, SOSTDC1 KO in purple). (D) Representative contour plots and corresponding bar graphs depict percentages of T_{fh} cells (CXCR5⁺PD-1⁺, color code as in C) and (E) T_{fh} cell helper capacity by CD40L/IL-21 double-positive cells and percentages of B_{GC} cells (CD38^{lo}GL7^{hi}) and plasma cells (CD19^{lo}CD138⁺, color code as in C) in SOSTDC1 KO and controls. (F) Percentages of immunoglobulin subclasses (gated on CD45.1⁺) in SOSTDC1 KO and controls. Bars depict mean, symbols

Results

represent individual animal. 5 or 6 animals were used for each group. Statistical analysis was performed using unpaired t-test or Mann-Whitney-U-test (* $p < 0.05$, ** $p < 0.01$, *** $p < 0.001$, ns $p > 0.05$).

In summary, the use of Cas9-transgenic animals and sgRNA-mediated knock out via retroviral infection provided an efficient method for the knock out of genes of interest. The use of a suitable fluorophore was found to critically affect stability of the transferred cells, enabling long-term detection of genetically modified transferred cells *in vivo*.

None of the eleven T_{fh} signature genes identified by unbiased transcriptome analysis showed an essential contribution to the generation and/or maintenance of T_{fh} cells when investigated using an adoptive transfer model. Detailed analysis of the particularly attractive T_{fh} cell signature gene *Sostdc1* did not indicate a strong involvement in general B cell and T cell function.

Given their strong differential expression in T_{fh} cells however, further detailed functional analyses of the remaining ten T_{fh} signature genes may be required to reconcile their differential expression with their functional role in T_{fh} cell physiology and pathophysiology.

4 Discussion

T_{fh} cells are a subpopulation of $CD4^+$ T cells mandatory for effective B cell help and thus the humoral immune response. By interaction with their cognate B cells within the germinal center, T_{fh} cell-mediated signals promote B cell differentiation into memory B cells and long-lived plasma cells, thereby enabling to the generation of high-affinity antibodies.

The aim of this thesis was the identification of T_{fh} signature genes and their functional characterization in T_{fh} cells. Genes involved in the maintenance of T_{fh} cells are of interest, since T_{fh} cell have been shown to broadly contribute to autoimmune disorders as well as allergies. Therefore, blocking T_{fh} -maintaining molecules would have high clinical and therapeutical relevance. Another clinically relevant aspect aims at promoting T_{fh} cell generation to enhance the generation of an effective and long-lasting humoral protection, e.g. in the context of vaccinations. Nevertheless, for both, inhibiting T_{fh} cells to counteract autoimmunity and (positively) modulating T_{fh} cell to support efficient vaccination, maintenance of T_{fh} cell activity within close physiological boundaries is thought to be essential, as exaggerated or diminished T_{fh} activation themselves bear the risk of inducing autoimmune disorders or immune incompetence, respectively. Thus, a targeted quantitative modification of T_{fh} cell activity would be of great benefit.







To identify new T_{fh} signature genes, a novel set of transcriptome data from the laboratory of Prof. Dr. Hutloff was compared to published analyses utilizing different experimental setups in order to obtain universal gene candidates independent from the adopted mouse model or immunization method. This comparison revealed 221 signature genes being either significantly up- or downregulated in T_{fh} compared to non- T_{fh} cells, 19 of which were considered particularly interesting based on their ascribed function in the literature. These genes were investigated by genetic manipulation in transgenic T cells via either selective overexpression for signature genes downregulated in T_{fh} cells, or CRISPR Cas9-mediated knock out of signature genes upregulated in T_{fh} cells, both followed by quantitative and functional T_{fh} cell investigation. To specifically study the function of RANKL, an available knock out mouse was used. Since under physiological circumstances (i.e. without immune

system activation) only very few T and B cells specifically recognize individual antigens (Moon *et al.*, 2007), an adoptive transfer system was used. To this end, transgenic T and B cells expressing the congenic markers Thy-1.1 and CD45.1, respectively, were transferred into syngeneic recipient animals *in vivo*. This allowed the tracking and unequivocal detection of transferred genetically modified lymphocytes in recipient animals.

It turned out that of the 19 genes examined, only one had an essential function in T_{fh} cell generation and maintenance: *Rara*. The 18 remaining genes showed no pronounced phenotypic changes within the T_{fh} cell population after overexpression or knock out. However, one intrinsic limitation of the adoptive transfer system is the lack of information on whether changes in target gene expression affected other cell types, such as for example regulatory T cells. Furthermore, a detailed functional analysis of the genes tested was beyond the scope of this work. Table 9 summarizes the examined genes and provides the modification paradigm (overexpression or knock out) as well as the investigated tissues.

Table 9 Summary of the experimental conditions of investigated T_{fh} cell signature genes

Novel T_{fh} cell signature genes identified based on transcriptome analysis were investigated by overexpression or knock out and analyzed in the tissues indicated by pictograms. The function of the genes in bold font was additionally studied in a chronic airway inflammation model.

Screening of Tfh signature genes	
Overexpression	Knockout
 Ccr2* 	
Plac8	Padi4
Fam129b	Sostdc1
Smad7	Tigit
Cish	Fam43a
 Cxcr6*	Rgs16
 Rara*	Angptl2
	Rnf157
	Dhrs3
	Hmox1
	Trpm6
	S100a11
additional analysis in airway inflammation model (KO and overexpression)	 Tnfsf11

4.1 T cell specific RANKL expression does not play a major role in T_{fh} cell generation, maintenance, and tissue inflammation

The co-stimulatory molecule RANKL plays a pivotal role in bone homeostasis and the immune system (Leibbrandt & Penninger, 2010; Mueller & Hess, 2012). Interestingly, the transcriptome analysis of T_{fh} and Non-T_{fh} cells (cf. Fig. 8) unraveled an increased expression of the RANKL-encoding gene *Tnfrsf11* in T_{fh} cells. Furthermore, previous preliminary results from the laboratory of Prof. Hutloff had shown significantly reduced T_{fh} cell numbers upon shRNA-mediated knock down of RANKL (unpublished observation). Thus, RANKL appeared to be involved in T_{fh} cell physiology and was considered an interesting candidate gene for functional investigation. It has already been shown that the RANKL/RANK axis is essential for T cell: DC interaction and the resulting cytokine production (Josien *et al.*, 1999). Therefore, the RANKL/RANK interaction might be essential for IL-6 production by DCs, itself being crucial in early T_{fh} cell generation (Choi *et al.*, 2013; Papillion *et al.*, 2019) and thereby essential for T_{fh} cell stabilization.

To study RANKL function in this context, inducible T cell specific RANKL-depletion was achieved by the generation of transgenic *Smarta.CreER^{T2}/RANKL^{fl/fl}* animals. First, the impact of an early RANKL KO was investigated, with the intention to confirm the preliminary results of shRNA-mediated knock down. However, previous results of shRNA-mediated RANKL knock down impacting T_{fh} cells could not be reproduced. Early knock out did not show an effect on T_{fh} cell generation and B cell helper capacity (Fig. 9). One explanation for the discrepancy compared to the effect of shRNA-mediated knock down could be unspecific off-target effects of the utilized shRNA, in contrast to the more precise genomic knock out achieved by using transgenic animals in this study. Moreover, shRNA-mediated knock down only reduced target gene expression, but did not fully abolish it. Supporting the hypothesis of shRNA effects potentially being attributed to undefined side effects, blockade of RANKL via monoclonal antibodies similarly did not reproduce prior findings (Fuhrmann, 2013; data not shown). Thus far, the functional role of early T_{fh} cell specific RANKL expression remains elusive and warrants further investigation.

Because of the lacking effects of early RANKL-depletion on T_{fh} cell number and function, we investigated whether interference with RANKL expression during later time points altered T_{fh} cell maintenance and generation of memory T_{fh} cells (Fig. 10). Generally, memory T cells and T_{fh} cells can be distinguished into 2 subpopulations: stationary cells located in secondary lymphoid organs like draining lymph nodes, and T cells (re)circulating between blood and tissues (Asrir *et al.*, 2017). Besides regarding their location, memory T cell subpopulations can be characterized by expression of distinct molecules. In contrast to other T cell populations, local memory T_{fh} cells residing within secondary lymphoid organs are $CD62L^lo$ (Asrir *et al.*, 2017; Fazilleau *et al.*, 2007), and they also show higher expression of characteristic T_{fh} cell markers such as CXCR5 and PD-1 and enable tissue residency by expression of CD69 (Asrir *et al.*, 2017).

Regarding these markers, we hypothesized a RANKL-dependent effect promoting the generation of local memory T_{fh} cells within the dLNs, which was reduced in RANKL depletion (cf. Fig. 10C) possibly resulting from poorer T cell activation. Reduced T cell activation might be confirmed by reduced CD44 expression in RANKL-depleted T cells in the spleen (cf. Fig. 10C). Moreover, CXCR3, a tissue residency marker for Th1-like T_{fh} cells, was lower in spleens of the RANKL KO group as well (cf. Fig. 10C).

Concluding, reduced memory T_{fh} cell populations and lower expression of linked markers might give a hint towards RANKL function in T_{fh} cell maintenance and long-term survival. However, these hypotheses are limited by the single iteration of these experiments and need to be repeated for statistical assessment.

There are several studies attributing a role to the RANK/RANKL axis in tissue inflammation (Bando *et al.*, 2018; Gregorczyk & Maślanka, 2020; Guerrini *et al.*, 2015; Loser *et al.*, 2006; Shimamura *et al.*, 2014) and excitingly, transcriptome analysis of T cells in lung and lung-dLN of our chronic airway inflammation model showed strong RANKL expression within the T_{fh} and T_{fh} -like population (cf. Figure 8A, unpublished data, raw data not shown).

So far, contradictory statements regarding the role of RANKL in tissue inflammation have been reported. In the brain, intestines and skin, RANKL signaling negatively enhanced immunoregulatory functions (Bando *et al.*, 2018; Loser *et al.*, 2006; Maruyama *et al.*, 2006; Shimamura *et al.*, 2014), e.g. by selectively upregulating molecules inducing immune tolerance (Lischke *et al.*, 2012). On the contrary, other

studies highlighted a pro-inflammatory role to RANKL by influencing cell migration in a local inflammation model (Gregorczyk & Maślanka, 2020; Guerrini *et al.*, 2015).

To further investigate T cell specific RANKL function in inflamed tissue, transgenic *Smarta.CreER^{T2}/RANKL^{fl/fl}* animals were used in our chronic airway inflammation model, enabling us to study T cell specific effects in non-lymphoid tissue and dLN.

In contrast to published reports, analysis of dLNs of WT and RANKL-depleted animals in our model did neither show changes in the frequency, nor the phenotype of transgenic T and B cells (cf. Fig. 11B, C, and D). However, in lungs of RANKL KO animals, T cells exhibited significantly higher levels of CXCR3 expression (cf. Fig. 11D), which was accompanied by reduced PC counts by up to 40% compared to wildtype littermates (cf. Fig. 11C).

The CXCR3 chemokine receptor is associated with effector T cell migration and especially linked to the Th₁ effector cell lineage (Groom & Luster, 2011). The observation of increased CXCR3 expression in RANKL KO mice supports the hypothesis of reduced T_{fh} cell activation as a consequence of lower DC interaction and priming of naïve T cells. Subsequently, RANKL KO cells might favor differentiation into T effector cell programs like Th₁ cells. To elaborate this hypothesis, future experiments should co-quantify master transcription factors T-bet and Bcl-6 to determine Th₁ and T_{fh} cell fractions, respectively. Furthermore, cytokine and chemokine/chemokine receptor profiles should be generated to confirm the findings.

An additional hint towards altered Th subsets was the observation of reduced PCs within RANKL KO mice. Reduced B cell helper capacity of transgenic T cells would reduce GC reactions and thereby proliferation and maturation of PCs and B_{mem} cells. Surprisingly, B_{GC} cell frequencies did not differ between the two groups and as in dLN (cf. Fig. 11B), T_{fh}-like cell frequencies were not altered in lungs of WT versus RANKL KO mice (cf. Fig. 11C). Since B cells, similar to DCs, express the RANKL receptors RANK and OPG, and since both are upregulated upon CD40 stimulation (Yun *et al.*, 1998), RANK/RANKL signaling within GC reactions may promote T_{fh}/B_{GC} cell interaction and support T_{fh} cell survival, the latter already being known for T cells in general (Yun *et al.*, 1998). To investigate GC reaction effectiveness, future experiments should address B cell functionality by the analysis of RANK expression or immunoglobulin subclasses.

These results are in contrast to the inflammation-promoting function of RANKL via enhanced migration, as seen e.g. in CNS inflammation and asthma (Gregorczyk & Maślanka, 2020; Guerrini *et al.*, 2015), but might support the hypothesis of regulatory functions of RANKL. The relatively minor effects of RANKL KO on T_{fh} cells could furthermore be explained using LPS as adjuvant in the immunization solution. LPS is known to promote Th₁ cell generation and IFN- γ secretion and both, LPS administration and IFN- γ can interfere with RANKL/RANK signaling (Maruyama *et al.*, 2006; Takayanagi *et al.*, 2000). Therefore, RANKL signaling in WT controls could be altered and additional experiments are required to address the impact of LPS administration onto RANKL signaling in the adopted model system. Finally, a transcriptome analysis comparing gene expression profiles of T_{fh} cells in WT and RANKL KO animals did not unravel RANKL-induced changes in the T_{fh} cell transcriptome (cf. Fig. 12), supporting the above findings of a small impact of RANKL on T and B cell function.

In summary, the use of RANKL KO animals revealed contradictory results compared to previous shRNA-mediated RANKL knock down experiments and no direct functional role of RANKL within T_{fh} cells was identified.

Of note however, possible functional redundancy of RANKL should be considered. Already in 1999, Bachmann and colleagues showed only minor contribution of RANKL/RANK to CD40L/CD40 signaling during viral infections (Bachmann *et al.*, 1999), and the authors favored an indirect involvement of RANKL in T-B cell-signaling, with functional impairment in antigen-presenting cells, such as DCs, and subsequent effects on viability and cytokine production, rather than a direct impact on T cells. The adaptor protein TRAF6, a downstream target of RANK, appears to be one of the central molecules in RANK signaling, as TRAF^{-/-} mice show the same phenotype as RANK^{-/-} mice (Mueller & Hess, 2012; Naito *et al.*, 1999). As shown before (Kadono *et al.*, 2005; Walsh & Choi, 2014), CD40 can activate this signaling cascade as well, albeit at reduced levels. Therefore, it would be important to analyze CD40, CD40L, related cytokines and the corresponding receptors (especially IL-6 and IL-6R) in future experiments in order to follow up the hypothesis of an indirect influence of RANKL/RANK interaction in T_{fh} cells via, e.g., IL-6 production by DCs.

4.2 RAR α signaling has a key role in the humoral immune response

Vitamin A is an essential vitamin for the human organism with important functions in growth, reproduction, cellular integrity, vision, and the immune system. For the latter, vitamin A and its derivative retinoic acid are known to influence immune cell regulation and function, migration, and differentiation (Friesen *et al.*, 2020; Liang *et al.*, 2020; Parastouei *et al.*, 2020; Scholz *et al.*, 2020). A special role is attributed to vitamin A and its metabolites in the context of allergic diseases, such as bronchial asthma. and various studies previously showed effects on T cell subsets, though reported results were often contradictory. The *Rara* gene, encoding the nuclear retinoic acid receptor α , emerged as one of the most strongly regulated genes in our transcriptome analysis comparing T_{fh} and Non-T_{fh} cells (cf. Fig. 8B). Since still very little is known about RA/RAR α signaling in T_{fh} cells, the functional analysis of this newly identified T_{fh} signature gene appeared of great interest. Firstly, the chronic allergy-like respiratory inflammation was investigated using the airway inflammation model described above. Secondly, characteristic, asthma-associated, and Th₂ cell-mediated responses (Hufnagl & Jensen-Jarolim, 2018; Matheu *et al.*, 2009) were evoked by Th₂ pre-polarization prior to adoptive transfer.

Successful Th₂ pre-polarization was confirmed by increased expression of Th₂-mediated cytokines such as IL-4, IL-5, and IL-13 (Fig. 14 C, also see Scholz *et al.*, 2020). RAR α overexpression strongly impacted the humoral immune response by affecting both transgenic T and B cells. Increased activation of RAR α significantly increased T_{fh} cells frequency in lungs and lung-dLNs, which was additionally accompanied by an increased generation of lung GC-like B cells (Fig. 14B and D). Finally, overexpression of *Rara* resulted in an additional downregulation of the Th₁-mediated cytokine IFN- γ and the lineage-defining transcription factor T-bet (Scholz *et al.*, 2020).

In line with altered T cell subtypes, differences in immunoglobulin subtype composition were detected: The Th₁ cell-related subtype IgG2a was significantly downregulated, while the IgG1 subtype and IgE, both preferentially produced in Th₂-mediated immune responses, were significantly upregulated (cf. Fig. 14E). No change was found in the production of IgA (cf. Fig. 14E), potentially due to the early time of analysis as a

sufficient amount of IgA cannot be detected until 15 days following the first immunization in our respiratory inflammation model (unpublished observation). In general, increased RAR α signaling led to an immunoglobulin class switch towards Th₂ subtypes and a concomitant IgM downregulation (Fig. 14E). The increased expression of IgE in Th₂ polarized environments has already been demonstrated previously (Gould & Sutton, 2008) and IgE subclass immunoglobulins are a known driver in allergies and bronchial asthma, with enhanced disease progression caused by vitamin A derivatives due to Th₂ induction (Gould & Sutton, 2008; Matheu *et al.*, 2009).

Conclusively, the impact of vitamin A and its derivatives has been studied mostly by hyper- or hypoalimentation in previous studies and often resulted in promotion of the Th₂ cells. In addition, regulatory T cell generation was often enhanced, while Th₁ and Th₁₇ cell responses were suppressed (Dawson *et al.*, 2006; Goswami & Kaplan, 2016; Liang *et al.*, 2020; Parastouei *et al.*, 2020; Penkert *et al.*, 2020; Xiao *et al.*, 2008).

Furthermore, Xie and colleagues investigated the effect of vitamin A derivatives on T_{fh} cells using an autoimmune myasthenia gravis disease model (Xie *et al.*, 2013). In contrast to the findings reported here, the authors showed an effect of ATRA supplementation on regulatory T cells, with decreased T_{fh} cells under ATRA supplementation and increased numbers of T_{fr} cells. Interestingly, a recent publication (Friesen *et al.*, 2020) uncovered a dual functionality of RAR α : In a ligand-bound state, RAR α exerted the known function as a transcription factor. Independent from ligand-binding however, RAR α was also involved in faster signaling via the PI3K/Akt/mTor pathway, affecting especially T cell activation and metabolism. The authors concluded that this ligand-independent RAR α activation led to a general, polarization-independent T cell activation and profiling. These effects seemed to be unique within T cells and, similar to other studies, strongly concentration dependent (Friesen *et al.*, 2020).

In contrast to most previous studies, the results presented here used T cell specific RAR α overexpression to study the role of RAR α signaling without the requirement of differential supplementation of vitamin A or vitamin A derivatives. This overexpression showed a general activation of T_{fh}, Th₂ and Th₁₇ cells, which was further supported by an increased expression of the respective transcription factors and cytokines (Scholz

et al., 2020) and correlated well with the data published by Friesen *et al.* (2020). Consistent with Friesen *et al.* (2020), a significant reduction in the Th₁-mediated immune response was detected upon RAR α overexpression. The fact that the transferred cells differentiated strongly towards T_{fh} cells despite Th₂ pre-polarization suggests RAR α as a strong stimulus for T_{fh} cell generation.

In summary, increased RAR α signaling led to an enhanced humoral immune reaction with a maintained Th₂ response. Thus, the administration of vitamin A and its derivatives may be contraindicated in e.g. asthma. In contrast, in the context of vaccines, vitamin A supplementation might be useful as it supports the generation of T_{fh} cells and thereby the production of high-affinity antibodies and long-lived plasma cells. Nevertheless, open aspects, e.g. the functional differences of ligand-independent versus ligand-bound RAR α states, the concentration-dependence of the recruited downstream signaling pathways (Friesen *et al.*, 2020), and possible means for supplementation warrant further investigation.

4.3 CRISPR Cas9-mediated knock out in transgenic T cells provides an efficient method for screening of gene function

For CRISPR Cas9 mediated knock out, Cas9-expressing *Smarta* or *Smarta.CreER^{T2}* animals were generated. The resulting mouse lines harbored the *Smarta* transgenic TCR, the congenic marker Thy-1.1, and the Cas9 either constitutively expressed or inducible at defined timed points. To validate functional KO induction of genes of interest in antigen-specific T cells in an adoptive transfer model, preliminary test trials were carried out assessing KO efficacy and cell survival. KO efficiency of various sgRNAs was systematically studied by the analysis of the sgRNA-targeted sequence by means of T7EI assays or Sanger sequencing (Fig. 16 and Table 7) to identify constructs with high KO efficacy. High KO efficacy was crucial since for most investigated genes no antibodies are available for rapid *post hoc* KO detection by e.g. flow cytometry. Sanger sequencing was used as the method of choice for most of the constructs and enabled reliable and quantitative determination of KO efficiency. After a successful KO verification *in vitro* and *in vivo* (cf. Fig. 17-19), retrovirally infected cells transferred into recipient animals were found to gradually diminish over the course of 13 days (Fig. 20). Several steps of the used protocol were subsequently

considered as potentially affecting T cell survival. One critical step was the T cell activation itself, though activation was necessary for retroviral infection. Another factor related to activation-induced cell loss could involve an upregulation of Fas and Fas ligands upon repeated TCR stimulation, which leads to activation-induced cell death (AICD). AICD physiologically serves as a feedback mechanism in ongoing immune responses (Varadhachary *et al.*, 1997) and in cell culture, comparatively strong stimulation of cells prior to transfer might result in T cell exhaustion and AICD induction. A third critical step affecting cell survival is the sorting procedure required to isolate retrovirally infected cells, which imposes mechanical stress caused by small nozzle size as well as sample and sheath pressure. Finally, sample handling and duration of the sorting procedure are known to impact the viability of sorted cells. Sorting was generally mandatory, since, first, the infection efficiency of transgenic T cells is only about 40% (data not shown). Second, without sorting possible effects of target gene KO could be concealed by functionally intact, genetically unmodified cells, especially given potential survival advantage of non-transfected over infected cells. To optimize cell viability, nozzle sizes of 85 μm or 100 μm were used in subsequent experiments (Fig. 13 and Fig. 22) and for future experiments, magnetic activated cell sorting (MACS) may be considered an alternative to flow-cytometry. Disadvantages of MACS however are the loss of cells during the purification process (own observations, data not shown) and the restriction to endogenously expressed or labeled surface markers instead of utilizing cytosolic fluorophore expression.

To exclude the sorting procedure as a major cause of transgenic T cells loss, control experiments were performed in which unsorted cells were transferred directly into recipient animals (cf. Fig 20 and 21). In these experiments, rejection was present even without prior cell sorting, but differential cell loss depending on the expressed fluorophore was noted, with most rapid loss in BFP⁺ T cells. BFP⁺ T cells were hardly detectable already 6 days post-transfer (Fig. 20), strongly suggestive of innate immune system-mediated rejection. Therefore, survival of cells transfected with the fluorescent markers dsRed, GFP, and mAmetrine were compared to BFP in a subsequent experiment (cf. Fig. 21). All markers except GFP showed a variable degree of rejection, with BFP showing the shortest survival times. GFP however could not be used as a marker for retroviral infection, since Cas9 expression was coupled to GFP expression in the utilized mouse model. Consequently, the second-most stable marker mAmetrine was used for retroviral transfection, which had previously provided

good results until at least day 17 post-transfer in overexpression experiments performed in CD28 knock out mice in the Hutloff laboratory.

4.4 Limitations of the adoptive transfer model at the example of *Sostdc1* knock out in antigen-specific T cells

After successful establishment of the CRISPR-Cas9 system in transgenic T cells, 11 genes of interest (see Table 6) were functionally investigated. Surprisingly, none of the examined genes affected the generation of T_{fh} cells. Furthermore, neither defects in B cell help, nor phenotypic effects on B cells or T cells were detected (cf. Fig. 22). *Sclerostin domain-containing-1* (*Sostdc1*) was selected for an in-depth functional analysis, since it was found as one of the most highly regulated genes in T_{fh} cells and because a recent study found it to play a crucial role in T_{fh} cell function (Wu *et al.*, 2020). SOSTDC1 is a secreted cell signaling regulator playing pivotal roles in developmental processes and the inhibition of cancer progression by interference with BMP and Wnt signaling (Bartolomé *et al.*, 2020; Cui *et al.*, 2019; Laurikkala *et al.*, 2003; Millan *et al.*, 2019; Zhou *et al.*, 2017). In addition, SOSTDC1 was already related functionally to the innate immune system via its regulation of NK cells (Millan *et al.*, 2019). However, SOSTDC1 KO neither lead to changed T_{fh} cell numbers, nor did it impact the expression of various surface molecules or cytokines. Only an increased expression of CD40L and IL-21 indicated an increased activation of SOSTDC1-deleted cells compared to WT control animals. No reduction in the capacity of the B cell help in SOSTDC1 KO animals was noted, as neither B_{GC} cells nor PCs were altered. In addition, there were no significant changes within immunoglobulin subclasses, indicative of an unaltered cytokine milieu within SOSTDC1 KO animals. In summary, SOSTDC1 seemed dispensable for the generation and maintenance of T_{fh} cells or T_{fh} cell function, specifically B cell help and the generation of high affinity antibodies (cf. Fig. 23).

Similar to our study, a recent study by Hu and colleagues investigated the function of SOSTDC1 in T_{fh} cells (Hu *et al.*, 2019). The authors adopted a Lymphocytic choriomeningitis virus (LCMV) infection model and confirmed high expression of *Sostdc1* in T_{fh} cells compared to Th_1 cells. In accordance with our findings, no effects of T cell specific SOSTDC1 KO on T_{fh} cells or B cells were detected. In addition to Th_1

cells, T_{reg} cells and T_{fr} cells were examined and similarly no changes were detected, leading the authors to conclude that SOSTDC1 had no regulatory function on T_{fh} cells. In contrast, based on an inhibition of Wnt signaling pathways by SOSTDC1, another recent study found evidence for an involvement of SOSTDC1⁺ T_{fh} cells in the generation and maintenance of T_{fr} cells, thus indicating an essential role SOSTDC1 in humoral immune regulation (Wu *et al.*, 2020).

Since both, the route of antigen delivery and the used mouse model very likely have a major influence on the gained results, the discrepant results on the role of SOSTDC1 in T_{fh} cells may be brought into accordance, first, by considering the different antigen delivery strategies. Here, a subcutaneous immunization model was used, while Hu and colleagues used a LCMV-based model with intraperitoneal injection and similarly found no involvement of SOSTDC1. The study by Wu *et al.* made use of both, an influenza model adopting intranasal immunization and a subcutaneous inflammation model. Regarding antigen delivery, it was found that intraperitoneal administration promotes tolerance rather than immunity due to quick antigen degradation, whereas subcutaneous antigen injection with Freund's adjuvant provided longer antigen activity and thereby promoted humoral immune response (Kearney *et al.*, 1994). Besides the mode of antigen delivery, the used adjuvant, the aggregate state, and the tissue residence time of the antigen are crucial determinants of the generation of a pro-inflammatory or regulatory immune response (Kearney *et al.*, 1994; Lischke *et al.*, 2012).

Second, in our study as well as in the study by Hu and colleagues, T cell-specific SOSTDC1 KO was investigated, while Wu and colleagues used a global (i.e. a non-T cell-specific) SOSTDC1 KO mouse model.

Moreover, in this study and partially in the study by Hu and colleagues, an adoptive transfer system was used that is ideally suited to specifically identify molecular mechanisms or key elements of T cell interaction within different tissues (Lischke *et al.*, 2012). In contrast, by introducing a global knock out, nonspecific non-T cell-derived effects might have been detected by the authors' experimental system. Moreover, one limitation of most adoptive transfer models is that effects on regulatory T cells or follicular regulatory T cells cannot be investigated, since the monoclonal TCR with given affinity against an individual epitope prevents generation of these cell types.

In conclusion, dissimilar experimental conditions could trigger differential immune responses and complicates a direct comparison of the effect on specific cell populations. With the conditions of the mouse system and the type of immunization chosen in this study, potential effects on populations such as T_{fr} cells might have been masked or biased, inferring an additional reason for the lacking effects of the remaining genes studied.

In summary, genetic modification of antigen-specific T cells by means of viral overexpression or CRISPR Cas9-mediated knock out was found to be an ideal method for fast and efficient screening for diverse gene's function. 19 of the most highly up- or downregulated T_{fh} cell signature genes were systematically investigated. Besides *Rara*, none of them individually seemed essential for the generation of T_{fh} cell. These findings could be related to the limitation of the utilized model system, as exemplified by the knock out of *SOSTDC1*. To overcome its limitations, diverse immunization models and organs might be studied. Moreover, this study primarily used constitutive knock out and overexpression of target genes. The use of an inducible system will expand future opportunities to e.g. investigate molecules essential for T_{fh} cell maintenance and memory formation during temporally well-defined, more restricted developmental episodes. Nevertheless, if the highly differential expression of the identified genes was taken as evidence for their essential role in T_{fh} cells and the functional immune responses, their indispensability might be evolutionarily disadvantageous. Therefore, functional redundancy of the investigated molecules may therefore potentially have occluded any apparent effect on T_{fh} cells upon KO or OE of individual signature genes. Proof of redundancy by parallel modification of multiple genes and transcriptome analysis allow for in-depth analysis. Combinatorial genetic interference or in-depth functional analysis of the identified signature genes may therefore represent worthwhile routes to be considered for further experimental work.

5 Conclusion

Due to the essential role of T_{fh} cells in the humoral immune response and their involvement in the generation of autoimmune disease, molecules generating and maintaining the T_{fh} phenotype are of particular interest. By comparing four different transcriptome analyses of T_{fh} versus non- T_{fh} cells, 19 molecules significantly over- or underexpressed in T_{fh} cells were identified and investigated functionally. To this end, transgenic T cells were genetically modified by CRISPR Cas9-mediated knock out or viral overexpression of the respective genes. The use of an adoptive transfer mouse model enabled tracking of modified antigen-specific T cells *in vivo* and the analysis of changes in T_{fh} cell function and phenotype, thereby establishing a fast and efficient screening paradigm for various gene's function. Of the 19 molecules examined, nuclear retinoc acid receptor RAR α (RAR α), showed an essential function for T_{fh} cells. *Rara* overexpression showed a significant increase in the humoral immune response, as shown by increased T_{fh} and GC B cells, revealing RAR α a potential target with clinical relevance. The 18 remaining molecules however were not found to have a significant impact on T_{fh} cell numbers as a first assessment of their involvement in T_{fh} cell physiology. Our transcriptome analysis, besides the 19 genes studied here, furthermore revealed a variety of differentially regulated T_{fh} signature genes that should be investigated further. To do so, the experimental approach established here provides an efficient tool.

The importance of a better understanding about T_{fh} cells has become increasingly clear in recent years, with regards to both, their pivotal role in the physiological adaptive immune response and their involvement in a multitude of immunological pathologies. In these challenging times, when the headstone to overcome a global pandemic has been the development of effective immunological treatments, T_{fh} cells residing at the crossroad between acute and maintained immune response have moved into the focus of contemporary science and promise further important insights to be revealed.

6 Literature

- Akkaya, M., Kwak, K., & Pierce, S. K. (2020). B cell memory: building two walls of protection against pathogens. *Nature Reviews Immunology*, *20*(4), 229–238.
- Alankus, B., Ecker, V., Vahl, N., Braun, M., Weichert, W., Macher-Göppinger, S., Gehring, T., Neumayer, T., Zenz, T., Buchner, M., & Ruland, J. (2020). Pathological RANK signaling in B cells drives autoimmunity and chronic lymphocytic leukemia. *Journal of Experimental Medicine*, *218*(2).
- Allen, C. D. C., Okada, T., & Cyster, J. G. (2007). Germinal-center organization and cellular dynamics. *Immunity*, *27*(2), 190–202.
- Allen, C. D. C., Okada, T., Tang, H. L., & Cyster, J. G. (2007). Imaging of germinal center selection events during affinity maturation. *Science*, *315*(5811), 528–531.
- Amadatsu, T., Morinaga, J., Kawano, T., Terada, K., Kadomatsu, T., Miyata, K., Endo, M., Kasamo, D., Kuratsu, J.-I., & Oike, Y. (2016). Macrophage-derived angiopoietin-like protein 2 exacerbates brain damage by accelerating acute inflammation after ischemia-reperfusion. *PloS One*, *11*(11), e0166285–e0166285.
- Anderson, D. M., Maraskovsky, E., Billingsley, W. L., Dougall, W. C., Tometsko, M. E., Roux, E. R., Teepe, M. C., DuBose, R. F., Cosman, D., & Galibert, L. (1997). A homologue of the TNF receptor and its ligand enhance T-cell growth and dendritic-cell function. *Nature*, *390*(6656), 175–179.
- Aruffo, A., Farrington, M., Hollenbaugh, D., Li, X., Milatovich, A., Nonoyama, S., Bajorath, J., Grosmaire, L. S., Stenkamp, R., Neubauer, M., Roberts, R. L., Noelle, R. J., Ledbetter, J. A., Francke, U., & Ochs, H. D. (1993). The CD40 ligand, gp39, is defective in activated T cells from patients with X-linked hyper-IgM syndrome. *Cell*, *72*(2), 291–300.
- Ashurst, A. S., Flórido, M., Lin, L. C. W., Quan, D., Armitage, E., Stifter, S. A., Stambas, J., & Britton, W. J. (2019). CXCR6-deficiency improves the control of pulmonary Mycobacterium tuberculosis and influenza infection independent of T-lymphocyte recruitment to the lungs. *Frontiers in Immunology*, *10*, 339.
- Asrir, A., Aloulou, M., Gador, M., Pérals, C., & Fazilleau, N. (2017). Interconnected subsets of memory follicular helper T cells have different effector functions. *Nature Communications*, *8*(1).
- Baaten, B., Tinoco, R., Chen, A., & Bradley, L. (2012). Regulation of antigen-experienced T cells: Lessons from the quintessential memory marker CD44. *Frontiers in Immunology*, *3*, 23.
- Bachmann, M. F., Wong, B. R., Josien, R., Steinman, R. M., Oxenius, A., & Choi, Y. (1999). TRANCE, a tumor necrosis factor family member critical for CD40 ligand-independent T helper cell activation. *The Journal of Experimental Medicine*, *189*(7), 1025–1031.

- Bakos, E., Thaïss, C. A., Kramer, M. P., Cohen, S., Radomir, L., Orr, I., Kaushansky, N., Ben-Nun, A., Becker-Herman, S., & Shachar, I. (2017). CCR2 regulates the immune response by modulating the interconversion and function of effector and regulatory T cells. *The Journal of Immunology*, *198*(12), 4659 – 4671.
- Baldeón Rojas, L., Weigelt, K., de Wit, H., Ozcan, B., van Oudenaren, A., Sempértegui, F., Sijbrands, E., Grosse, L., van Zonneveld, A.-J., Drexhage, H. A., & Leenen, P. J. M. (2016). Study on inflammation-related genes and microRNAs, with special emphasis on the vascular repair factor HGF and miR-574-3p, in monocytes and serum of patients with T2D. *Diabetology & Metabolic Syndrome*, *8*, 6.
- Ballesteros-Tato, A., León, B., Graf, B. A., Moquin, A., Adams, P. S., Lund, F. E., & Randall, T. D. (2012). Interleukin-2 inhibits germinal center formation by limiting T follicular helper cell differentiation. *Immunity*, *36*(5), 847–856.
- Bando, J. K., Gilfillan, S., Song, C., McDonald, K. G., Huang, S. C. C., Newberry, R. D., Kobayashi, Y., Allan, D. S. J., Carlyle, J. R., Cella, M., & Colonna, M. (2018). The tumor necrosis factor superfamily member RANKL suppresses effector cytokine production in group 3 innate lymphoid cells. *Immunity*, *48*(6), 1208-1219.
- Baptista, A. P., Gola, A., Huang, Y., Milanez-Almeida, P., Torabi-Parizi, P., Urban Jr., J. F., Shapiro, V. S., Gerner, M. Y., & Germain, R. N. (2019). The chemoattractant receptor Ebi2 drives ontranodal naive CD4⁺ T cell peripheralization to promote effective adaptive immunity. *Immunity*, *50*(5), 1188-1201.
- Baron-Cohen, S., Cassidy, S., Auyeung, B., Allison, C., Achoukhi, M., Robertson, S., Pohl, A., & Lai, M.-C. (2014). Attenuation of typical sex differences in 800 adults with autism vs. 3,900 controls. *PloS One*, *9*(7), e102251–e102251.
- Bartleson, J. M., Viehmann Milam, A. A., Donermeyer, D. L., Horvath, S., Xia, Y., Egawa, T., & Allen, P. M. (2020). Strength of tonic T cell receptor signaling instructs T follicular helper cell-fate decisions. *Nature Immunology*, *21*(11), 1384–1396.
- Bartolomé, R. A., Pintado-Berninches, L., Jaén, M., de Los Ríos, V., Imbaud, J. I., & Casal, J. I. (2020). SOSTDC1 promotes invasion and liver metastasis in colorectal cancer via interaction with ALCAM/CD166. *Oncogene*, *39*(38), 6085–6098.
- Baumjohann, D., Preite, S., Reboldi, A., Ronchi, F., Ansel, K. M., Lanzavecchia, A., & Sallusto, F. (2013). Persistent antigen and germinal center B cells sustain T follicular helper cell responses and phenotype. *Immunity*, *38*(3), 596–605.
- Bauquet, A. T., Jin, H., Paterson, A. M., Mitsdoerffer, M., Ho, I.-C., Sharpe, A. H., & Kuchroo, V. K. (2009). The costimulatory molecule ICOS regulates the expression of c-Maf and IL-21 in the development of follicular T helper cells and TH-17 cells. *Nature Immunology*, *10*(2), 167–175.

- Beadling, C., Druey, K. M., Richter, G., Kehrl, J. H., & Smith, K. A. (1999). Regulators of G protein signaling exhibit distinct patterns of gene expression and target G protein specificity in human lymphocytes. *The Journal of Immunology*, *162*(5), 2677–2682.
- Bélanger, S., & Crotty, S. (2016). Dances with cytokines, featuring TFH cells, IL-21, IL-4 and B cells. *Nature Immunology*, *17*(10), 1135–1136.
- Benjamini, Y., & Hochberg, Y. (1995). Controlling the false discovery rate - A practical and powerful approach to multiple testing. *J. Royal Statist. Soc., Series B*, *57*, 289–300.
- Bocharnikov, A. V., Keegan, J., Wacleche, V. S., Cao, Y., Fonseka, C. Y., Wang, G., Muise, E. S., Zhang, K. X., Arazi, A., Keras, G., Li, Z. J., Qu, Y., Gurish, M. F., Petri, M., Buyon, J. P., Putterman, C., Wofsy, D., James, J. A., Guthridge, J. M., Rao, D. A. (2019). PD-1hiCXCR5+ T peripheral helper cells promote B cell responses in lupus via MAF and IL-21. *JCI Insight*, *4*(20), e130062.
- Boettcher, M., & McManus, M. T. (2015). Choosing the right tool for the job: RNAi, TALEN, or CRISPR. *Molecular Cell*, *58*(4), 575–585.
- Bolduc, A., Long, E., Stapler, D., Cascalho, M., Tsubata, T., Koni, P. A., & Shimoda, M. (2010). Constitutive CD40L expression on B cells prematurely terminates germinal center response and leads to augmented plasma cell production in T cell areas. *Journal of Immunology*, *185*(1), 220–230.
- Bolger-Munro, M., Choi, K., Scurll, J. M., Abraham, L., Chappell, R. S., Sheen, D., Dang-Lawson, M., Wu, X., Priatel, J. J., Coombs, D., Hammer, J. A., & Gold, M. R. (2019). Arp2/3 complex-driven spatial patterning of the BCR enhances immune synapse formation, BCR signaling and B cell activation. *ELife*, *8*, e44574.
- Bono, M. R., Tejon, G., Flores-Santibañez, F., Fernandez, D., Roseblatt, M., & Sauma, D. (2016). Retinoic acid as a modulator of T cell immunity. *Nutrients*, *8*(6), 1–15.
- Boyle, J. (2008). Molecular biology of the cell, 5th edition by B. Alberts, A. Johnson, J. Lewis, M. Raff, K. Roberts, and P. Walter. *Biochemistry and Molecular Biology Education*, *36*(4), 317–318.
- Brandao, K., Deason-Towne, F., Perraud, A.-L., & Schmitz, C. (2013). The role of Mg²⁺ in immune cells. *Immunologic Research*, *55*(1), 261–269.
- Breitfeld, D., Ohl, L., Kremmer, E., Ellwart, J., Sallusto, F., Lipp, M., & Förster, R. (2000). Follicular B helper T cells express CXC chemokine receptor 5, localize to B cell follicles, and support immunoglobulin production. *Journal of Experimental Medicine*, *192*(11), 1545–1551.
- Cannons, J. L., Qi, H., Lu, K. T., Dutta, M., Gomez-Rodriguez, J., Cheng, J., Wakeland, E. K., Germain, R. N., & Schwartzberg, P. L. (2010). Optimal germinal center responses require a multistage T cell:B cell adhesion process involving integrins, SLAM-associated protein, and CD84. *Immunity*, *32*(2), 253–

265.

- Carmona-Fernandes, D., Santos, M. J., Perpétuo, I. P., Fonseca, J. E., & Canhão, H. (2011). Soluble receptor activator of nuclear factor κ B ligand/osteoprotegerin ratio is increased in systemic lupus erythematosus patients. *Arthritis Research & Therapy*, *13*(5), R175.
- Carow, B., Gao, Y., Terán, G., Yang, X. O., Dong, C., Yoshimura, A., & Rottenberg, M. E. (2017). CISH controls bacterial burden early after infection with *Mycobacterium tuberculosis* in mice. *Tuberculosis*, *107*, 175–180.
- Catron, D. M., Rusch, L. K., Hataye, J., Itano, A. A., & Jenkins, M. K. (2006). CD4+ T cells that enter the draining lymph nodes after antigen injection participate in the primary response and become central-memory cells. *Journal of Experimental Medicine*, *203*(4), 1045–1054.
- Chen, J., Trounstine, M., Kurahara, C., Young, F., Kuo, C. C., Xu, Y., Loring, J. F., Alt, F. W., & Huszar, D. (1993). B cell development in mice that lack one or both immunoglobulin κ light chain genes. *EMBO Journal*, *12*(3), 821–830.
- Chen, S., Evans, H. G., & Evans, D. R. (2011). FAM129B/MINERVA, a novel adherens junction-associated protein, suppresses apoptosis in HeLa cells. *The Journal of Biological Chemistry*, *286*(12), 10201–10209.
- Choi, Y. S., Eto, D., Yang, J. A., Lao, C., & Crotty, S. (2013). Cutting edge: STAT1 is required for IL-6–mediated Bcl6 induction for early follicular helper cell differentiation. *The Journal of Immunology*, *190*(7), 3049–3053.
- Chu, V. T., Graf, R., Wirtz, T., Weber, T., Favret, J., Li, X., Petsch, K., Tran, N. T., Sieweke, M. H., Berek, C., Kühn, R., & Rajewsky, K. (2016). Efficient CRISPR-mediated mutagenesis in primary immune cells using CrispRGold and a C57BL/6 Cas9 transgenic mouse line. *Proceedings of the National Academy of Sciences of the United States of America*, *113*(44), 12514–12519.
- Chu, V. T., Weber, T., Graf, R., Sommermann, T., Petsch, K., Sack, U., Volchkov, P., Rajewsky, K., & Kühn, R. (2016). Efficient generation of Rosa26 knock-in mice using CRISPR/Cas9 in C57BL/6 zygotes. *BMC Biotechnology*, *16*(1), 1–15.
- Coquet, J. M., Schuijs, M. J., Smyth, M. J., Deswarte, K., Beyaert, R., Braun, H., Boon, L., Hedestam, G. B. K., Nutt, S. L., Hammad, H., & Lambrecht, B. N. (2015). Interleukin-21-producing CD4⁺ T cells promote type 2 immunity to house dust mites. *Immunity*, *43*(2), 318–330.
- Cossarizza, A., Chang, H.-D., Radbruch, A., Akdis, M., Andrä, I., Annunziato, F., Bacher, P., Barnaba, V., Battistini, L., Bauer, W. M., Baumgart, S., Becher, B., Beisker, W., Berek, C., Blanco, A., Borsellino, G., Boulais, P. E., Brinkman, R. R., Büscher, M., ... Zimmermann, J. (2017). Guidelines for the use of flow cytometry and cell sorting in immunological studies. *European Journal of Immunology*, *47*(10), 1584–1797.
- Crotty, S. (2019). T follicular helper cell biology: A decade of discovery and diseases.

- Immunity*, 50(5), 1132–1148.
- Cui, Y., Zhang, F., Jia, Y., Sun, L., Chen, M., Wu, S., Verhoeft, K., & Li, Y. (2019). The BMP antagonist, *SOSTDC1*, restrains gastric cancer progression via inactivation of *c-Jun* signaling. *9*(11), 2331–2348.
- Dawson, H. D., Collins, G., Pyle, R., Key, M., Weeraratna, A., Deep-Dixit, V., Nadal, C. N., & Taub, D. D. (2006). Direct and indirect effects of retinoic acid on human Th2 cytokine and chemokine expression by human T lymphocytes. *BMC Immunology*, 7, 1–15.
- De Silva, N. S., & Klein, U. (2015). Dynamics of B cells in germinal centres. *Nature Reviews Immunology*, 15(3), 137–148.
- Deenick, E. K., Chan, A., Ma, C. S., Gatto, D., Schwartzberg, P. L., Brink, R., & Tangye, S. G. (2010). Follicular helper T cell differentiation requires continuous antigen presentation that is independent of unique B cell signaling. *Immunity*, 33(2), 241–253.
- Deenick, E. K., & Ma, C. S. (2011). The regulation and role of T follicular helper cells in immunity. *Immunology*, 134(4), 361–367.
- Depoil, D., Zaru, R., Guiraud, M., Chauveau, A., Harriague, J., Bismuth, G., Utzny, C., Müller, S., & Valitutti, S. (2005). Immunological synapses are versatile structures enabling selective T cell polarization. *Immunity*, 22(2), 185–194.
- Diehl, S. A., Schmidlin, H., Nagasawa, M., Blom, B., & Spits, H. (2012). IL-6 Triggers IL-21 production by human CD4⁺ T cells to drive STAT3-dependent plasma cell differentiation in B cells. *Immunology & Cell Biology*, 90(8), 802–811.
- Dienz, O., Eaton, S. M., Bond, J. P., Neveu, W., Moquin, D., Noubade, R., Briso, E. M., Charland, C., Leonard, W. J., Ciliberto, G., Teuscher, C., Haynes, L., & Rincon, M. (2009). The induction of antibody production by IL-6 is indirectly mediated by IL-21 produced by CD4⁺ T cells. *Journal of Experimental Medicine*, 206(1), 69–78.
- Ding, Y., Li, J., Wu, Q., Yang, P., Luo, B., Xie, S., Druey, K. M., Zajac, A. J., Hsu, H.-C., & Mountz, J. D. (2013). IL-17RA is essential for optimal localization of follicular T_h cells in the germinal center light zone to promote autoantibody-producing B cells. *The Journal of Immunology*, 191(4), 1614–1624.
- DiToro, D., Winstead, C. J., Pham, D., Witte, S., Andargachew, R., Singer, J. R., Wilson, C. G., Zindl, C. L., Luther, R. J., Silberger, D. J., Weaver, B. T., Kolawole, E. M., Martinez, R. J., Turner, H., Hatton, R. D., Moon, J. J., Way, S. S., Evavold, B. D., & Weaver, C. T. (2018). Differential IL-2 expression defines developmental fates of follicular versus nonfollicular helper T cells. *Science*, 361(6407), eaao2933.
- Dogan, T., Gnad, F., Chan, J., Phu, L., Young, A., Chen, M. J., Doll, S., Stokes, M. P., Belvin, M., Friedman, L. S., Kirkpatrick, D. S., Hoeflich, K. P., & Hatzivassiliou, G. (2017). Role of the E3 ubiquitin ligase RNF157 as a novel downstream effector linking PI3K and MAPK signaling pathways to the cell

- cycle. *The Journal of Biological Chemistry*, 292(35), 14311–14324.
- Dong, L., He, Y., Cao, Y., Wang, Y., Jia, A., Wang, Y., Yang, Q., Li, W., Bi, Y., & Liu, G. (2020). Functional differentiation and regulation of follicular T helper cells in inflammation and autoimmunity. *Immunology*, 163(1), 19–32.
- Doudna, J. A., & Charpentier, E. (2014). The new frontier of genome engineering with CRISPR-Cas9. *Science*, 346(6213).
- El Khoury, L. Y., Campbell, J. M., & Clark, K. J. (2018). Chapter 17 - The transition of zebrafish functional genetics from random mutagenesis to targeted integration. In *Molecular-Genetic and Statistical Techniques for Behavioral and Neural Research*, (N. R. Gerlai, pp. 401–416). Academic Press.
- Elgueta, R., Benson, M. J., De Vries, V. C., Wasiuk, A., Guo, Y., & Noelle, R. J. (2009). Molecular mechanism and function of CD40/CD40L engagement in the immune system. *Immunological Reviews*, 229(1), 152–172.
- Fantini, M. C., Becker, C., Monteleone, G., Pallone, F., Galle, P. R., & Neurath, M. F. (2004). Cutting edge: TGF- β induces a regulatory phenotype in CD4⁺CD25⁻ T cells through Foxp3 induction and down-regulation of Smad7. *The Journal of Immunology*, 172(9), 5149–5153.
- Fazilleau, N., Eisenbraun, M. D., Malherbe, L., Ebright, J. N., Pogue-Caley, R. R., McHeyzer-Williams, L. J., & McHeyzer-Williams, M. G. (2007). Lymphoid reservoirs of antigen-specific memory T helper cells. *Nature Immunology*, 8(7), 753–761.
- Fonseca JE, Cortez-Dias N, Francisco A, Sobral M, Canhão H, Resende C, Castelão W, Macieira C, Sequeira G, Saraiva F, da Silva JA, Carmo-Fonseca M, V. Q. M. (2005). Inflammatory cell infiltrate and RANKL/OPG expression in rheumatoid synovium: comparison with other inflammatory arthropathies and correlation with outcome. *Clin Exp Rheumatol.*, 23(2), 185–192.
- Förster, R., Mattis, A. E., Kremmer, E., Wolf, E., Brem, G., & Lipp, M. (1996). A Putative Chemokine Receptor, BLR1, Directs B cell migration to defined lymphoid organs and specific anatomic compartments of the spleen. *Cell*, 87(6), 1037–1047.
- Friesen, L. R., Gu, B., & Kim, C. H. (2020). A ligand-independent fast function of RAR α promotes exit from metabolic quiescence upon T cell activation and controls T cell differentiation. *Mucosal Immunology*, 14, 1–13.
- Fuhrmann, F. (2013). *Charakterisierung ICOS-regulierter Moleküle in der Entwicklung von folliculären T-Helferzellen*. Dissertation. Fachbereich der Biologie, Chemie, Pharmazie der Freien Universität Berlin.
- Gao, X., Wang, H., Chen, Z., Zhou, P., & Yu, D. (2020). An optimized method to differentiate mouse follicular helper T cells in vitro. *Cellular & Molecular Immunology*, 17(7), 779–781.
- Garo, L. P., Ajay, A. K., Fujiwara, M., Beynon, V., Kuhn, C., Gabriely, G., Sadhukan,

- S., Raheja, R., Rubino, S., Weiner, H. L., & Murugaiyan, G. (2019). Smad7 controls immunoregulatory PDL2/1-PD1 signaling in intestinal inflammation and autoimmunity. *Cell Reports*, 28(13), 3353-3366.
- Gatto, D., & Brink, R. (2013). B cell localization: Regulation by EBI2 and its oxysterol ligand. *Trends in Immunology*, 34(7), 336–341.
- Gitlin, A. D., Shulman, Z., & Nussenzweig, M. C. (2014). Clonal selection in the germinal centre by regulated proliferation and hypermutation. *Nature*, 509(7502), 637–640.
- Good-Jacobson, K. L., & Shlomchik, M. J. (2010). Plasticity and heterogeneity in the generation of memory B cells and long-lived plasma cells: The influence of germinal center interactions and dynamics. *The Journal of Immunology*, 185(6), 3117–3125.
- Gorelik, L., Fields, P. E., & Flavell, R. A. (2000). Cutting edge: TGF- β inhibits T_h type 2 development through inhibition of GATA-3 expression. *The Journal of Immunology*, 165(9), 4773–4777.
- Goswami, R., & Kaplan, M. H. (2016). Essential vitamins for an effective T cell response. *World Journal of Immunology*, 6(1), 39.
- Gould, H. J., & Sutton, B. J. (2008). IgE in allergy and asthma today. *Nature Reviews Immunology*, 8(3), 205–217.
- Grant, S. M., Lou, M., Yao, L., Germain, R. N., & Radtke, A. J. (2020). The lymph node at a glance - how spatial organization optimizes the immune response. *Journal of Cell Science*, 133(5), 1–7.
- Green, H. N., & Mellanby, E. (1928). Vitamin A as an anti-infective agent. *British Medical Journal*, 2(3537), 691–696.
- Green, J. A., & Cyster, J. G. (2012). S1PR2 links germinal center confinement and growth regulation. *Immunological Reviews*, 247(1), 36–51.
- Gregorczyk, I., & Maślanka, T. (2020). Blockade of RANKL/RANK and NF- κ B signalling pathways as novel therapeutic strategies for allergic asthma: A comparative study in a mouse model of allergic airway inflammation. *European Journal of Pharmacology*, 879, 173129.
- Grimbacher, B., Hutloff, A., Schlesier, M., Glocker, E., Warnatz, K., Dräger, R., Eibel, H., Fischer, B., Schäffer, A. A., Mages, H. W., Kroczeck, R. A., & Peter, H. H. (2003). Homozygous loss of ICOS is associated with adult-onset common variable immunodeficiency. *Nature Immunology*, 4(3), 261–268.
- Groom, J. R., & Luster, A. D. (2011). CXCR3 in T cell function. *Experimental Cell Research*, 317(5), 620–631.
- Guerrini, M. M., Okamoto, K., Komatsu, N., Sawa, S., Danks, L., Penninger, J. M., Nakashima, T., & Takayanagi, H. (2015). Inhibition of the TNF family cytokine RANKL prevents autoimmune inflammation in the central nervous system.

Immunity, 43(6), 1174–1185.

- Guittard, G., Dios-Esponera, A., Palmer, D. C., Akpan, I., Barr, V. A., Manna, A., Restifo, N. P., & Samelson, L. E. (2018). The Cish SH2 domain is essential for PLC- γ 1 regulation in TCR stimulated CD8⁺ T cells. *Scientific Reports*, 8(1), 5336.
- Haeseleer, F., & Palczewski, K. B. T.-M. in E. (2000). [24] Short-chain dehydrogenases/reductases in retina. In *Vertebrate Phototransduction and the Visual Cycle, Part B* (Vol. 316, pp. 372–383). Academic Press.
- Hauptelshofer, S., Leichsenring, T., Berg, S., Pedreiturria, X., Joachim, S. C., Tischoff, I., Otte, J.-M., Bopp, T., Fantini, M. C., Esser, C., Willbold, D., Gold, R., Faissner, S., & Kleiter, I. (2019). Smad7 in intestinal CD4⁺ T cells determines autoimmunity in a spontaneous model of multiple sclerosis. *Proceedings of the National Academy of Sciences of the United States of America*, 116(51), 25860–25869.
- Haynes, N. M., Allen, C. D. C., Lesley, R., Ansel, K. M., Killeen, N., & Cyster, J. G. (2007). Role of CXCR5 and CCR7 in follicular T_h cell positioning and appearance of a programmed cell death gene-1 high germinal center-associated subpopulation. *The Journal of Immunology*, 179(8), 5099–5108.
- Heath, W. R., Kato, Y., Steiner, T. M., & Caminschi, I. (2019). Antigen presentation by dendritic cells for B cell activation. *Current Opinion in Immunology*, 58, 44–52.
- Heine, G., Hollstein, T., Treptow, S., Radbruch, A., & Worm, M. (2018). 9-cis retinoic acid modulates the type I allergic immune response. *Journal of Allergy and Clinical Immunology*, 141(2), 650-658.
- Heizmann, C. W. (2019). *Ca²⁺-binding proteins of the EF-hand superfamily: Diagnostic and prognostic biomarkers and novel therapeutic targets*. In *Calcium-binding proteins of the EF-Hand Superfamily: From Basics to Medical Applications* (C. W. Heizmann; pp. 157–186). Springer New York.
- Hille, F., Richter, H., Wong, S. P., Bratovič, M., Ressel, S., & Charpentier, E. (2018). The biology of CRISPR-Cas: Backward and forward. *Cell*, 172(6), 1239–1259.
- Hilligan, K. L., & Ronchese, F. (2020). Antigen presentation by dendritic cells and their instruction of CD4⁺ T helper cell responses. *Cellular & Molecular Immunology*, 17(6), 587–599.
- Hiramatsu, Y., Suto, A., Kashiwakuma, D., Kanari, H., Kagami, S., Ikeda, K., Hirose, K., Watanabe, N., Grusby, M. J., Iwamoto, I., & Nakajima, H. (2010). c-Maf activates the promoter and enhancer of the IL-21 gene, and TGF- β inhibits c-Maf-induced IL-21 production in CD4⁺ T cells. *Journal of Leukocyte Biology*, 87(4), 703–712.
- Howell, M. D., Fairchild, H. R., Kim, B. E., Bin, L., Boguniewicz, M., Redzic, J. S., Hansen, K. C., & Leung, D. Y. M. (2008). Th2 cytokines act on S100/A11 to downregulate keratinocyte differentiation. *Journal of Investigative Dermatology*,

128(9), 2248–2258.

- Hu, Jianjun, Wu, J., Li, Y., Wang, Z., Tang, J., Li, Z., Hu, L., Huang, Q., Ye, L., & Xu, L. (2019). Sclerostin domain-containing protein 1 is dispensable for the differentiation of follicular helper and follicular regulatory T cells during acute viral infection. *American Journal of Translational Research*, 11(6), 3722–3736.
- Hu, Joyce, Havenar-Daughton, C., & Crotty, S. (2013). Modulation of SAP dependent T/B cell interactions as a strategy to improve vaccination. *Current Opinion in Virology*, 3(3), 363–370.
- Hu, R., Kagele, D. A., Huffaker, T. B., Runtsch, M. C., Alexander, M., Liu, J., Bake, E., Su, W., Williams, M. A., Rao, D. S., Möller, T., Garden, G. A., Round, J. L., & O'Connell, R. M. (2014). miR-155 promotes T follicular helper cell accumulation during chronic, low-grade inflammation. *Immunity*, 41(4), 605–619.
- Huet, S., Groux, H., Caillou, B., Valentin, H., Prieur, A. M., & Bernard, A. (1989). CD44 contributes to T cell activation. *The Journal of Immunology*, 143(3), 798–801.
- Hufnagl, K., & Jensen-Jarolim, E. (2018). Vitamin A and D in allergy: From experimental animal models and cellular studies to human disease. *Allergo Journal International*, 27(3), 72–78.
- Hutloff, A. (2018). *T follicular helper-like cells inflamed non-lymphoid tissues*. *Frontiers in Immunology*, 9, 1707.
- Hutloff, A., Büchner, K., Reiter, K., Baelde, H. J., Odendahl, M., Jacobi, A., Dörner, T., & Kroczeck, R. A. (2004). Involvement of inducible costimulator in the exaggerated memory B cell and plasma cell generation in systemic lupus erythematosus. *Arthritis & Rheumatism*, 50(10), 3211–3220.
- Hwang, I.-Y., Park, C., Harrison, K., & Kehrl, J. H. (2017). Normal thymocyte egress, T cell trafficking, and CD4⁺ T cell homeostasis require interactions between RGS proteins and Gα_{i2}. *Journal of Immunology*, 198(7), 2721–2734. h
- Hwang, J.-R., Byeon, Y., Kim, D., & Park, S.-G. (2020). Recent insights of T cell receptor-mediated signaling pathways for T cell activation and development. *Experimental & Molecular Medicine*, 52(5), 750–761.
- Isaac, R. S., Jiang, F., Doudna, J. A., Lim, W. A., Narlikar, G. J., & Almeida, R. (2016). Nucleosome breathing and remodeling constrain CRISPR-Cas9 function. *eLife*, 5, 1–14.
- Jensen, K. T., Fløe, L., Petersen, T. S., Huang, J., Xu, F., Bolund, L., Luo, Y., & Lin, L. (2017). Chromatin accessibility and guide sequence secondary structure affect CRISPR-Cas9 gene editing efficiency. *FEBS Letters*, 591(13), 1892–1901.
- Ji, H., Lee, J.-H., Wang, Y., Pang, Y., Zhang, T., Xia, Y., Zhong, L., Lyu, J., & Lu, Z. (2016). EGFR phosphorylates FAM129B to promote Ras activation. *Proceedings of the National Academy of Sciences of the United States of*

America, 113(3), 644–649.

- Jia, Y., Ying, X., Zhou, J., Chen, Y., Luo, X., Xie, S., Wang, Q. chuan, Hu, W., & Wang, L. (2018). The novel KLF4/PLAC8 signaling pathway regulates lung cancer growth. *Cell Death & Disease*, 9(6), 603.
- Jimenez-Preitner, M., Berney, X., Uldry, M., Vitali, A., Cinti, S., Ledford, J. G., & Thorens, B. (2011). Plac8 is an inducer of C/EBP β required for brown fat differentiation, thermoregulation, and control of body weight. *Cell Metabolism*, 14(5), 658–670.
- Jin, Y., Andersen, G., Yorgov, D., Ferrara, T. M., Ben, S., Brownson, K. M., Holland, P. J., Birlea, S. A., Siebert, J., Hartmann, A., Lienert, A., Van Geel, N., Lambert, J., Luiten, R. M., Wolkerstorfer, A., Wietze Van Der Veen, J. P., Bennett, D. C., Taïeb, A., Ezzedine, K., ... Spritz, R. A. (2016). Genome-wide association studies of autoimmune vitiligo identify 23 new risk loci and highlight key pathways and regulatory variants. *Nature Genetics*, 48(11), 1418–1424.
- Johnson, R. M., Kerr, M. S., & Slaven, J. E. (2012). Plac8-dependent and inducible NO synthase-dependent mechanisms clear *Chlamydia muridarum* infections from the genital tract. *The Journal of Immunology*, 188(4), 1896–1904.
- Johnston, R. J., Choi, Y. S., Diamond, J. A., Yang, J. A., & Crotty, S. (2012). STAT5 is a potent negative regulator of TFH cell differentiation. *The Journal of Experimental Medicine*, 209(2), 243–250.
- Johnston, R. J., Poholek, A. C., DiToro, D., Yusuf, I., Eto, D., Barnett, B., Dent, A. L., Craft, J., & Crotty, S. (2009). Bcl6 and Blimp-1 are reciprocal and antagonistic regulators of T follicular helper cell differentiation. *Science*, 325(5943), 1006–1010.
- Josien, R., Wong, B. R., Li, H.-L., Steinman, R. M., & Choi, Y. (1999). TRANCE, a TNF family member, is differentially expressed on T cell subsets and induces cytokine production in dendritic cells. *The Journal of Immunology*, 162(5), 2562–2568.
- Kadono, Y., Okada, F., Perchonock, C., Jang, H. D., Lee, S. Y., Kim, N., & Choi, Y. (2005). Strength of TRAF6 signalling determines osteoclastogenesis. *EMBO Reports*, 6(2), 171–176.
- Kang, S. G., Liu, W.-H., Lu, P., Jin, H. Y., Lim, H. W., Shepherd, J., Fremgen, D., Verdin, E., Oldstone, M. B. A., Qi, H., Teijaro, J. R., & Xiao, C. (2013). MicroRNAs of the miR-17~92 family are critical regulators of T_{FH} differentiation. *Nature Immunology*, 14(8), 849–857.
- Kara, E. E., McKenzie, D. R., Bastow, C. R., Gregor, C. E., Fenix, K. A., Ogunniyi, A. D., Paton, J. C., Mack, M., Pombal, D. R., Seillet, C., Dubois, B., Liston, A., MacDonald, K. P. A., Belz, G. T., Smyth, M. J., Hill, G. R., Comerford, I., & McColl, S. R. (2015). CCR2 defines in vivo development and homing of IL-23-driven GM-CSF-producing Th17 cells. *Nature Communications*, 6(1), 8644.

- Kawabe, T., Naka, T., Yoshida, K., Tanaka, T., Fujiwara, H., Suematsu, S., Yoshida, N., Kishimoto, T., & Kikutani, H. (1994). The immune responses in CD40-deficient mice: Impaired immunoglobulin class switching and germinal center formation. *Immunity*, 1(3), 167–178.
- Kearney, E. R., Pape, K. A., Loh, D. Y., & Jenkins, M. K. (1994). Visualization of peptide-specific T cell immunity and peripheral tolerance induction in vivo. *Immunity*, 1(4), 327–339.
- Kim, D., Pertea, G., Trapnell, C., Pimentel, H., Kelley, R., & Salzberg, S. L. (2013). TopHat2: accurate alignment of transcriptomes in the presence of insertions, deletions and gene fusions. *Genome Biology*, 14(4), R36.
- Kleiter, I., Song, J., Lukas, D., Hasan, M., Neumann, B., Croxford, A. L., Pedré, X., Hövelmeyer, N., Yogev, N., Mildner, A., Prinz, M., Wiese, E., Reifenberg, K., Bittner, S., Wiendl, H., Steinman, L., Becker, C., Bogdahn, U., Neurath, M. F., ... Waisman, A. (2010). Smad7 in T cells drives T helper 1 responses in multiple sclerosis and experimental autoimmune encephalomyelitis. *Brain : A Journal of Neurology*, 133(4), 1067–1081.
- Kosacka, J., Nowicki, M., Paeschke, S., Baum, P., Blüher, M., & Klötting, N. (2018). Up-regulated autophagy: as a protective factor in adipose tissue of WOKW rats with metabolic syndrome. *Diabetology & Metabolic Syndrome*, 10, 13.
- Kumar, B. V., Connors, T. J., & Farber, D. L. (2018). Human T cell development, localization, and function throughout life. *Immunity*, 48(2), 202–213.
- Künzli, M., Schreiner, D., Pereboom, T. C., Swarnalekha, N., Litzler, L. C., Lötscher, J., Ertuna, Y. I., Roux, J., Geier, F., Jakob, R. P., Maier, T., Hess, C., Taylor, J. J., & King, C. G. (2020). Long-lived T follicular helper cells retain plasticity and help sustain humoral immunity. *Science Immunology*, 5(45), eaay5552.
- Lahmann, A., Kuhrau, J., Fuhrmann, F., Heinrich, F., Bauer, L., Durek, P., Mashreghi, M.-F., & Hutloff, A. (2019). Bach2 controls T follicular helper cells by direct repression of Bcl-6. *The Journal of Immunology*, 202(8), 2229–2239.
- Langmead, B., & Salzberg, S. L. (2012). Fast gapped-read alignment with Bowtie 2. *Nature Methods*, 9(4), 357–359.
- Latham, L. E., Wikenheiser, D. J., & Stumhofer, J. S. (2020). ICOS signaling promotes a secondary humoral response after re-challenge with *Plasmodium chabaudi chabaudi* AS. *PLoS Pathogens*, 16(4), 1–28.
- Latta, M., Mohan, K., & Issekutz, T. B. (2007). CXCR6 is expressed on T cells in both T helper type 1 (Th1) inflammation and allergen-induced Th2 lung inflammation but is only a weak mediator of chemotaxis. *Immunology*, 121(4), 555–564.
- Laurikkala, J., Kassai, Y., Pakkasjärvi, L., Thesleff, I., & Itoh, N. (2003). Identification of a secreted BMP antagonist, ectodin, integrating BMP, FGF, and SHH signals from the tooth enamel knot. *Developmental Biology*, 264(1), 91–105.

- Ledford, J. G., Kovarova, M., & Koller, B. H. (2007). Impaired host defense in mice lacking ONZIN. *The Journal of Immunology*, 178(8), 5132–5143.
- Lee, D. J. (2020). The relationship between TIGIT⁺ regulatory T cells and autoimmune disease. *International Immunopharmacology*, 83, 106378.
- Lee, J.-Y., Skon, C. N., Lee, Y. J., Oh, S., Taylor, J. J., Malhotra, D., Jenkins, M. K., Rosenfeld, M. G., Hogquist, K. A., & Jameson, S. C. (2015). The transcription factor KLF2 restrains CD4⁺ T follicular helper cell differentiation. *Immunity*, 42(2), 252–264.
- Leibbrandt, A., & Penninger, J. M. (2010). Novel functions of RANK(L) signaling in the immune system. *Advances in Experimental Medicine and Biology*, 658(L), 77–94.
- Li, J., Lu, E., Yi, T., & Cyster, J. G. (2016). EB12 augments Tfh cell fate by promoting interaction with IL-2-queenching dendritic cells. *Nature*, 533(7601), 110–114.
- Li, P., Li, M., Lindberg, M. R., Kennett, M. J., Xiong, N., & Wang, Y. (2010). PAD4 is essential for antibacterial innate immunity mediated by neutrophil extracellular traps. *Journal of Experimental Medicine*, 207(9), 1853–1862.
- Liang, Y., Yi, P., Wang, X., Zhang, B., Jie, Z., Soong, L., & Sun, J. (2020). Retinoic acid modulates hyperactive T cell responses and protects vitamin A-deficient mice against persistent lymphocytic choriomeningitis virus infection. *The Journal of Immunology*, 204(11), 2984–2994.
- Liao, Y., Smyth, G. K., & Shi, W. (2014). featureCounts: an efficient general purpose program for assigning sequence reads to genomic features. *Bioinformatics*, 30(7), 923–930.
- Linterman, M. A., Pierson, W., Lee, S. K., Kallies, A., Kawamoto, S., Rayner, T. F., Srivastava, M., Divekar, D. P., Beaton, L., Hogan, J. J., Fagarasan, S., Liston, A., Smith, K. G. C., & Vinuesa, C. G. (2011). Foxp3⁺ follicular regulatory T cells control the germinal center response. *Nature Medicine*, 17(8), 975–982.
- Lischke, T., Hegemann, A., Gurka, S., Vu Van, D., Burmeister, Y., Lam, K.-P., Kershaw, O., Mollenkopf, H.-J., Mages, H. W., Hutloff, A., & Kroczek, R. A. (2012). Comprehensive analysis of CD4⁺ T cells in the decision between tolerance and immunity in vivo reveals a pivotal role for ICOS. *The Journal of Immunology*, 189(1), 234–244.
- Liu, R., Wu, Q., Su, D., Che, N., Chen, H., Geng, L., Chen, J., Chen, W., Li, X., & Sun, L. (2012). A regulatory effect of IL-21 on T follicular helper-like cell and B cell in rheumatoid arthritis. *Arthritis Research and Therapy*, 14(6), R255.
- Liu, X., Yan, X., Zhong, B., Nurieva, R. I., Wang, A., Wang, X., Martin-Orozco, N., Wang, Y., Chang, S. H., Esplugues, E., Flavell, R. A., Tian, Q., & Dong, C. (2012). Bcl6 expression specifies the T follicular helper cell program in vivo. *Journal of Experimental Medicine*, 209(10), 1841–1852.
- Liu, Y., Lightfoot, Y. L., Seto, N., Carmona-Rivera, C., Moore, E., Goel, R., O’Neil, L.,

- Mistry, P., Hoffmann, V., Mondal, S., Premnath, P. N., Gribbons, K., Dell'Orso, S., Jiang, K., Thompson, P. R., Sun, H.-W., Coonrod, S. A., & Kaplan, M. J. (2018). Peptidylarginine deiminases 2 and 4 modulate innate and adaptive immune responses in TLR-7-dependent lupus. *JCI Insight*, 3(23), e124729.
- Loser, K., Mehling, A., Loeser, S., Apelt, J., Kuhn, A., Grabbe, S., Schwarz, T., Penninger, J. M., & Beissert, S. (2006). Epidermal RANKL controls regulatory T-cell numbers via activation of dendritic cells. *Nature Medicine*, 12(12), 1372–1379.
- Love, M. I., Huber, W., & Anders, S. (2014). Moderated estimation of fold change and dispersion for RNA-seq data with DESeq2. *Genome Biology*, 15(12), 550.
- Lozano, E., Dominguez-Villar, M., Kuchroo, V., & Hafler, D. A. (2012). The TIGIT/CD226 axis regulates human T cell function. *Journal of Immunology (Baltimore, Md. : 1950)*, 188(8), 3869–3875.
- Lu, K. T., Kanno, Y., Cannons, J. L., Handon, R., Bible, P., Elkahloun, A. G., Anderson, S. M., Wei, L., Sun, H., O'Shea, J. J., & Schwartzberg, P. L. (2011). Functional and epigenetic studies reveal multistep differentiation and plasticity of in vitro-generated and in vivo-derived follicular T helper cells. *Immunity*, 35(4), 622–632.
- Lu, L. L., Suscovich, T. J., Fortune, S. M., & Alter, G. (2018). Beyond binding: antibody effector functions in infectious diseases. *Nature Reviews Immunology*, 18(1), 46–61.
- Lu, P., Shih, C., & Qi, H. (2017). Germinal centers: Ephrin B1-mediated repulsion and signaling control germinal center T cell territoriality and function. *Science*, 356(6339).
- Ma, C. S., Avery, D. T., Chan, A., Batten, M., Bustamante, J., Boisson-Dupuis, S., Arkwright, P. D., Kreins, A. Y., Averbuch, D., Engelhard, D., Magdorf, K., Kilic, S. S., Minegishi, Y., Nonoyama, S., French, M. A., Choo, S., Smart, J. M., Peake, J., Wong, M., ... Tangye, S. G. (2012). Functional STAT3 deficiency compromises the generation of human T follicular helper cells. *Blood*, 119(17), 3997–4008.
- Manzo, A., Vitolo, B., Humby, F., Caporali, R., Jarrossay, D., Dell'Accio, F., Ciardelli, L., Ugucioni, M., Montecucco, C., & Pitzalis, C. (2008). Mature antigen-experienced T helper cells synthesize and secrete the B cell chemoattractant CXCL13 in the inflammatory environment of the rheumatoid joint. *Arthritis & Rheumatism*, 58(11), 3377–3387.
- Mao, L., Hou, H., Wu, S., Zhou, Y., Wang, J., Yu, J., Wu, X., Lu, Y., Mao, L., Bosco, M. J., Wang, F., & Sun, Z. (2017). TIGIT signalling pathway negatively regulates CD4⁺ T-cell responses in systemic lupus erythematosus. *Immunology*, 151(3), 280–290.
- Maruyama, K., Takada, Y., Ray, N., Kishimoto, Y., Penninger, J. M., Yasuda, H., & Matsuo, K. (2006). Receptor activator of NF- κ B ligand and osteoprotegerin

- regulate proinflammatory cytokine production in mice. *The Journal of Immunology*, 177(6), 3799–3805.
- Matheu, V., Berggård, K., Barrios, Y., Barrios, Y., Arnau, M. R., Zubeldia, J. M., Baeza, M. L., Back, O., & Issazadeh-Navikas, S. (2009). Impact on allergic immune response after treatment with vitamin A. *Nutrition and Metabolism*, 6, 1–11.
- Matz, A., Lee, S.-J., Schwedhelm-Domeyer, N., Zanini, D., Holubowska, A., Kannan, M., Farnworth, M., Jahn, O., Göpfert, M. C., & Stegmüller, J. (2015). Regulation of neuronal survival and morphology by the E3 ubiquitin ligase RNF157. *Cell Death and Differentiation*, 22(4), 626–642.
- McHeyzer-Williams, M., Okitsu, S., Wang, N., & McHeyzer-Williams, L. (2012). Molecular programming of B cell memory. *Nature Reviews Immunology*, 12(1), 24–34.
- Meli, A. P., Fontés, G., Avery, D. T., Leddon, S. A., Tam, M., Elliot, M., Ballesteros-Tato, A., Miller, J., Stevenson, M. M., Fowell, D. J., Tangye, S. G., & King, I. L. (2016). The integrin LFA-1 controls T follicular helper cell generation and maintenance. *Immunity*, 45(4), 831–846.
- Millan, A. J., Elizaldi, S. R., Lee, E. M., Aceves, J. O., Muruges, D., Loots, G. G., & Manilay, J. O. (2019). *Sostdc1* regulates NK cell maturation and cytotoxicity. *The Journal of Immunology*, 202(8), 2296–2306.
- Moon, J. J., Chu, H. H., Pepper, M., McSorley, S. J., Jameson, S. C., Kedl, R. M., & Jenkins, M. K. (2007). Naive CD4⁺ T cell frequency varies for different epitopes and predicts repertoire diversity and response magnitude. *Immunity*, 27(2), 203–213.
- Moriyama, S., Takahashi, N., Green, J. A., Hori, S., Kubo, M., Cyster, J. G., & Okada, T. (2014). Sphingosine-1-phosphate receptor 2 is critical for follicular helper T cell retention in germinal centers. *Journal of Experimental Medicine*, 211(7), 1297–1305.
- Mueller, C. G., & Hess, E. (2012). Emerging functions of RANKL in lymphoid tissues. *Frontiers in Immunology*, 3(216), 1–7.
- Mulle, J. G., Dodd, A. F., McGrath, J. A., Wolyniec, P. S., Mitchell, A. A., Shetty, A. C., Sobreira, N. L., Valle, D., Rudd, M. K., Satten, G., Cutler, D. J., Pulver, A. E., & Warren, S. T. (2010). Microdeletions of 3q29 confer high risk for schizophrenia. *American Journal of Human Genetics*, 87(2), 229–236.
- Murphy, K., & Weaver, C. (2016). *Janeway's Immunobiology* (9th revise). New York: Garland Science.
- Naito, A., Azuma, S., Tanaka, S., Miyazaki, T., Takaki, S., Takatsu, K., Nakao, K., Nakamura, K., Katsuki, M., Yamamoto, T., & Inoue, J. I. (1999). Severe osteopetrosis, defective interleukin-1 signalling and lymph node organogenesis in TRAF6-deficient mice. *Genes to Cells*, 4(6), 353–362.

- Nurieva, R. I., Chung, Y., Hwang, D., Yang, X. O., Soon, H., Ma, L., Wang, Y., Watowich, S. S., Jetten, A. M., Tian, Q., & Dong, C. (2008). Generation of T follicular helper cells is mediated by interleukin-21 but independent of T helper 1, 2, or 17 cell lineages. *Immunity*, 29(1), 138-149.
- Nurieva, R. I., Chung, Y., Martinez, G. J., Yang, X. O., Tanaka, S., Matskevitch, T. D., Wang, Y.-H., & Dong, C. (2009). Bcl6 mediates the development of T follicular helper cells. *Science*, 325(5943), 1001–1005.
- Nurieva, R. I., Podd, A., Chen, Y., Alekseev, A. M., Yu, M., Qi, X., Huang, H., Wen, R., Wang, J., Li, H. S., Watowich, S. S., Qi, H., Dong, C., & Wang, D. (2012). STAT5 protein negatively regulates T follicular helper (Tfh) cell generation and function. *The Journal of Biological Chemistry*, 287(14), 11234–11239.
- O'Connor, R. A., Li, X., Blumerman, S., Anderton, S. M., Noelle, R. J., & Dalton, D. K. (2012). Adjuvant immunotherapy of experimental autoimmune encephalomyelitis: immature myeloid cells expressing CXCL10 and CXCL16 attract CXCR3⁺CXCR6⁺ and myelin-specific T cells to the draining lymph nodes rather than the central nervous system. *Journal of Immunology*, 188(5), 2093–2101.
- Oishi, H., Itoh, S., Matsumoto, K., Ishitobi, H., Suzuki, R., Ema, M., Kojima, T., Uchida, K., Kato, M., Miyata, T., & Takahashi, S. (2012). Delayed cutaneous wound healing in Fam129b/Minerva-deficient mice. *The Journal of Biochemistry*, 152(6), 549–555.
- Okada, Takaharu, Miller, M. J., Parker, I., Krummel, M. F., Neighbors, M., Hartley, S. B., O'Garra, A., Cahalan, M. D., & Cyster, J. G. (2005). Antigen-engaged B cells undergo chemotaxis toward the T zone and form motile conjugates with helper T cells. *PLoS Biology*, 3(6), 1047–1061.
- Okada, Tatsuya, Tsukano, H., Endo, M., Tabata, M., Miyata, K., Kadomatsu, T., Miyashita, K., Semba, K., Nakamura, E., Tsukano, M., Mizuta, H., & Oike, Y. (2010). Synoviocyte-derived angiopoietin-like protein 2 contributes to synovial chronic inflammation in rheumatoid arthritis. *The American Journal of Pathology*, 176(5), 2309–2319.
- Ono, T., Hayashi, M., Sasaki, F., & Nakashima, T. (2020). RANKL biology: Bone metabolism, the immune system, and beyond. *Inflammation and Regeneration*, 40(1), 1–16.
- Oxenius, A., Bachmann, M. F., Zinkernagel, R. M., & Hengartner, H. (1998). Virus-specific MHC class II-restricted TCR-transgenic mice: Effects on humoral and cellular immune responses after viral infection. *European Journal of Immunology*, 28(1), 390–400.
- Ozaki, K., Spolski, R., Feng, C. G., Qi, C. F., Cheng, J., Sher, A., Morse, H. C., Liu, C., Schwartzberg, P. L., & Leonard, W. J. (2002). A critical role for IL-21 in regulating immunoglobulin production. *Science*, 298(5598), 1630–1634.
- Papa, I., & Vinuesa, C. G. (2018). Synaptic interactions in germinal centers.

Frontiers in Immunology, 9, 1858.

- Papillion, A., Powell, M. D., Chisolm, D. A., Bachus, H., Fuller, M. J., Weinmann, A. S., Villarino, A., O'Shea, J. J., León, B., Oestreich, K. J., & Ballesteros-Tato, A. (2019). Inhibition of IL-2 responsiveness by IL-6 is required for the generation of GC-TFH cells. *Science Immunology*, 4(39).
- Parastouei, K., Solaymani-Mohammadi, F., Shiri-Shahsavari, M. R., Chahardoli, R., Nasl-Khameneh, A. M., Zarandi, M. B., Ghotloo, S., & Saboor-Yaraghi, A. A. (2020). The effect of calcitriol and all-trans retinoic acid on T-bet, IFN- γ , GATA3 and IL-4 genes expression in experimental autoimmune encephalomyelitis. *Apmis*, 128(11), 583–592.
- Penkert, R. R., Smith, A. P., Hrinicus, E. R., McCullers, J. A., Vogel, P., Smith, A. M., & Hurwitz, J. L. (2020). Effect of vitamin A deficiency in dysregulating immune responses to influenza virus and increasing mortality rates after bacterial coinfections. *The Journal of Infectious Diseases*, 223(10), 1806–1816.
- Pennock, N. D., White, J. T., Cross, E. W., Cheney, E. E., Tamburini, B. A., & Kedl, R. M. (2013). T cell responses: Naïve to memory and everything in between. *American Journal of Physiology*, 37(4), 273–283.
- Perfetto, S. P., Chattopadhyay, P. K., Lamoreaux, L., Nguyen, R., Ambrozak, D., Koup, R. A., & Roederer, M. (2006). Amine reactive dyes: An effective tool to discriminate live and dead cells in polychromatic flow cytometry. *Journal of Immunological Methods*, 313(1), 199–208.
- Periasamy, S., Dhiman, R., Barnes, P. F., Paidipally, P., Tvinnereim, A., Bandaru, A., Valluri, V. L., & Vankayalapati, R. (2011). Programmed death 1 and cytokine inducible SH2-containing protein dependent expansion of regulatory T cells upon stimulation with Mycobacterium tuberculosis. *The Journal of Infectious Diseases*, 203(9), 1256–1263.
- Perraud, A.-L., Knowles, H. M., & Schmitz, C. (2004). Novel aspects of signaling and ion-homeostasis regulation in immunocytes: The TRPM ion channels and their potential role in modulating the immune response. *Molecular Immunology*, 41(6), 657–673.
- Phan, T. G., Gray, E. E., & Cyster, J. G. (2009). The microanatomy of B cell activation. *Current Opinion in Immunology*, 21(3), 258–265.
- Ponta, H., Sherman, L., & Herrlich, P. A. (2003). CD44: From adhesion molecules to signalling regulators. *Nature Reviews Molecular Cell Biology*, 4(1), 33–45.
- Pontarini, E., Murray-Brown, W. J., Croia, C., Lucchesi, D., Conway, J., Rivellese, F., Fossati-Jimack, L., Astorri, E., Prediletto, E., Corsiero, E., Romana Delvecchio, F., Coleby, R., Gelbhardt, E., Bono, A., Baldini, C., Puxeddu, I., Ruscitti, P., Giacomelli, R., Barone, F., ... Bombardieri, M. (2020). Unique expansion of IL-21⁺ Tfh and Tph cells under control of ICOS identifies Sjögren's syndrome with ectopic germinal centres and MALT lymphoma. *Annals of the Rheumatic Diseases*, 79(12), 1588–1599.

- Pratama, A., Srivastava, M., Williams, N. J., Papa, I., Lee, S. K., Dinh, X. T., Hutloff, A., Jordan, M. A., Zhao, J. L., Casellas, R., Athanasopoulos, V., & Vinuesa, C. G. (2015). MicroRNA-146a regulates ICOS-ICOSL signalling to limit accumulation of T follicular helper cells and germinal centres. *Nature Communications*, *6*, 6436.
- Qi, H., Cannons, J. L., Klauschen, F., Schwartzberg, P. L., & Germain, R. N. (2008). SAP-controlled T-B cell interactions underlie germinal centre formation. *Nature*, *455*(7214), 764–769.
- Qi, H., Kastenmüller, W., & Germain, R. N. (2014). Spatiotemporal basis of innate and adaptive immunity in secondary lymphoid tissue. *Annual Review of Cell and Developmental Biology*, *30*(1), 141–167.
- Rao, D. A., Gurish, M. F., Marshall, J. L., Slowikowski, K., Fonseka, C. Y., Liu, Y., Donlin, L. T., Henderson, L. A., Wei, K., Mizoguchi, F., Teslovich, N. C., Weinblatt, M. E., Massarotti, E. M., Coblyn, J. S., Helfgott, S. M., Lee, Y. C., Todd, D. J., Bykerk, V. P., Goodman, S. M., ... Brenner, M. B. (2017). Pathologically expanded peripheral T helper cell subset drives B cells in rheumatoid arthritis. *Nature*, *542*(7639), 110–114.
- Rao, D. D., Senzer, N., Cleary, M. A., & Nemunaitis, J. (2009). Comparative assessment of siRNA and shRNA off target effects: what is slowing clinical development. *Cancer Gene Therapy*, *16*(11), 807–809.
- Reif, K., Ekland, E. H., Ohl, L., Nakano, H., Lipp, M., Förster, R., & Cyster, J. G. (2002). Balanced responsiveness to chemoattractants from adjacent zones determines B-cell position. *Nature*, *416*(6876), 94–99.
- Renton, A. E., Pliner, H. A., Provenzano, C., Evoli, A., Ricciardi, R., Nalls, M. A., Marangi, G., Abramzon, Y., Arepalli, S., Chong, S., Hernandez, D. G., Johnson, J. O., Bartoccioni, E., Scuderi, F., Maestri, M., Gibbs, J. R., Errichiello, E., Chiò, A., Restagno, G., ... Traynor, B. J. (2015). A genome-wide association study of myasthenia gravis. *JAMA Neurology*, *72*(4), 396–404.
- Ripamonti, A., Provasi, E., Lorenzo, M., De Simone, M., Ranzani, V., Vangelisti, S., Curti, S., Bonnal, R. J. P., Pignataro, L., Torretta, S., Geginat, J., Rossetti, G., Pagani, M., & Abrignani, S. (2017). Repression of miR-31 by BCL6 stabilizes the helper function of human follicular helper T cells. *Proceedings of the National Academy of Sciences of the United States of America*, *114*(48), 12797–12802.
- Rolf, J., Fairfax, K., & Turner, M. (2010). Signaling pathways in T follicular helper cells. *The Journal of Immunology*, *184*(12), 6563–6568.
- Sagar, A., Bishop, J. R., Tessman, D. C., Guter, S., Martin, C. L., & Cook, E. H. (2013). Co-occurrence of autism, childhood psychosis, and intellectual disability associated with a de novo 3q29 microdeletion. *American Journal of Medical Genetics. Part A*, *161A*(4), 845–849.
- Sage, P. T., Paterson, A. M., Lovitch, S. B., & Sharpe, A. H. (2014). The coinhibitory receptor CTLA-4 controls B cell responses by modulating T follicular helper, T

- follicular regulatory, and T regulatory cells. *Immunity*, 41(6), 1026–1039.
- Sallusto, F., Geginat, J., & Lanzavecchia, A. (2004). Central memory and effector memory T cell subsets: Function, generation, and maintenance. *Annual Review of Immunology*, 22(1), 745–763.
- Sander, J. D., & Joung, J. K. (2014). CRISPR-Cas systems for editing, regulating and targeting genomes. *Nature Biotechnology*, 32(4), 347–355.
- Santamaria-Kisiel, L., Rintala-Dempsey, A. C., & Shaw, G. S. (2006). Calcium-dependent and -independent interactions of the S100 protein family. *The Biochemical Journal*, 396(2), 201–214.
- Sasaki, Y., Ohta, M., Desai, D., Figueiredo, J.-L., Whelan, M. C., Sugano, T., Yamabi, M., Yano, W., Faits, T., Yabusaki, K., Zhang, H., Mlynarchik, A. K., Inoue, K., Mizuno, K., & Aikawa, M. (2015). Angiopoietin like protein 2 (ANGPTL2) promotes adipose tissue macrophage and T lymphocyte accumulation and leads to insulin resistance. *PloS One*, 10(7), e0131176–e0131176.
- Schipper, H. M. (2011). Heme oxygenase-1 in Alzheimer disease: a tribute to Moussa Youdim. *Journal of Neural Transmission*, 118(3), 381–387.
- Scholz, J., Kuhrau, J., Heinrich, F., Heinz, G. A., Hutloff, A., Worm, M., & Heine, G. (2020). Vitamin A controls the allergic response through T follicular helper cell as well as plasmablast differentiation. *Allergy: European Journal of Allergy and Clinical Immunology*, 76(4), 1109–1122.
- Schuster, G. U., Kenyon, N. J., & Stephensen, C. B. (2008). Vitamin A deficiency decreases and high dietary vitamin A increases disease severity in the mouse model of asthma. *The Journal of Immunology*, 180(3), 1834–1842.
- Seibler, J., Zevnik, B., Küter-Luks, B., Andreas, S., Kern, H., Hennek, T., Rode, A., Heimann, C., Faust, N., Kauselmann, G., Schoor, M., Jaenisch, R., Rajewsky, K., Kühn, R., & Schwenk, F. (2003). Rapid generation of inducible mouse mutants. *Nucleic Acids Research*, 31(4), e12.
- Sentmanat, M. F., Peters, S. T., Florian, C. P., Connelly, J. P., & Pruett-Miller, S. M. (2018). A survey of validation strategies for CRISPR-Cas9 editing. *Scientific Reports*, 8(1), 888.
- Seyfarth, J., Ahlert, H., Rosenbauer, J., Baechle, C., Roden, M., Holl, R. W., Mayatepek, E., Meissner, T., & Jacobsen, M. (2018). CISH promoter polymorphism effects on T cell cytokine receptor signaling and type 1 diabetes susceptibility. *Molecular and Cellular Pediatrics*, 5(1), 2.
- Shahinian, A., Pfeffer, K., Lee, K. P., Kundig, T. M., Kishihara, K., Wakeham, A., Kawai, K., Ohashi, P. S., Thompson, C. B., & Mak, T. W. (1993). Differential T cell costimulatory requirements in CD28-deficient mice. *Science*, 261(5121), 609–612.
- Shankar, S. P., Wilson, M. S., DiVietro, J. A., Mentink-Kane, M. M., Xie, Z., Wynn, T.

- A., & Druey, K. M. (2012). RGS16 Attenuates Pulmonary Th2/Th17 Inflammatory Responses. *The Journal of Immunology*, *188*(12), 6347–6356.
- Sharma, P., Azebi, S., England, P., Christensen, T., Møller-Larsen, A., Petersen, T., Batsché, E., & Muchardt, C. (2012). Citrullination of histone H3 interferes with HP1-mediated transcriptional repression. *PLoS Genetics*, *8*(9), e1002934–e1002934.
- Shi, J., Hou, S., Fang, Q., Liu, X., Liu, X., & Qi, H. (2018). PD-1 controls follicular T helper cell positioning and function. *Immunity*, *49*(2), 264–274.e4.
- Shimamura, M., Nakagami, H., Osako, M. K., Kurinami, H., Koriyama, H., Zhengda, P., Tomioka, H., Tenma, A., Wakayama, K., & Morishita, R. (2014). OPG/RANKL/RANK axis is a critical inflammatory signaling system in ischemic brain in mice. *Proceedings of the National Academy of Sciences of the United States of America*, *111*(22), 8191–8196.
- Shulman, Z., Gitlin, A. D., Targ, S., Jankovic, M., Pasqual, G., Nussenzweig, M. C., & Victora, G. D. (2013). T follicular helper cell dynamics in germinal centers. *Science*, *341*(6146), 673–677.
- Shulman, Z., Gitlin, A. D., Weinstein, J. S., Lainez, B., Esplugues, E., Flavell, R. A., Craft, J. E., & Nussenzweig, M. C. (2014). Dynamic signaling by T follicular helper cells during germinal center B cell selection. *Science*, *345*(6200), 1058–1062.
- Simpson N, Gatenby PA, Wilson A, Malik S, Fulcher DA, Tangye SG, Manku H, Vyse TJ, Roncador G, Huttley GA, Goodnow CC, Vinuesa CG, C. M. (2010). Expansion of circulating T cells resembling follicular helper T cells is a fixed phenotype that identifies a subset of severe systemic lupus erythematosus. *Arthritis Rheum.*, *62*(1), 234–244.
- Sonoda, E., Pewzner-Jung, Y., Schwers, S., Taki, S., Jung, S., Eilat, D., & Rajewsky, K. (1997). B cell development under the condition of allelic inclusion. *Immunity*, *6*(3), 225–233.
- Spolski, R., & Leonard, W. J. (2008). Interleukin-21: Basic biology and implications for cancer and autoimmunity. *Annual Review of Immunology*, *26* 57–79.
- Stebegg, M., Kumar, S. D., Silva-Cayetano, A., Fonseca, V. R., Linterman, M. A., & Graca, L. (2018). Regulation of the germinal center response. *Frontiers in Immunology*, *9*, 2469.
- Suan, D., Nguyen, A., Moran, I., Bourne, K., Hermes, J. R., Arshi, M., Hampton, H. R., Tomura, M., Miwa, Y., Kelleher, A. D., Kaplan, W., Deenick, E. K., Tangye, S. G., Brink, R., Chtanova, T., & Phan, T. G. (2015). T follicular helper cells have distinct modes of migration and molecular signatures in naive and memory immune responses. *Immunity*, *42*(4), 704–718.
- Suzuki, A., Kochi, Y., Shoda, H., Seri, Y., Fujio, K., Sawada, T., Yamada, R., & Yamamoto, K. (2016). Decreased severity of experimental autoimmune arthritis in peptidylarginine deiminase type 4 knockout mice. *BMC Musculoskeletal*

Disorders, 17, 205.

- Takayanagi, H., Ogasawara, K., Hida, S., Chiba, T., Murata, S., Sato, K., Takaoka, A., Yokochi, T., Oda, H., Tanaka, K., Nakamura, K., & Taniguchi, T. (2000). T-cell-mediated regulation of osteoclastogenesis by signalling cross-talk between RANKL and IFN- γ . *Nature*, 408(6812), 600–605.
- Thorin-Trescases, N., & Thorin, E. (2017). High circulating levels of ANGPTL2: beyond a clinical marker of systemic inflammation. *Oxidative Medicine and Cellular Longevity*, 2017, 1096385.
- Tibbitt, C. A., Stark, J. M., Martens, L., Ma, J., Mold, J. E., Deswarte, K., Oliynyk, G., Feng, X., Lambrecht, B. N., De Bleser, P., Nylén, S., Hammad, H., Arsenian Henriksson, M., Saeys, Y., & Coquet, J. M. (2019). Single-Cell RNA sequencing of the T helper cell response to house dust mites defines a distinct gene expression signature in airway Th2 cells. *Immunity*, 51(1), 169–184.
- Tomura, M., Itoh, K., & Kanagawa, O. (2010). Naive CD4⁺ T lymphocytes circulate through lymphoid organs to interact with endogenous antigens and upregulate their function. *The Journal of Immunology*, 184(9), 4646–4653.
- Troncone, E., Marafini, I., Stolfi, C., & Monteleone, G. (2018). Transforming growth factor- β 1/Smad7 in intestinal immunity, inflammation, and cancer. *Frontiers in Immunology*, 9, 1407.
- Ueno, H., Banchereau, J., & Vinuesa, C. G. (2015). Pathophysiology of T follicular helper cells in humans and mice. *Nature Immunology*, 16(2), 142–152.
- Varadhachary, A. S., Perdow, S. N., Hu, C., Ramanarayanan, M., & Salgame, P. (1997). Differential ability of T cell subsets to undergo activation-induced cell death. *Proceedings of the National Academy of Sciences of the United States of America*, 94(11), 5778–5783.
- Vinuesa, C. G., Linterman, M. A., Yu, D., & MacLennan, I. C. M. (2016). Follicular Helper T cells. *Annual Review of Immunology*, 34(1), 335–368.
- Vogelzang, A., McGuire, H. M., Yu, D., Sprent, J., Mackay, C. R., & King, C. (2008). A fundamental role for interleukin-21 in the generation of T follicular helper cells. *Immunity*, 29(1), 127–137.
- Vu Van, D., Beier, K. C., Pietzke, L.-J., Al Baz, M. S., Feist, R. K., Gurka, S., Hamelmann, E., Kroczeck, R. A., & Hutloff, A. (2016). Local T/B cooperation in inflamed tissues is supported by T follicular helper-like cells. *Nature Communications*, 7(1), 10875.
- Walsh, M. C., & Choi, Y. (2014). Biology of the RANKL-RANK-OPG system in immunity, bone, and beyond. *Frontiers in Immunology*, 5, 1–11.
- Wan, Z., Lin, Y., Zhao, Y., & Qi, H. (2019). TFH cells in bystander and cognate interactions with B cells. *Immunological Reviews*, 288(1), 28–36.
- Webb, L. M. C., & Linterman, M. A. (2017). Signals that drive T follicular helper cell

- formation. *Immunology*, 152(2), 185–194.
- Weber, J. P., Fuhrmann, F., Feist, R. K., Lahmann, A., Al Baz, M. S., Gentz, L.-J., Vu Van, D., Mages, H. W., Haftmann, C., Riedel, R., Grün, J. R., Schuh, W., Kroczek, R. A., Radbruch, A., Mashreghi, M.-F., & Hutloff, A. (2015). ICOS maintains the T follicular helper cell phenotype by down-regulating Krüppel-like factor 2. *Journal of Experimental Medicine*, 212(2), 217–233.
- Weber, J. P., Fuhrmann, F., & Hutloff, A. (2012). T-follicular helper cells survive as long-term memory cells. *European Journal of Immunology*, 42(8), 1981–1988.
- Weinstein, J. S., Herman, E. I., Lainez, B., Licona-Limón, P., Esplugues, E., Flavell, R., & Craft, J. (2016). TFH cells progressively differentiate to regulate the germinal center response. *Nature Immunology*, 17(10), 1197–1205.
- Willatt, L., Cox, J., Barber, J., Cabanas, E. D., Collins, A., Donnai, D., FitzPatrick, D. R., Maher, E., Martin, H., Parnau, J., Pindar, L., Ramsay, J., Shaw-Smith, C., Sistermans, E. A., Tettenborn, M., Trump, D., de Vries, B. B. A., Walker, K., & Raymond, F. L. (2005). 3q29 microdeletion syndrome: clinical and molecular characterization of a new syndrome. *American Journal of Human Genetics*, 77(1), 154–160.
- Williams, J. W., Tjota, M. Y., & Sperling, A. I. (2012). The contribution of allergen-specific IgG to the development of Th2-mediated airway inflammation. *Journal of Allergy*, 2012, 236075.
- Wong, B. R., Rho, J., Arron, J., Robinson, E., Orlinick, J., Chao, M., Kalachikov, S., Cayani, E., Bartlett, F. S., Frankel, W. N., Lee, S. Y., & Choi, Y. (1997). TRANCE is a novel ligand of the tumor necrosis factor receptor family that activates c-Jun N-terminal kinase in T cells. *Journal of Biological Chemistry*, 272(40), 25190–25194.
- Wu, X., Wang, Y., Huang, R., Gai, Q., Liu, H., Shi, M., Zhang, X., Zuo, Y., Chen, L., Zhao, Q., Shi, Y., Wang, F., Yan, X., Lu, H., Xu, S., Yao, X., Chen, L., Zhang, X., Tian, Q., ... Liu, X. (2020). SOSTDC1-producing follicular helper T cells promote regulatory follicular T cell differentiation. *Science*, 369(6506), 984–988.
- Xiao, S., Jin, H., Korn, T., Liu, S. M., Oukka, M., Lim, B., & Kuchroo, V. K. (2008). Retinoic acid increases Foxp3⁺ regulatory T cells and inhibits development of Th17 cells by enhancing TGF- β -driven Smad3 signaling and inhibiting IL-6 and IL-23 receptor expression. *The Journal of Immunology*, 181(4), 2277–2284.
- Xie, X., Mu, L., Yao, X., Li, N., Sun, B., Li, Y., Zhan, X., Wang, X., Kang, X., Wang, J., Liu, Y., Zhang, Y., Wang, G., Wang, D., Liu, X., Kong, Q., & Li, H. (2013). ATRA alters humoral responses associated with amelioration of EAMG symptoms by balancing Tfh/Tfr helper cell profiles. *Clinical Immunology*, 148(2), 162–176.
- Xiong, J., Onal, M., Jilka, R. L., Weinstein, R. S., Manolagas, S. C., & O'Brien, C. A. (2011). Matrix-embedded cells control osteoclast formation. *Nature Medicine*, 17(10), 1235–1241.

- Xu, H., Li, X., Liu, D., Li, J., Zhang, X., Chen, X., Hou, S., Peng, L., Xu, C., Liu, W., Zhang, L., & Qi, H. (2013). Follicular T-helper cell recruitment governed by bystander B cells and ICOS-driven motility. *Nature*, *496*(7446), 523–527.
- Yang, H., Chen, J. si, Zou, W. jing, Tan, Q., Xiao, Y. zhu, Luo, X. yan, Gao, P., Fu, Z., & Wang, H. (2020). Vitamin A deficiency exacerbates extrinsic atopic dermatitis development by potentiating type 2 helper T cell-type inflammation and masT cell activation. *Clinical and Experimental Allergy*, *50*(8), 942–953.
- Yang, X. O., Zhang, H., Kim, B.-S., Niu, X., Peng, J., Chen, Y., Kerketta, R., Lee, Y.-H., Chang, S. H., Corry, D. B., Wang, D., Watowich, S. S., & Dong, C. (2013). The signaling suppressor CIS controls proallergic T cell development and allergic airway inflammation. *Nature Immunology*, *14*(7), 732–740.
- Yu, D., Rao, S., Tsai, L. M., Lee, S. K., He, Y., Sutcliffe, E. L., Srivastava, M., Linterman, M., Zheng, L., Simpson, N., Ellyard, J. I., Parish, I. A., Ma, C. S., Li, Q.-J., Parish, C. R., Mackay, C. R., & Vinuesa, C. G. (2009). The ranscriptional repressor Bcl-6 directs T follicular helper cell lineage commitment. *Immunity*, *31*(3), 457–468.
- Yuen, G., Khan, F. J., Gao, S., Stommel, J. M., Batchelor, E., Wu, X., & Luo, J. (2017). CRISPR/Cas9-mediated gene knockout is insensitive to target copy number but is dependent on guide RNA potency and Cas9/sgRNA threshold expression level. *Nucleic Acids Research*, *45*(20), 12039–12053.
- Yugami, M., Odagiri, H., Endo, M., Tsutsuki, H., Fujii, S., Kadomatsu, T., Masuda, T., Miyata, K., Terada, K., Tanoue, H., Ito, H., Morinaga, J., Horiguchi, H., Sugizaki, T., Akaike, T., Gotoh, T., Takai, T., Sawa, T., Mizuta, H., & Oike, Y. (2016). Mice deficient in angiopoietin-like protein 2 (Angptl2) gene show increased susceptibility to bacterial infection due to attenuated macrophage activity. *The Journal of Biological Chemistry*, *291*(36), 18843–18852.
- Yun, T. J., Chaudhary, P. M., Shu, G. L., Frazer, J. K., Ewings, M. K., Schwartz, S. M., Pascual, V., Hood, L. E., & Clark, E. A. (1998). OPG/FDCR-1, a TNF receptor family member, is expressed in lymphoid cells and is up-regulated by ligating CD40. *Journal of Immunology (1950)*, *161*(11), 6113–6121.
- Zeiträg, J., Dahlström, F., Chang, Y., Alterauge, D., Richter, D., Niemietz, J., & Baumjohann, D. (2020). T cell-expressed microRNAs critically regulate germinal center T follicular helper cell function and maintenance in acute viral infection in mice. *European Journal of Immunology*, *51*(2), 408–413.
- Zhou, Q., Chen, J., Feng, J., Xu, Y., Zheng, W., & Wang, J. (2017). SOSTDC1 inhibits follicular thyroid cancer cell proliferation, migration, and EMT via suppressing PI3K/Akt and MAPK/Erk signaling pathways. *Molecular and Cellular Biochemistry*, *435*(1), 87–95.
- Zhu, J., & Paul, W. E. (2008). CD4 T cells: fates, functions, and faults. *Blood*, *112*(5), 1557–1569.
- Zou, Y. R., Takeda, S., & Rajewsky, K. (1993). Gene targeting in the Igk locus:

Efficient generation of λ chain-expressing B cells, independent of gene rearrangements in Igk. *EMBO Journal*, 12(3), 811–820.

7 Acknowledgements

First, I would like to thank my supervisor Prof. Dr. Andreas Hutloff, who enabled the realization of this project and the finalization of my thesis. He always gave me advice and support, was available to answer questions and solve problems and shared his extensive expertise with me - I am very grateful for his mentorship. Furthermore, I thank Prof. Dr. Thomas Bosch for taking over my supervision and for reviewing my thesis within the Faculty of Mathematics and Natural Sciences at the Christian-Albrechts-University in Kiel. I would like to thank my working group for the professional discussions, methodical instructions, the indispensable help on long analysis days, and the pleasant and fun atmosphere in and outside the laboratory. I would especially like to thank Phine, who has always supported me mentally and has become a good friend. I would like to thank Prof. Dr. Leif Erik Sander and Dr. Mir-Farzin Mashreghi for their willingness to be part of my Advisory Committee and the exciting discussions regarding my project. I would like to thank all the staff of the Robert Koch Institute in Berlin, especially the members of the laboratory of Prof. Dr. Richard A. Kroczeck and the opportunity to become part of this team. Furthermore, I would like to thank all the staff of the DRFZ and all those involved in this project. I would also like to express my special thanks to the staff of the Institute of Immunology in Kiel, who gave us a warm welcome and made our start in Kiel as easy as possible.

Special thanks go to my family, especially my parents and my brother, who have always supported me and stood by my side. I am grateful for my friends who have accompanied me for many years and on whom I can always rely. Many thanks to Jamina and Annika - without you, I would have never come this far.

Finally, the person who has supported me the most, always stood by me and believed in me is my partner and best friend Andy - thank you for everything!

The Curriculum Vitae on the following page is not included in the public version for privacy reasons.

8 Curriculum Vitae

9 List of publications

Lahmann, A., **Kuhrau, J.**, Fuhrmann, F., Heinrich, F., Bauer, L., Durek, P., Mashreghi, M.-F., & Hutloff, A. (2019). Bach2 Controls T Follicular Helper Cells by Direct Repression of Bcl-6. *The Journal of Immunology*, 202(8), 2229–2239. <https://doi.org/10.4049/jimmunol.1801400>

Scholz, J., **Kuhrau, J.**, Heinrich, F., Heinz, G. A., Hutloff, A., Worm, M., & Heine, G. (2020). Vitamin A controls the allergic response through T follicular helper cell as well as plasmablast differentiation. *Allergy*, 76(4):1109-1122. <https://doi.org/10.1111/all.14581>

Declaration

I, Julia Ritzau-Jost, born on August 14, 1991, in Stuttgart, hereby declare that I have written this dissertation entitled "Generation and Maintenance of T Follicular Helper Cells" independently and without unauthorized assistance and that I have identified all aids used as such.

Furthermore, I affirm that this work has never been the subject of a previous doctoral dissertation or has already been submitted for publication. The present work has been carried out in compliance with the rules of good scientific practice of the German Research Foundation. Furthermore, I assure that no academic degree has been withdrawn from me.

A handwritten signature in black ink, appearing to read 'Julia Ritzau-Jost', written in a cursive style.

Julia Ritzau-Jost